The mechanism of action of Interleukin-1 (IL-1) in acute neurodegeneration.

Hiren C Patel

A thesis submitted to the University of Manchester for the degree of Doctor of Philosophy in the Faculty of Medicine, Dentistry, Nursing and Pharmacy.

April 2003

Division of Neuroscience
School of Biological Sciences

(EF5WF)

Contents

List of Tables

List of Figures

Abstract

The cytokine Interleukin-1 (IL-1) has been implicated in traumatic, ischaemic and excitotoxic neuronal cell death. Striatal injection of S-AMPA with IL-1 in the rat results in 'distant' ipsilateral cortical cell death in addition to the 'local' striatal cell death observed in response to S-AMPA alone. The mechanism by which IL-1 exacerbates S-AMPA induced cell death is unknown. The cortical cell death induced by S-AMPA with IL-1 is considered to be IL-1 specific, as it is not induced by injection of S-AMPA with other pro-inflammatory cytokines or by S-AMPA alone. The primary aim of this thesis was to investigate the mechanisms by which IL-1 induces cortical cell death.

Co-infusion of S-AMPA with IL-1 increased the volume of cell death by 3-fold compared to that induced by striatal injection of S-AMPA alone. Consistent with previous reports, the increase in damage resulted predominantly from ipsilateral cortical cell death. Unlike previous reports however, S-AMPA with IL-1 significantly (2-fold) increased subcortical cell death compared to S-AMPA. Ipsilateral cortical cell death was also observed in response to S-AMPA alone in a small proportion of rats. In addition, 'distant' cell death was also seen in many similar subcortical and allocortical regions in response to striatal injection of S-AMPA with IL-1 and S-AMPA alone. These data suggested that 'distant' cell death is an S-AMPA dependent process, and that 'distant' cortical death is a result of the effects of IL-1 on an S-AMPA dependent process.

It has been suggested that cortical cell death in response to intrastriatal injection of S-AMPA with IL-1 results from IL-1 acting through particular sites (hypothalamus, striatum) in the brain. Immunohistochemical assessment of IL-1β expression was performed 4 h, 8 h, and 16 h after striatal injections of S-AMPA or S-AMPA with IL-1 to determine/ identify the 'putative pathway(s)' of IL-1 action in the brain. Immunoreactive IL-1β (irIL-1β) was identified in similar subcortical and cortical brain regions in response to both treatments. Neuronal damage was also seen in similar brain regions in which irIL-1β observed. In general, the temporo-spatial progression of both irIL-1β and neuronal damage was variable. However, irIL-1β in the cortex was consistent in its progression, and was observed earlier and more frequently in response to S-AMPA with IL-1, *vs* rats treated with S-AMPA alone. IrIL-1β was observed in the cortex 8 h after intrastriatal injection of S-AMPA with IL-1, and preceded neuronal degeneration in most animals. These data further suggested that 'distant' cell death and

IL-1β expression resulted from S-AMPA dependent mechanisms. Little hypothalamic irIL-1β was observed in this experiment suggesting also that hypothalamic IL-1 expression is not critical in mediating the effects of IL-1 in acute neurodegeneration as previously suggested.

'Distant' cell death has also been reported in response to intrahippocampal S-AMPA and kainic acid in the rats, and has been related to seizure activity. IL-1 increases seizures, and therefore it was hypothesised that IL-1 exacerbated excitotoxin induced cell death by increasing seizure activity. Consistent with this, increased seizure duration (3522 ± 660 s (SEM) *vs* 1415 ± 301 s; P<0.001), frequency (185 ± 20 *vs* 119 ± 16 P<0.05), and cell death volume (140 ± 20mm^3 *vs* 52mm^3 ± 6 <0.001) were observed in response to co-infusion of S-AMPA with IL-1 vs S-AMPA alone. In addition, diazepam (i.p) reduced cell death (P<0.001) and seizure duration (P<0.001) induced by S-AMPA with IL-1.

Intrastriatal injection of S-AMPA or S-AMPA with IL-1 increased c-Fos expression in regions similar to those in which c-Fos has been reported previously in response to seizures. Further, convulsive behaviours quantified as seizures were associated with EEG changes consistent with epileptiform, activity suggesting that intrastriatal injection of S-AMPA or S-AMPA with IL-1 was epileptogenic. In addition, a significant increase in cortical neuronal activity (number of c-Fos positive cells) was observed in response to S-AMPA with IL-1 compared to S-AMPA (8 h after injection) in the rat.

These data support the hypothesis that IL-1 exacerbates excitotoxin induced cell death by increasing seizure activity. Seizures are observed in stroke and head injury, and can contribute to outcome in these conditions. These data therefore also suggest that IL-1 causes or contributes to neuronal death by exacerbating seizures.

Declaration

I, the undersigned, declare that no portion of the work referred to in this thesis has been submitted in support of an application for another degree or qualification of this or any other institute of learning.

Hiren Patel

Copyright

Acknowledgement of assistance.

I would like to thank all the BSU staff for their high standards of animal husbandry. I would also like to thank Ralph Davies and Laura Heenan for their assistance during the seizure and immunohistochemistry experiments.

Finally, I thank the MRC for their financial support.

Personal Acknowledgement

Without initial funding and enthusiasm from the neurosurgeons at Hope hospital this thesis would not have been possible - Thank-you. Special thanks also to all my registrar colleagues- particular thanks to Shafqat, Khalid, Arup and John who made my life easier during the early days. Jerard also deserves special mention here – for too many reasons to mention individually!

My trial and tribulations at Hope aside, the Rothwell lab has been my daytime 'home' for the last three years. During this time many people have helped and contributed to various parts of this thesis happening, and I thank you all. Laura and Ralph thanks again for your help throughout, and Fiona, although the electrophysiology stuff did not make it to this thesis thanks for all your time and effort. I am sure something will come form all those results!

Stuart and Nancy. Whilst I may have disagreed with you both over many things, I could not have imagined working two nicer bosses. Thank you for all your help, advise, guidance and support over the last three years. Nancy, I hope that your relationship with the neurosurgeons remains fruitful. Your enthusiasm and hard work has certainly galvanised certain sections of Manchester neurosurgery. Long may it continue!

Finally Harriet thanks for being my taxi service, my punch bag, my organiser etc. I hope these last few months have not been too painful.

Abbreviations

°C	degrees centigrade
µg	microgram
AMPA	α-amino-3-hydroxy-methyl-4-isoxazolepropionate
ANOVA	analysis of variance
APES	3-aminoproylmethoxysilane
AcP	accessory protein
BSA	bovine serum albumin
BBB	blood brain barrier
BST	bed nucleus of the stria terminalis
Ca^{2+}	calcium
CBF	cerebral blood flow
CNS	central nervous system
CO_2	carbon dioxide
COX	cyclo-oxygenase
CSF	cerebrospinal fluid
Ctx	cortex
DAB	3,3-diaminobenzidine tetrahydrochloride
DMT	dorsomedial thalamus
EEG	electroencephalogram
EPN	enteropiriform mucleus
FITC	flourecin isothiocynate
h	hour (s)
H_2O_2	hydrogen peroxide
hrIL-1β	human recombinant interleukin-1beta
IL-1	interleukin-1
IL-6	interleukin-6
IL-1RI or II	interleukin-1 receptor type 1 or type 2
IL-1ra	interleukin –1 receptor antagonist
ICE	interleukin –1 converting enzyme
ICAM	intercellular adhesion molecule
icv	intracerebroventricular
i.p.	intraperitoneal
IU	international unit
kDa	kilo Dalton
MANOVA	multivariate analysis of variance
M	molar
MCAO	middle cerebral artery occlusion
mg	milligram
ml	millilitre
mmol	millimole
min	minute
Na	Sodium
NMDA	N-methyl-D-aspartate
MGlu	cis-2,4-methanoglutamate
mM	millimolar
mRNA	messenger RNA
min	minutes(s)
ng	nanogram
nl	nanolitre

NR	nucleus reuniens
nmol	nanomoles
N_2O	nitrous oxide
PFA	paraformaldhyde
PBS	phosphate buffered saline
p	probability
ROS	reactive oxygen species
SEM	standard error of the mean
S-AMPA	(S)-α-amino-3-hydroxy-methyl-4-isoxazolepropionate
Sec	second(s)
SI	substansia innominata
Rt th/ZI	reticular thalamus/Zona incerta
th	thalamus
Tx	triton X
TNFα	tumour necrosis factor alpha
µg	microgram
µl	microlitre
UK	United Kingdom
USA	United States of America
VCAM	vascular cell adhesion molecule
vs	*versus*
Zn	Zinc

'The Author'

I graduated from the University of Sheffield medical school in July 1995. I then undertook my basic surgical training in Cambridge, and completed my postgraduate surgical exams in before taking up this research post in April 2000. During my PhD, I undertook duties as a neurosurgical registrar at Hope hospital, and my long-term aim is to be a consultant neurosurgeon with an academic interest.

Chapter 1: General Introduction

1.1 The problem of acute neurodegeneration

Over one hundred thousand new cases of stroke are reported every year in the UK {Bath & Lees 2000}. The mortality in this group of patients is at least 20%, making stroke the third largest cause of death in this country. Morbidity is also a significant problem, such that stroke is the leading cause of disability in the UK {Bath & Lees 2000}. The outcome from other acute neurodegenerative conditions is also poor, with 30-43% of patients dying after severe head injury, {Marshall, Gautille, et al. 1991} and 40-50% following subarachnoid haemorrhage{Kassel, Sasaki, et al. 1985}. As with stroke, morbidity is also a common feature of these conditions{Kassel, Sasaki, et al. 1985; Marshall, Gautille, et al. 1991}.

Experimental studies have revealed numerous potential therapeutic targets for these conditions {Barone & Feuerstein 1999; Ginsberg 1998; Doble A 1999}. However, no significant improvement in outcome has been demonstrated in any of the clinical trials of 'neuroprotective' agents to date {Keyser, Sulter, et al. 2000}. Differences between human and animal pathophysiology, poor experimental modelling of clinical conditions, timing of drug administration, harmful side effects, and limitations of the design of clinical trials are some of the reasons put forward to explain why these trials have failed {Keyser, Sulter, et al. 2000}. However, failure of these clinical trials also suggests that we are some way from completely understanding and treating brain injury.

1.2 Cell death in stroke and head injury

Despite differences in the aetiology of neuronal cell death, the progression of neuronal damage is similar for stroke or head injury. Both can be considered to have a central region of cell death (core) resulting from the primary insult and a surrounding region of

vulnerable tissue (penumbra) that may die as a result of secondary insults {Leker & Shohami 2002}.

Occlusion of a cerebral blood vessel is the most common cause of stroke {Siesjo 1992a; Siesjo 1992b}. This leads to a reduction in the blood flow to part(s) of the brain distal to the occluded vessel {Siesjo 1992a; Siesjo 1992b}. Cell death ensues rapidly in regions where blood flow falls below critical levels (blood flow<10-12 ml/100g/min) necessary to maintain cellular functions {Siesjo 1992a}. The region of the brain distal to an occluded vessel is classically described as having a core (region of cell death and critically reduced blood flow) and a surrounding penumbral region where blood flow is reduced (but not to critical levels), and where neurones are viable but highly vulnerable to secondary insults {Siesjo 1992a}. The initial cell death in response to head injury results from direct mechanical injury. The neurones in the tissue surrounding the area of initial insult exhibit similar vulnerability to that seen in the ischaemic penumbra which result from similar pathological processes such as oedema and ischaemia {Siesjo 1992a; Siesjo 1993}.

Cells in the 'penumbral' regions may be recruited into the core lesion by ongoing secondary insults {Siesjo 1992a; Leker & Shohami 2002}. Prevention of secondary insults to this vulnerable brain region has been the key target for neuroprotective strategies as the primary damage is considered to be largely irreversible. Whilst a number of pathophysiological processes act as secondary insults (hypoxia, hyperglycaemia, hypotension, seizures, pyrexia) {Siesjo 1992a; Siesjo 1993; Ginsberg 1998}, at a cellular level, excitatory amino acids particularly glutamate are considered to be critical in mediating neuronal cell death in this region {Doble A 1999}.

1.3 Excitatory amino acids

Glutamate is the principle excitatory amino acid in the brain and is present in about one third of all synapses in the brain {Watkins & Evans 1981}. Under physiological conditions, glutamate is released from presynaptic vesicles in a calcium (Ca^{2+}) dependent manner upon depolarisation of the presynaptic membrane {Nicholls & Attwell 1990}. During normal synaptic functioning, efficient removal of glutamate through high affinity sodium (Na^{+}) dependent glutamate transporters, which are present on nerve terminals and glial cells, limits the excitatory action of glutamate {Nicholls & Attwell 1990}.

Glutamate acts by binding to two main categories of receptors, the ion-channel forming, 'ionotropic receptors' and the G-protein coupled, 'metabotropic receptors'. Three types of ionotropic receptor types, NMDA, AMPA, and kainate are currently recognised. Each of these ionotropic receptors is further divided into various subtypes as shown in Table 1.1 {Bleakman & Lodge 1998; Ozawa, Kamiya, et al. 1998; Doble A 1999}. Metabotropic receptors are not discussed further here because the work in this thesis is mainly related to ionotropic receptor activation.

GLUTAMATE RECEPTORS

METABOTROPIC			IONOTROPIC		
Group 1	Group 2	Group 3	NMDA	AMPA	KAINATE
mGluR1	mGluR2	mGluR4	NR1	GluR1	GluR5
mGluR5	mGluR3	mGluR6	NR2A	GluR2	GluR6
		mGluR7	NR2B	GluR3	GluR7
		mGluR8	NR2C	GluR4	KA1
			NR2D		KA2

Table 1.1 Representation of the major glutamatergic receptor subunits in the brain.

1.3.1 NMDA receptor

Glutamate activation via the NMDA receptors has been the subject of most investigation because of the availability of selective agonists and antagonists. These receptors are distributed widely throughout the brain (cortex, hippocampus, striatum, septum, amygdala) with the greatest density of receptor observed in the CA1 region of the hippocampus {Ozawa, Kamiya, et al. 1998}.

NMDA receptors are ligand-gated ion channels that are readily permeable to Ca^{2+}, Na^{+} and K^{+} {Ozawa, Kamiya, et al. 1998; Doble A 1999}. The NMDA receptor is complex, and has a number of modulatory sites. One of these sites binds glycine which is required as a co-agonist with glutamate for activation of the receptor {Ozawa, Kamiya, et al. 1998; Doble A 1999}. Binding of Mg^{2+} ions blocks activation of the receptor {Ozawa, Kamiya, et al. 1998; Doble A 1999} but this block is voltage-dependent, and is released in the event of neuronal depolarisation. NMDA receptor function may also be modulated through binding of spermine or spermidine to a polyamine site which enhances ion channel opening, or by binding of extracellular zinc (Zn^{2+}) which prevents ion channel opening {Ozawa, Kamiya, et al. 1998; Doble A 1999} .

1.3.2 AMPA receptor

Until recently, ionotropic glutamate receptors were classified into NMDA or non-NMDA receptors {Bleakman & Lodge 1998}. Non-NMDA receptors were initially subdivided into quisqualate and kainate receptors, and it was not until the development of the agonist AMPA, and the recognition that quisqualate activated metabotropic receptors, that non-NMDA receptors were re-categorised into AMPA and kainate receptor types {Bleakman & Lodge 1998}. In addition, it was not until the advent of expression cloning studies that the difference between AMPA receptors and kainate receptors was truly appreciated because most AMPA and kainate agonists activate both types of receptors. *In vivo*, this remains an issue as kainate or AMPA receptor specific antagonists are not yet widely available {Bleakman & Lodge 1998}.

Like NMDA receptors, AMPA receptors are distributed widely in the CNS. Radioligand binding studies show greatest binding of [^{3}H]-AMPA binding in the CA1 region and pyramidal cell layer of the hippocampus, and superficial layer of the cortex {Olsen, Szamraj, et al. 1987}. Intermediate levels of binding are seen in the deeper cortical layers and striatum, with low levels in the diencephalon, and midbrain and brainstem {Olsen, Szamraj, et al. 1987; Ozawa, Kamiya, et al. 1998}.

AMPA receptors exist as pentameric or tetrameric assemblies {Bleakman & Lodge 1998; Ozawa, Kamiya, et al. 1998}. Each assembly is made up of a combination (homomeric or hetromeric) of 4-5 subunits (GluR1-GluR4). Each subunit consists of three trans-membrane domains (denoted M1, M3, M4) and one hairpin, re-entrant loop within the membrane (M2), which forms the ion channel wall. As with the NMDA receptor, all AMPA receptor combinations are readily permeable to Na^+ and K^+

{Bleakman & Lodge 1998; Ozawa, Kamiya, et al. 1998}. However, only those subunits that do not express the GluR2 subunit are permeable to Ca^{2+}. In addition these Ca^{2+} permeable AMPA receptors exhibit increased permeability to Zn^{2+} {Bleakman & Lodge 1998; Ozawa, Kamiya, et al. 1998; {Weiss & Sensi 2000}.

AMPA receptors are rapidly desensitised by AMPA agonists {Bleakman & Lodge 1998; Ozawa, Kamiya, et al. 1998} . However, desensitisation rates can be modulated and are determined by whether AMPA receptors exist as 'flip' or 'flop' isoforms, with the flip isoform desensitising less rapidly. 'Flip' or 'flop' isoforms occur as a result of alternative splicing of an exon that encodes a 38 amino acid sequence that precedes the M4 region of each subunit {Bleakman & Lodge 1998; Ozawa, Kamiya, et al. 1998}.

1.3.3 Kainate receptors

Kainate receptors are also distributed widely in the CNS with highest levels being observed in the hippocampus {Bleakman & Lodge 1998; Ozawa, Kamiya, et al. 1998}. Kainate receptors exist as homomeric or hetromeric combinations of the various receptor subunits documented in Table 1.1. The combination of these subunits, and RNA editing similar to that described for AMPA receptors, determines the ion channel permeability of these receptors. The effects of kainate receptor activation however, remain poorly understood as kainate specific antagonists are not widely available{Bleakman & Lodge 1998; Ozawa, Kamiya, et al. 1998}.

1.3.4 Glutamate receptor activation

Glutamate receptor activation mediates fast and slow excitatory transmission in the brain {Watkins & Evans 1981}. Glutamate receptor activation is critical for the development and maintenance of long term potentiation (LTP) {Collingridge & Singer

1990}. Glutamate receptor activation also plays a role in the development and maturation of neurones and synapses {McDonald & Johnston 1990}, and has been implicated in the regulation of physiological processes such as respiration and blood pressure{Foutz, Champagnat, et al. 1988; Faraci & Breese 1994}.

Glutamate is also an important mediator of various pathological processes. Abnormalities in the glutamatergic system, resulting from either excessive endogenous glutamate release, or failure of glutamate uptake has been implicated in various neurological diseases such as epilepsy, amyotrophic lateral sclerosis, Parkinson's disease, and Alzheimers in addition to the acute neurodegenerative conditions of stroke and head injury {Doble A 1999}.

Excess glutamate or glutamate receptor over-activation is neurotoxic *in vitro* and *in vivo* {Choi 1985; Choi 1994}. Cell death in response to stroke or head injury leads to a massive increase in extracellular glutamate release, and the extent of this glutamate release can be correlated to the extent of injury induced experimentally by middle cerebral artery occlusion (MCAO) in the rat {Choi 1988; Doble A 1999}. Administration of glutamate receptor antagonists reduces cell death induced by experimental ischaemic or traumatic brain injury in rodents {Choi 1988; Doble A 1999}. Cell death due to over activation of glutamate receptors is termed excitotoxic cell death, and this is thought to be one of the key mechanisms through which cells die in response to ischaemic or traumatic insults to the brain.

1.4 Excitotoxic cell death

The mechanisms of excitotoxic cell death are not yet fully understood. Neuronal depolarisation leading to an influx of Na^+ and Ca^{2+} are important events in this process

{Choi 1988; Doble A 1999}. Na^+ is associated with the passive entry of Cl^- into the cell which leads to cell swelling and may ultimately cause cell death. Influx of Ca^{2+} and NMDA receptor mediated increase in intracellular Ca^{2+} stores leads to activation of a number of intracellular nucleases, proteases, lipases resulting in cell destruction. Increased intracellular Ca^{2+} also leads to the generation of free radicals which also contributes to the progression of cell death {Choi 1988; Doble A 1999}.

Ca^{2+} entry is the critical feature of excitotoxic cell death, as removal of extracellular Ca^{2+} (but not Na^+) prevents the neurotoxicity of glutamate *in vitro* {Choi 1985}. As NMDA receptors are the only 'freely' Ca^{2+} permeable glutamate receptors, excitotoxic cell death is thought to be mediated predominantly through NMDA receptors {Ozawa, Kamiya, et al. 1998}.

1.4.1 AMPA receptor mediated excitotoxic cell death

A role for AMPA receptors activation in mediating cell death in acute neurodegenerative conditions has also been demonstrated. AMPA agonists induce neuronal cell death *in vivo* in rodents {Lawrence, Allan, et al. 1998} and *in vitro* of cerebellar or spinal motor neurones {Garthwaite & Garthwaite 1991; Vandenberghe, Robberecht, et al. 2000}, and AMPA antagonists reduce cell death induced by experimental traumatic or ischaemic brain injury (See Table 1.2). In some cases, AMPA antagonists have been shown to be neuroprotective even when administered after induction of experimental brain injury (see Table 1.2). As this delayed neuroprotective effect is not observed with NMDA antagonists in the same setting, some investigators have suggested a greater role for AMPA receptor-mediated neuronal cell death in acute neurodegeneration {Xue, Huang, et al. 1994}. The mechanism(s) of cell death induced by activation of AMPA receptors is, however, not as clear as that for NMDA receptor -

mediated cell death. This is mainly due to two factors: firstly, AMPA receptors are thought to be poor conductors of Ca^{2+} influx, the critical component of NMDA receptor mediated excitotoxic cell death {Ozawa, Kamiya, et al. 1998}. Secondly, the AMPA receptor desensitises rapidly in the continued presence of glutamate to steady state levels {Ozawa, Kamiya, et al. 1998}.

1.4.1.1 AMPA receptors and Ca^{2+} permeability

Whilst in situ hybridisation and immunohistochemical studies suggest that Ca^{2+} permeable AMPA receptors are not the predominant AMPA receptor subtype expressed in the rodent brain, electrophysiological characterisation of ionic currents activated by AMPA receptors has suggested that Ca^{2+} permeable neurones are present in the hippocampus, cerebral cortex, retinal bipolar cells, cerebellar purkinje cells, and medial septal neurones {Bleakman & Lodge 1998}. In addition, insults such as global forebrain ischaemia and kainic acid induced status epilepticus in rats, induce a pronounced suppression of GluR2 receptors which can lead to a relative increase in the number of Ca^{2+} permeable receptors {Weiss & Sensi 2000}.

Antagonist	*Experimental model*	*Species*	*Timing (t) of antagonist administration after injury*	*Reference*
NBQX	Global cerebral ischaemia	Gerbil	t= 0	Sheardown, Nielsen, et al. 1990
NBQX	Global cerebral ischaemia	Gerbil	t= 4-24 h	Sheardown, Suzdak, et al. 1993
NBQX	Global cerebral ischaemia	Rat	t= 15-30 min	Buchan, Li, et al. 1991
NBQX	Traumatic brain injury	Rat	t= 0-6 h	Bernert & Turski 1996
NBQX	Focal ischaemia	Rat	t=0 and repeated at t= 1 h	Gill, Nordholm, et al. 1992
NBQX	Focal ischaemia	Rat	t= 90 min	Xue, Huang, et al. 1994
LY-293558	Focal cerebral ischaemia	Cat	t= 30 min prior to injury induction	Bullock, Graham, et al. 1994
YM90K	Focal cerebral ischaemia	Cat	t=10 min	Yatsugi, Takahashi, et al. 1996
LY215490	Focal cerebral ischaemia	Rat	t= 30 min prior to injury induction	Gill & Lodge 1994
LY293558	Spinal ischaemia	Rabbit	t= 15-90 min	Bowes, Swanson, et al. 1996

Table 1.2: Summary of AMPA antagonists that reduce cell death induced by traumatic brain injury, or global or focal cerebral ischaemia.

Oxygen-glucose deprivation of hippocampal neurones in culture increases AMPA receptor-dependent intracellular Ca^{2+} accumulation, and sensitivity to AMPA receptor-mediated excitotoxicity {Ying, Weishaupt, et al. 1997}. Cultured cortical neurones that exhibit Ca^{2+} permeable AMPA receptors are also more sensitive (compared to neurones that express the GluR2 subunit) to the excitotoxic effects of AMPA agonists. Electrophysiological and Ca^{2+} imaging studies also show increased AMPA receptor mediated Ca^{2+} influx in cells destined to die in the CA1 region in response to global ischaemia in the gerbil {Lu, Yin, et al. 1996; Carriedo, Sensi, et al. 2000; Tanaka, Grooms, et al. 2000; Weiss & Sensi 2000}.

Rapid release of Zn^{2+} occurs in experimental epilepsy, ischaemia, and trauma and has been implicated in neuronal cell death {Weiss & Sensi 2000}. Zn^{2+} accumulation is observed in neurones that subsequently die, and Zn^{2+} chelators reduce neuronal cell death {Weiss & Sensi 2000}. Ca^{2+} permeable AMPA receptors are also permeable to Zn^{2+}, and Zn^{2+} entry has been implicated in abrupt loss of mitochondrial membrane potential leading to development of reactive oxygen species, and cell death {Sensi, Yin, et al. 2000; Weiss & Sensi 2000} (see Figure 1.1).

These data suggest that cell death in response to AMPA receptor activation may proceed along the 'classical' excitotoxic pathway as described for NMDA in some neurones (see above).

1.4.1.2 AMPA receptor desensitisation

Differences in AMPA receptor desensitisation have been implicated in the selective vulnerability of cerebellar neurones to AMPA receptor mediated cell death {Brorson, Manzolillo, et al. 1995; Rosa, Jefferys, et al. 1999; Seifert, Schroder, et al. 2002},and

pharmacological reduction of desensitisation, enhances AMPA receptor mediated cell death {Brorson, Manzolillo, et al. 1995; Carriedo, Sensi, et al. 2000}.

Although receptor subtype is important in AMPA receptor mediated cell death, it has been shown that co-expression of the GluR2 flip and GluR4 flip in the HEK23 cell line has a lethal effect compared to other homomeric or hetromeric combinations suggests that combinations of GluR subtypes are also important. In addition, s in response to injury and inflammation flip/flop isoforms exhibit considerable spatial and temporal variation {Alsbo, Wrang, et al. 2000; Zhou, Imbe, et al. 2001}. Given the variation, and the number of subtype/isoform combinations of AMPA receptors, definitive studies are not yet available for the impact of receptor combination or desensitisation on cell death. Finally, AMPA receptor activation also leads to the release of endogenous glutamate. Therefore it has been suggested that glutamate acting through NMDA receptors may also mediate cell death induced by AMPA receptor activation *in vivo* {Berman & Murray 1997}.

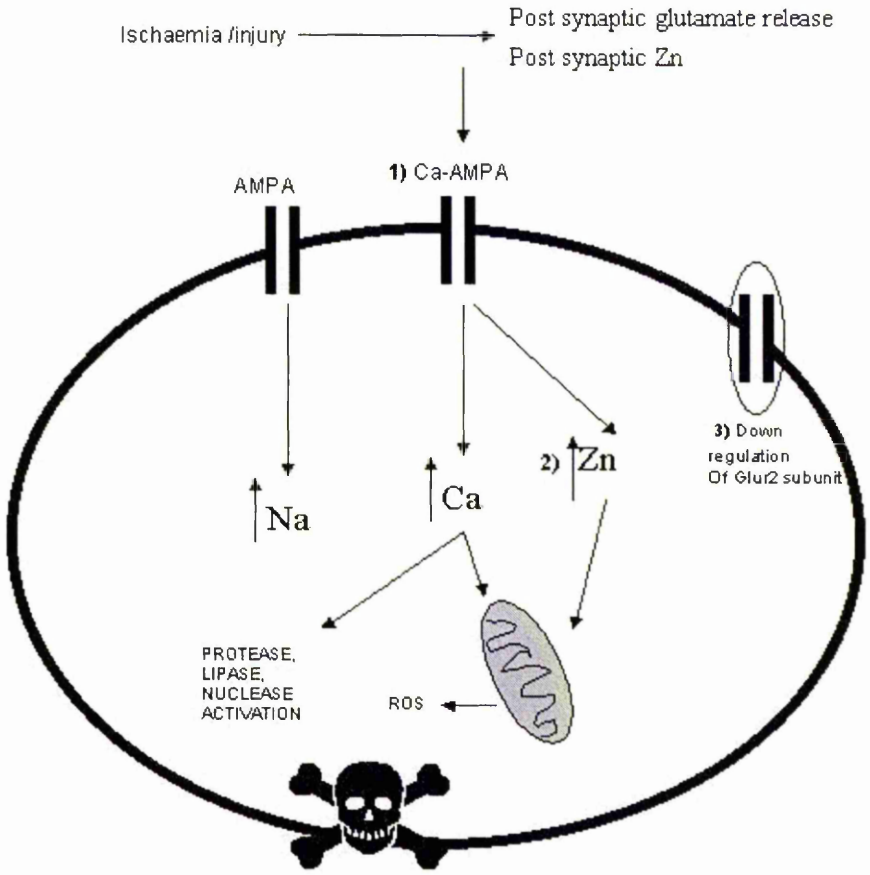

Figure 1.1 Schematic representation of the potential mechanism(s) involved in AMPA receptor mediated 'excitotoxic' cell death. Cell death is thought to occur as a result of 1) intracellular increase in Ca^{2+} entry via Ca-AMPA (Ca^{2+} permeable AMPA receptors), 2) intracellular entry of Zn^{2+} and generation of ROS (reactive oxygen species), and 3) down-regulation of GluR2 subunit, and a relative increase in Ca-AMPA.

1.5 CNS inflammation

More recently the inflammatory response to trauma or ischaemia has been implicated in mediating or exacerbating neuronal injury {Barone & Feuerstein 1999}. The CNS has long been considered an immune privileged site, and has been thought to be unable to mount an immune response. This immune privilege is based on the observations that heterologous tissue implanted into the brain survives longer than if implanted into peripheral tissue; and that the entry of inflammatory cells (leucocytes) a fundamental characteristic of the inflammatory process is blunted. This concept has been further supported by observations that the brain/ CNS shares features that confer immune privilege to other such sites, such as absence of lymphatics, lack of the constitutive expression of MHC antigens (important for antigen recognition) and the presence of a physical barrier, the blood brain barrier.

1.5.1 Inflammatory response in the central nervous system

Inflammation in the central nervous system is not generally visible because the 'classical' redness, and swelling are not immediately obvious. Loss of function, pain and fever, are all features associated with CNS insults, although rarely appreciated as part of the inflammatory response of the nervous system. However, evidence that the CNS may partake in the inflammatory process is provided by observations that most components required for the inflammatory response (cellular and non-cellular) are observed in response to CNS injury {Perry, Bell, et al. 1995; Barone & Feuerstein 1999}. As in the periphery, this process has been demonstrated as a co-ordinated stepwise process. In the CNS, the earliest component of the inflammatory response appears to be microglial activation {Kreutzberg 1996}.

1.5.2 Microglial activation

The earliest and most consistent CNS response to injury is microglial activation {Kreutzberg 1996}. Microglial activation is characterised by a change in morphology (cell body becomes rounded, cellular processes are retracted, and phagolysosomes become apparent) and immunophenotype (up-regulation of the constitutively expressed CB3 receptor, expression of the MHC class I and II antigens) {Kreutzberg 1996}. Microglia are activated from within 20 minutes to one hour after global, or focal cerebral ischaemia in experimental animals, and within 5 h in response to cortical stab injury in the rat {Stoll, Jander, et al. 1998; Stoll & Jander 1999}. The microglial response to injury is hypertrophy, migration to the site of injury, and proliferation {Kreutzberg 1996}. Microglia are key phagocytic cells, and have the ability to produce reactive oxygen species, nitric oxide, cytokines, arachidonic acid metabolites, proteolytic enzymes, all of which are components of the classical inflammatory response {Stoll & Jander 1999; Stoll, Jander, et al. 1998}. Microglia, by virtue of their early responsiveness and ability to secrete various pro-inflammatory mediators are thought to initiate the inflammatory response of the CNS to injury.

1.6 Cytokines

Cytokines are a diverse group of polypeptides that are traditionally recognised as prime mediators of the local and systemic responses of the host to injury and inflammation {Hopkins & Rothwell 1995; Rothwell & Hopkins 1995; Rothwell 1999}. Cytokines can act in a paracrine, autocrine or endocrine manner, and are noted to have many overlapping functions {Hopkins & Rothwell 1995; Rothwell & Hopkins 1995; Rothwell 1999}. Over 100 cytokines have been identified, and these have been categorised into interleukins, interferons, chemokines, tumour necrosis factors, neurotrophins and

growth factors {Hopkins & Rothwell 1995; Rothwell & Hopkins 1995; Rothwell 1999}. Cytokines are produced at low levels in the normal state, but are rapidly upregulated during times of stress (Table 1.3) {Hopkins & Rothwell 1995; Rothwell & Hopkins 1995; Rothwell 1999}.

Stimulus	*Cytokines produced*	*Cellular source*	*References*
LPS (peripheral infection)	IL-1, IL-6, L-10, IL-13	Microglia, neurones	{Hopkins & Rothwell 1995}
malaria, meningitis, CMV, HIV (CNS infections)	IL-1, IL-6, TNFα, TGFβ,INF, MIP-1α, MIP-1β, RANTES,	Microglia, astrocytes	{Asensio & Campbell 1999}
Trauma / cerebral ischaemia	IL-1, IL-2, IL-6, TNFα, IL-8, LIF, MCP-1, RANTES, FGF, PDGF	Microglia, astrocytes, neurones	{Barone & Feuerstein 1999} {Benveniste 1998}
Seizures	IL-1, IL-6, TNFα, NGF, BDNF, FGF, LIF	Microglia, neurones, astrocytes	{Munoz-Fernandez & Fresno 1998} {Jankowsky & Patterson 2001}

Table 1.3: Cytokine synthesis in response to CNS injury or inflammation. Abbreviations: BDNF, brain derived neurotrophic factor; EGF, epidermal growth factor; FGF, fibroblast growth factor; INF interferon; IL, Interleukin; LIF, leukaemia inhibitory factor; MIP, macrophage inflammatory protein; NGF nerve growth factor; PDGF, platelet derived growth factor; TGF, transforming growth factor; TNF, tumour necrosis factor; RANTES, regulated on activation normal T cell expressed and secreted.

Cytokines have recently been implicated in acute and chronic brain injury. The cytokines TNFα, IL-6, TGF-β as well as IL-1 (the first cytokine to be identified to influence the CNS) are currently considered to be the most important cytokine mediators of cell death in acute brain injury. A short summary of the effects of the aforementioned cytokines in brain injury is given below, but this review concentrates on the effects of IL-1 in acute neurodegeneration as it is the cytokine under investigation in this thesis.

TNFα, IL-6, and TGFβ are all up-regulated rapidly in response to experimental brain injury (see Table 1.3). Intracerebral administration of TNFα exacerbates, and antagonism of endogenous TNFα by soluble TNFα receptor or neutralising antibody reduces cell death induced by experimental brain injury {Nawashiro, Martin, et al. 1997; Mayne, Ni, et al. 2001}. TNFα induces cell death of cultured hippocampal neuronal and PC12 cells {Reimann-Philipp, Ovase, et al. 2001; Zhao, Bausano, et al. 2001}. In contrast, other *in vitro* studies have reported that TNFα is neuroprotective {Cheng, Christakos, et al. 1994; Bruce, Boling, et al. 1996}, and mice lacking the TNF receptor (p55 or P55 and P75) show enhanced cell death in response to excitotoxic or ischaemic brain injury compared to their wild type counterparts {Gary, Bruce-Keller, et al. 1998}. These latter data support a neuroprotective role for TNFα in brain injury. The reason for the discrepancy between these results is not clear.

Similarly inconsistent data have also arisen from studies investigating the role of the pro-inflammatory cytokine IL-6 in brain injury. Intracerebroventricular (icv) injection of IL-6 reduces infarct volume in response to middle cerebral artery occlusion in rats {Loddick, Turnbull, et al. 1998a}. A neuroprotective role for IL-6 is also suggested by

the observation that cell death induced by cold injury is increased in IL-6 knockout mice {Penkowa, Moos, et al. 1999}. However, as no reduction in cell death is seen in response to cerebral ischaemia in wild type mice compared to IL-6 knockout mice the neuroprotective role of IL-6 has been questioned. The lack of IL-6 specific antagonists has limited further investigation of the role of IL-6 in brain injury {Clark, Rinker, et al. 2000}.

Unlike TNFα or IL-6, TGFβ is an 'anti-inflammatory' cytokine and its role in acute CNS pathology appears to be better defined. Administration of TGFβ reduces glutamate-induced neuronal cell death *in vitro*, as well as ischaemic cell death mice {Prehn, Backhauss, et al. 1993}. TGFβ also reduces hippocampal neurones degeneration in response to transient global ischaemic insults in rats {Prehn, Backhauss, et al. 1993}. Antagonism of TGFβ exacerbates ischaemic and excitotoxic brain injury in rats further suggesting that TGFβ is a neuroprotective cytokine {Ruocco, Nicole, et al. 1999}.

1.7 Interleukin-1 (IL-1)

IL-1 is a 17-kDa polypeptide that exists as a barrel shaped molecule composed of 12-14β strands. Although other putative IL-1 homologues / family members have been identified recently, IL-1 exists as two, well characterised isoforms, IL-1α and IL-1β {Dinarello 1994}. A naturally occurring, specific IL-1 receptor antagonist (IL-1ra) has also been identified and characterised {Dinarello 1994}. IL-1α and IL-1β are the products of separate genes located on chromosome 2 {Dinarello 1994}. They share some structural homology and are both produced as precursors, which lack leader sequences and require enzymatic cleavage to the mature form by specific cellular

proteases. Whilst pro-IL-1α is active, inactive pro-IL-1β depends on activation by IL–1 converting enzyme (ICE), otherwise known as caspase-1 {Alnemri, Fernandes-Alnemri, et al. 1995; Enari, Hug, et al. 1995}. IL-1α and IL-1β act through binding to the IL-1 receptor I (IL-1RI, 80 kDa) which requires association with an accessory protein (AcP) for cellular activation {Greenfeder, et al. 1995; Parnet, Kelley, et al. 2002}. The other IL-1 known receptor, IL-1 RII has no intracellular domain and is unable to transduce intracellular signals {Loddick, Liu, et al. 1998b}.

Functional (IL-1R1) receptors have been localised using radiolabelled IL-1 to neurones and astrocytes, and are reported to be widely distributed throughout the brain {Farrar, Kilian, et al. 1987; Ban 1994}. However, in situ studies have suggested that IL-1R1 receptors are localised mainly to the meninges, choroid plexus, ependymal cells, and vascular endothelium {Ericsson, Liu, et al. 1995}. Limited brain parenchymal IL-1R1 mRNA is localised in the hypothalamus {Ericsson, Liu, et al. 1995}. Protein localisation has been problematic because of the lack of specific antibodies to IL-1R1 receptors (personal communication E Pinteaux). In contrast to IL-1 RI, the AcP is constitutively expressed and abundant in the rat brain {Loddick, Liu, et al. 1998b}. The IL-1RII receptor is also expressed widely in the CNS with high levels of IL-1RII in the hippocampus and cerebellum {French, VanHoy, et al. 1999}.

The IL-1 receptor antagonist (IL-1ra) has a molecular weight of 22KDa, and binds to the IL-1 receptor without inducing cellular activation. IL-1ra mRNA and protein are both up-regulated in response to similar stimuli as for IL-1 (e.g. LPS, trauma, ischaemia, excitotoxins, seizures) {Toulmond & Rothwell 1995; Eriksson, Winblad, et al. 1998; Gayle, Ilyin, et al. 1999; Allan, Harrison, et al. 2001; Hosoi, Okuma, et al. 2002}, although protein expression of IL-1ra does appear to lag behind IL-1

expression{Toulmond & Rothwell 1995}. This well characterised, endogenous antagonist has proved extremely useful in studying the actions of IL-1 and has great potential as a therapeutic agent {Freeman & Buchman 2001; Hallegua & Weisman 2002}.

1.8 Actions of IL-1

Consistent with most other cytokines, IL-1 is not generally expressed or secreted in normal healthy tissues {Dinarello 1994}. Its main role appears to be limited to disease states, when it is expressed in a wide range of tissues {Dinarello 1994}.

IL-1 is a key mediator of the inflammatory response. Local up regulation of IL-1 promotes vascular permeability {Marcus, Wyble, et al. 1996} increases neutrophil and monocyte adhesion and migration {Issekutz 1995; Rogers, Tripp, et al. 1994}, and induces nitric oxide and prostaglandin synthesis {Cao, Matsumura, et al. 2001}. IL-1 also up-regulates other pro-inflammatory cytokines and chemokines, that interact and orchestrate the inflammatory response {Kaplanski, Farnarier, et al. 1994; Asensio & Campbell 1999}. In addition to these local effects, IL-1 induces acute phase protein production and suppresses the production of factors not critical in the inflammatory response such as albumin, lipoprotein lipase and cytochromes {Dinarello 1994; Hopkins & Rothwell 1995; Rothwell & Luheshi 2000; Rothwell 1999}.

IL-1 also induces systemic responses of inflammation such as fever, anorexia, and increased slow wave sleep {Hopkins & Rothwell 1995; Rothwell & Hopkins 1995; Terao, Matsumura, et al. 1998; Parnet, Kelley, et al. 2002}. These changes can be reproduced by intracerebral injections of IL-1 in rodents at concentrations of one-thousandth the necessary peripheral dose, suggesting that endogenous brain IL-1, rather

than peripheral IL-1 mediates these effects. IL-1 cannot cross the blood brain barrier (BBB) passively and circulating concentrations are usually low {Hopkins & Rothwell 1995;Rothwell & Hopkins 1995; Rothwell & Luheshi 2000; Anforth, Bluthe, et al. 1998}, supporting a role for IL-1 production and action within the brain.

In addition to these systemic responses many of which may be effected via the hypothalamus, IL-1 also exerts local pro-inflammatory effects in response to CNS injury and infection, and is expressed in inflamed or injured brain regions {Davies, Loddick, et al. 1999; Pearson, Rothwell, et al. 1999}. IL-1 induced by injury is mainly expressed in microglia, although IL-1 is also localised in the brain in neurones, astrocytes, and oligodendocytes {Blasi, Riccio, et al. 1999; Pearson, Rothwell, et al. 1999; Vitkovic, Bockaert, et al. 2000}.

1.9 IL-1 and acute brain injury

The local inflammatory response to acute brain injury may contribute dramatically to CNS damage in acute neurodegenerative states {Barone & Feuerstein 1999}. Since IL-1 has well documented pro-inflammatory actions in the CNS (Table 1.4), it has attracted much attention as a potential therapeutic target in such conditions {Rothwell & Luheshi 2000}.

Effect of IL-1	*IL-1 application*	*Species/ culture system*	*Reference*
Up regulation of IL-6	Bath application	Mixed rat glial cultures	Pinteaux, Parker, et al. 2002
Up regulation of TNFα	Bath application	Human glioma cell line	Bethea, Chung, et al. 1992
	Bath application of IL-1 with interferon-gamma	Rat astrocyte cell culture	Chung & Benveniste 1990
Up regulation of COX-2/ prostaglandin	icv injection of IL-1	Rat	Cao, Matsumura, et al. 2001
	Bath application	Rat microglial culture	Basu, Krady, et al. 2002
	Bath application	Human neuroblastoma cell line	Hoozemans, Veerhuis, et al. 2001
Intercellular adhesion molecules (ICAM-1, VCAM-1, E-Selectin)	Bath application	Human cultured brain endothelial cells	Stanimirovic & Satoh 2000
Neutrophil recruitment	Systemic (i.p) injection of IL-1	Rats	Sutcliffe, Smith, et al. 2001
	Intracerebral injection of IL-1	Rats	Anthony, Dempster, et al. 1998

Table 1.4 Effects of IL-1 on various inflammatory mediators in the brain/brain parenchymal cells.

Elevated levels of IL-1 and IL-1ra have been noted in the cerebrospinal fluid of patients with severe head injury, or subarachnoid haemorrhage {McClain, Cohen, et al. 1987; Mathiesen, Edner, et al. 1997}. Furthermore, expression of IL-1 mRNA (within 15 min of MCAO in the rat) and protein (within 1 h of ischaemic or traumatic injury) increase in response to experimental brain injury caused by excitotoxin infusion, cerebral

ischaemia or traumatic brain injury in rodents {Minami, Kuraishi, et al. 1992; Ianotti, Kida, et al. 1993; Liu, McDonnell, et al. 1993;Yabuuchi, Minami, et al. 1993; Buttini, Sauter, et al. 1994; Davies, Loddick, et al. 1999; Pearson, Rothwell, et al. 1999; Allan, Parker, et al. 2000}. Whilst IL-1 itself does not cause neuronal cell death, intrastriatal or icv injection of IL-1 results in a significant increase in the magnitude of cell death caused by excitotoxic, ischaemic or traumatic brain injury in rodents {Loddick & Rothwell 1996a; Lawrence, Allan, et al. 1998}.

The greatest evidence supporting a causal role for IL-1 in brain injury comes from experiments in which IL-1ra (the naturally occurring specific IL-1 receptor antagonist) has been used. Injection of IL-1ra, icv, intrastriatally, or peripherally reduces cell death induced by MCAO by 50% in rodents {Relton & Rothwell 1992; Loddick & Rothwell 1996a; Betz, Schielke, et al. 1996; Stroemer & Rothwell 1997}. IL-1ra is neuroprotective after temporary and permanent focal cerebral ischaemia in rats{Yamasaki, Matsuura, et al. 1995; Loddick & Rothwell 1996a}. The neuroprotective effects of IL-1ra in focal ischaemia are observed even when IL-1ra is administered up to 3 h after temporary MCAO in the rat {Ross et al unpublished}. IL-1ra also reduces cell death induced by fluid percussion injury, intrastriatal excitotoxin injection, hypoxic ischaemic injury and experimental allergic encephalitis in rats {Relton & Rothwell 1992; Martin, Chinookoswong, et al. 1994; Martin & Near 1995; Badovinac, Mostarica-Stojkovic, et al. 1998; Sanderson, Raghupathi, et al. 1999}.

Furthermore, cell death induced by MCAO is reduced by administration of ICE inhibitors or IL-1β antibody in rats {Yamasaki, Matsuura, et al. 1995 ; Loddick, MacKenzie, et al. 1996b} . Mice lacking both the IL-1 α and IL-1 β genes also have a

reduction in damage induced by middle cerebral artery occlusion {Boutin, LeFeuvre, et al. 2001}.

In contrast to the deleterious effects of IL-1 in brain injury *in vivo* described above, IL-1 reduces neuronal damage induced by excitotoxins in primary cultured neurones {Strijbos & Rothwell 1995}. *In vitro* studies have also suggested that IL-1 depresses Ca^{2+} response in hippocampal neurones, enhances GABA receptor function, and inhibits glutamate release, all of which support a potential neuroprotective role for IL-1 in the brain {Miller, Galpern, et al. 1991; Plata-Salaman & Ffrench-Mullen 1992; Murray, McGahon, et al. 1997}. However, IL-1 is toxic to cells in mixed glial and neuronal culture, suggesting that IL-1 actions may be dependent on interactions between various cell types {Giulian, Vaca, et al. 1993; Rothwell 1999}.

1.10 How does IL-1 contribute to brain injury?

Despite the discrepancy observed between *in vitro* and *in vivo* experiments there is considerable evidence to implicate IL-1 as a primary mediator of brain injury *in vivo*. However, the mechanism by which IL-1 exacerbates brain injury is not clear. Given the diverse effects of IL-1 it is perhaps unlikely that one factor alone contributes to cell death. It is well recognised that IL-1 can increase body temperature, causes blood brain barrier (BBB) disruption, induce cerebral oedema, and potentiate seizure activity, all of which can influence the progression of brain injury {Hopkins & Rothwell 1995; Rothwell, Allan, et al. 1997; Vezzani, Conti, et al. 1999; Rothwell & Luheshi 2000}. In addition, recent data suggests that IL-1 mediates its effects in neurodegeneration by activating specific brain regions {Rothwell, Allan, et al. 1997}.

1.10.1 Site specific actions of IL-1

The hypothesis that IL-1 acts through specific sites in the brain is based on a number of observations. When IL-1 is co-injected into the striatum with the excitotoxin S-AMPA (a glutamate agonist), ipsilateral cortical damage is dramatically increased {Lawrence, Allan, et al. 1998; Grundy 2000} (Figure 1.2). The damage affects the whole ipsilateral hemisphere and is distant to the site of injection. As cell death is not increased upon co-injection of S-AMPA with IL-1 in the cortex {Lawrence, Allan, et al. 1998}, it has been proposed that IL-1 exacerbates neurodegeneration by acting at specific sites in the brain (Figure 1.2).

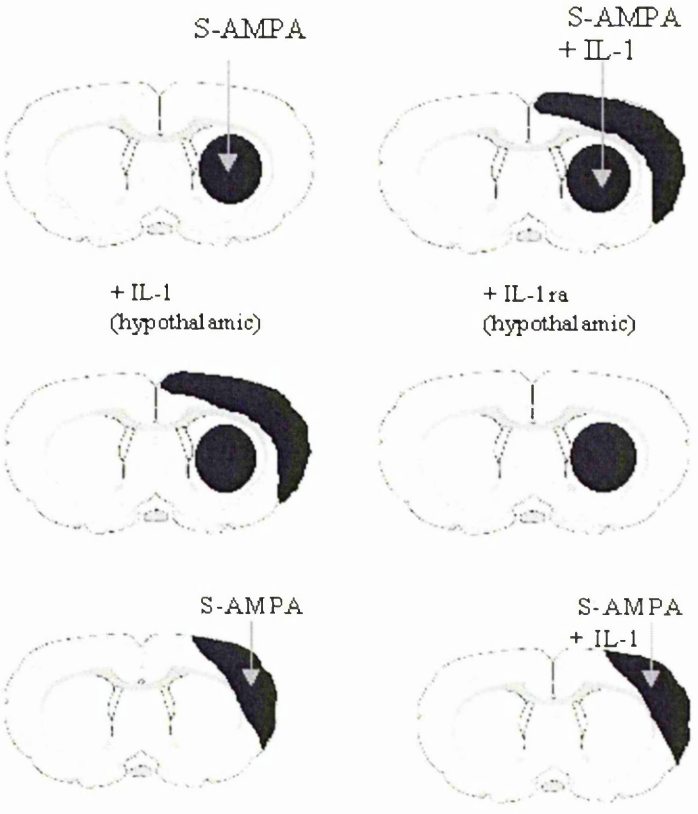

Figure 1.2: Diagrammatic representation of lesions induced by intrastriatal or intracortical injection of S-AMPA ± IL-1. The effects on cell death of intrastriatal S-AMPA with intrahypothalamic IL-1, and intrahypothalamic IL-1ra with intrastriatal injection of S-AMPA with IL-1 are also represented {Lawrence, Allan, et al. 1998}.

Consistent with observations of increased cortical death induced by striatal injection of IL-1 with S-AMPA, increased infarct volume (70% increase) is seen when IL-1 is injected into the striatum or into the cerebral ventricles of rats subjected to MCAO. However, no effect on ischaemic brain damage was seen when IL-1 is injected directly injected into the ischaemic cortex {Stroemer & Rothwell 1998} supporting the site specific hypothesis for the action of IL-1 on excitotoxic brain injury.

The observation that IL-1ra is neuroprotective effects only when injected into the striatum or given icv but not when injected directly into the site of cortical damage {Stroemer & Rothwell 1997; Lawrence, Allan, et al. 1998} further supports the postulate that IL-1 mediates it neurodegenerative effects through specific sites in the brain.

More recently the hypothalamus has also been identified as a potential site through which IL-1 acts. This is based on the observation that IL-1 mRNA and protein expression (8 h after striatal injection) precedes cortical cell death induced by intrastriatal injection of IL-1 with S-AMPA (first observed 12 h). Further, infusion of IL-1 into the hypothalamus exacerbates cell death induced by striatal injection of S-AMPA, and hypothalamic injection of IL-1ra reduces cell death induced by intrastriatal injection of S-AMPA with IL-1 in the rat {Allan, Parker, et al. 2000}. The ventral striatum and the nucleus accumbens shell are also considered to be important sites for IL-1 action, as injection of IL-1 with S-AMPA in these areas results in a greater frequency and volume of cortical death than observed with co-infusion of IL-1 with S-AMPA into the dorsal striatum or nucleus accumbens core {Grundy, Rothwell, et al. 2002}.

1.10.2 IL-1 and temperature

It is well documented that body temperature can influence neurodegeneration in both animals and humans. In humans, mild hypothermia at presentation has been equated with a better outcome after stroke, whilst fever in the first seven days after a stroke has been correlated with a poor outcome {Reith, Jorgensen, et al. 1996; Ginsberg 1998}. Experimental paradigms investigating the relationship between body or brain temperature and the magnitude of neuronal cell death have also reported beneficial effects of hypothermia {Ginsberg 1998}. Reduction of brain temperature to 33° C (*vs* 36° C) for 2 h reduces the infarct volume induced by permanent or reversible focal cerebral ischaemia in the rat {Morikawa, Ginsberg, et al. 1992; Karibe, Chen, et al. 1994}. Neuroprotective effects of hypothermia have also been observed in experimental paradigms of head injury and global cerebral ischaemia in the rat {Busto, Dietrich, et al. 1987; Clifton, Jiang, et al. 1991}. Conversely, increasing body or brain temperature after induction of cerebral ischaemia (focal or global) increases neuronal damage, further suggesting that the progression of neuronal injury may be influenced by temperature {Busto, Dietrich, et al. 1987; Ginsberg 1998}.

The role of IL-1 as an endogenous pyrogen is well established. Intravenous, intrastriatal, or icv injections of IL-1 all induce fever {Kluger, Kozak, et al. 1995; Rothwell & Luheshi 2000}. Thus the effects of IL-1 in exacerbating brain injury may depend on its pyrogenic actions. However, studies of ischaemic brain damage in the rat have not shown any significant difference in core body temperature following the injection of intracortical or intrastriatal IL-1, noting only an accelerated return to basal temperature from hyperthermia during recovery from anaesthesia after surgery {Stroemer & Rothwell 1998; Loddick & Rothwell 1996a}. Similarly, no change has been observed in

the core body temperature in response to injection of IL-1ra into the striatum, cortex or icv in rats exposed to cerebral ischaemia {Loddick & Rothwell 1996a}. Intrastriatal or icv injection of IL-1 administered with intrastriatal S-AMPA does conversely, result in a significant increase in body temperature (compared to striatal injection of S-AMPA alone) {Grundy, Rothwell, et al. 1999}. However, although IL-1 causes an increase in body temperature when injected icv with intrastriatal S-AMPA, it causes only a modest increase in cortical injury. This implies that the effects of IL-1 on AMPA receptor mediated cell damage in the striatum can be dissociated from its pryogenic effect. {Grundy, Rothwell, et al. 1999}. These data together suggest that the impact of IL-1 in acute neurodegeneration is independent of its effects on temperature. However, all these studies report core (peritoneal or rectal) body temperature, which is poorly reflective of brain temperature {Busto, Dietrich, et al. 1987}. The effects of IL-1 on brain temperature and its relation to the cell death in experimental brain injury have not been reported.

1.10.3 Effect of IL-1 on cerebral blood flow and oedema

Cerebral blood flow (CBF) plays a critical role in brain injury regardless of aetiology. Whilst its contribution to stroke is obvious, it is less well known that up to 90% of people dying following severe head injury have evidence of ischaemic damage and up to a third of patients suffering a subarachnoid haemorrhage have evidence of vasospasm {Kassel, Sasaki, et al. 1985}.

Current evidence to suggest that IL-1 influences CBF is limited. Increased expression of IL-1 mRNA has been reported in cerebrovascular endothelial cells {Zhang, Chopp, et al. 1998}. IL-1RI is expressed constitutively by the cerebral microvasculature and perivascular glia, and IL-1 has a dose-dependent dilatory effect on porcine pial vessels

{Shibata, Parfenova, et al. 1996}. Intrastriatal injection of IL-1 is also increases cerebral blood flow in juvenile rodents {Blamire, Anthony, et al. 2000}. However, IL-1 may also have vasoconstrictor effects, as it can cause increased in endothelin (a potent vasoconstrictor) expression in brain microvessel endothelium {Katabami, Shimizu, et al. 1992}. Further, IL-1 has also been shown to reduce pial vessel blood flow in rats after transient MCAO {Fabian, Perez-Polo, et al. 2000}.

Administration of IL-1 (icv) increases, and IL-1β antibody decreases brain water content (oedema) by 3-5% in rats in response to MCAO {Yamasaki, Matsuura, et al. 1995}. Intraparenchymal injection of IL-1 in adult rats results in extravasation of albumin (indicating BBB breakdown) and increase in brain water content {Holmin & Mathiesen 2000}. IL-1 also induces BBB breakdown and therefore the development of vasogenic oedema in juvenile rodents {Blamire, Anthony, et al. 2000}. Removal of neutrophils prior to IL-1 administration prevents BBB breakdown in juvenile rodents suggesting that this process is dependent on neutrophils {Anthony, Bolton, et al. 1997}. I*n vitro* data also suggests that IL-1 increases the permeability of brain derived endothelial monolayers {de Vries, Blom-Roosemalen, et al. 1996}. Further, persistent changes in the apparent diffusion coefficient in rats after intrastriatal injection of IL-1 suggests that IL-1 may also induce cytotoxic oedema (cell swelling) {Blamire, Anthony, et al. 2000} . However, the temporal relationship between IL-1 induction, development of cell death, and BBB breakdown or blood flow has yet to be determined.

1.10.4 Effect of IL-1 on seizures

1.10.4.1 Epilepsy

Seizures are the motor, or electrophysiological expression of the process of epilepsy. Epilepsy is a common condition, which affects about 1% of the population. It comprises

a diverse group of disorders that result from an abnormal electrical discharge from a large group of neurones {Shin & McNamara 1994}. Seizures may be classified into focal (or partial) when they are localized, or into generalized types if they show widespread involvement of both hemispheres from the outset (primary generalization) {Shin & McNamara 1994}. Examples of generalized seizures are absence seizures (characterized clinically by vacant episodes, or 'drop attacks' etc), myoclonic (seizures characterized with repetitive flexor spasms), or tonic-clonic (seizures characterized by alternating flexor and extensor spasms (grand-mal)) seizures. Seizures may also be further categorized into 'simple', or if associated with loss of consciousness, 'complex' subtypes. In addition, partial seizures may progress to generalized seizures (secondary generalization), and prolonged seizure episodes are termed status epilepticus {Shin & McNamara 1994}.

Complex partial seizures (temporal lobe epilepsy) are considered to be the most common and severe form of adult epilepsy. This has been modeled *in vivo*, and is termed 'limbic epilepsy'. It is characterized by the progressive development of seizures which evolve through the following five stages: 1) immobility, facial clonus, eye twitching, 2) head nodding, and severe facial clonus, 3) unilateral forelimb clonus, 4) rearing often associated with bilateral forelimb clonus, and 5) rearing and falling. This behaviour pattern is observed in response to kainic acid, or electrical and chemical kindling {Ben Ari 1985; Sperk 1994; Loscher 1998}.

Cell death is a key feature of 'limbic seizures' {Ben Ari 1985; Sperk 1994; Loscher 1998}. It is observed in prominent limbic (hippocampus, amygdala, bed nucleus of the stria terminalis), and allocortical (piriform, entorhinal cortex) regions {Sperk 1994}. High metabolic and electrical activity is seen in these regions that subsequently die, and

cell death {Ben Ari 1985} is reduced by anticonvulsants suggesting that cell death results from seizure activity {Ben Ari 1985}. Metabolic data also suggest that cell death induced by seizures is related to the intensity of seizures {Ben Ari 1985}.

1.10.4.2 IL-1 and seizures

Autoptic brains of patients with temporal lobe epilepsy show increased IL-1 immunoreactivity {Sheng, Boop, et al. 1994}, while increased IL-1 protein and mRNA expression are also evident in rodents with self-sustained status epilepticus {Vezzani, Conti, et al. 1999}. Furthermore, intracerebral injection of IL-1 increases fit frequency and duration in kainate-induced and audiogenic seizures in rats {Vezzani, Conti, et al. 1999} whilst icv injection of IL-1ra in rodents significantly reduces seizure frequency {de Simoni, Perego, et al. 2000}. The onset of seizures is delayed in IL-1R1 knockout mice, compared to their wild type counterparts, in which seizures induced by bicuculline are inhibited by intrahippocampal injection of IL-1ra {Vezzani, Moneta, et al. 2000}. IL-1 may therefore increase cell death by increasing duration of seizure activity.

1.11 Aims

The aims of this thesis were to investigate the mechanism by which IL-1 exacerbates neuronal death *in vivo*. Striatal injection of S-AMPA with IL-1 results in 'distant' cortical cell death in addition to the 'local' striatal cell death seen in response to striatal injection of S-AMPA alone. Cortical cell death is thought to be IL-1 specific, and therefore, studying cortical cell death in this paradigm allows for the investigation of the effects of IL-1 on cell death *in vivo*.

The immediate aim of this thesis was to reproduce cortical cell death induced by striatal injection of IL-1 with S-AMPA. After validating this model of brain injury, the aim was to test the hypothesis that IL-1 acts through specific sites to induce cortical cell death. Identification of putative sites of IL-1 action was undertaken by studying the temporo-spatial pattern of immunoreactive IL-1 expression in response to intrastriatal injection of S-AMPA *vs* IL-1 with S-AMPA.

Results obtained during the course of this thesis suggested that in this experimental paradigm, IL-1 exacerbated cell death by increasing S-AMPA induced seizure activity. Seizures in response to S-AMPA or S-AMPA with IL-1 were therefore characterised, and the effect of the anticonvulsant on seizures and cell death was investigated to test the hypothesis that IL-1 increases excitotoxin induced cell death by exacerbating seizures.

Chapter 2: Methods

2.1 Animals

Male, Sprague-Dawley rats (Charles River, UK) weighing 250-350 grams were used for all experiments. All animals were maintained under a 12-hour light–dark cycle in a temperature (21-23°C) and humidity (60%± 5) constant environment. All experiments were conducted in accordance with the UK Animals (scientific procedures) Act, 1986.

2.2 Materials

All materials were obtained from Sigma, UK unless stated otherwise.

2.2.1 α-amino-3-hydroxy-5-methyl-4-isoxazolepropionic acid (S-AMPA)

S-AMPA (Tocris Cookson, UK) was dissolved in phosphate buffered saline (PBS) to concentrations of 20 mM and 15 mM and then aliquoted and frozen at -70°C. Striatal injections were performed using 500nl of the 20 mM (10nmol injected) or 15mM (7.5nmol injected) solution of S-AMPA.

2.2.2 Interleukin–1β (IL-1β)

Human recombinant IL-1β (referred to as IL-1 in this thesis) was obtained from two separate sources (E.I. Dupont de Nemours and Co, USA and NIBSC, UK). Both were of a similar specific activity (1.3-2.5 × 10^8 IU/mg, E.I. Dupont de Nemours and Co, USA, and 1.5-2.8 × 10^8 IU/mg, NIBSC, UK). IL-1 obtained from Dupont was dissolved in a sterile 0.1% bovine serum albumin (BSA), 0.9% saline solution, whilst IL-1 acquired though NIBSC was dissolved in sterile 0.5% bovine serum albumin (BSA), 0.9% saline solution. Both solutions were stored at -70°C, and all experiments were performed using 500nl of a 20ng/μl solution (10ng injected). NIBSC IL-1 was only used in the EEG

experiments (see chapter 6). A volume of 500nl of sterile 0.1% (or 0.5%) BSA, 0.9% saline solution was injected as vehicle.

2.2.3 Diazepam

The anticonvulsant Diazepam was dissolved in a mixture of 0.9% saline, propylene glycol, and ethanol (3:3:4) (vehicle) and used at a concentration of 1mg/μl. Diazepam (5mg/kg i.p.), or the equivalent volume of vehicle, was administered 30 min before striatal injections, and then hourly for a further 5 h. In all experiments, the intracranial injection volume was 1 μl and the total intraperitoneal treatment volume did not exceed 1 ml.

2.3 Surgical Procedures

2.3.1 Striatal injections.

All animals were anaesthetised in an anaesthetic flow chamber filled with 2.5% halothane (Fluothane, Zeneca, UK). After induction of anaesthesia, (loss of withdrawal reflexes) animals were placed in a stereotactic frame (Stoetling Co, USA) and anaesthesia was maintained using a mixture of nitrous oxide (1.2 L/min) and 2% halothane. Oxygen was supplied at a rate of 800ml/min. The skull was exposed through a midline scalp incision and a hole, 0.7 mm anterior to and 2.7 mm lateral to bregma, was drilled {Paxinos & Watson 1986}. At this point, a 26-gauge needle attached to a 1μl Hamilton syringe (World Precision Instruments, USA), was lowered to a point 5.5mm below the skull surface and striatal infusions performed. These were done using the Micro-4 infusion pump (World Precision Instruments, USA) at a rate of 200nl/min. The injection needle was removed 5 min after completion of infusion and the scalp wound sutured (4.0 mersilk suture, Ethicon, Johnson and Johnson International, UK).

Animals were subsequently removed from the frame and allowed to recover in a heated recovery cage.

2.3.2 Implantation of EEG leads and abdominal transmitters.

Prior to implantation, a small amount of the silastic sheath over the EEG leads was trimmed, and the electrode was pulled into a loop. Some low temperature heat shrink wrap (length of about 4mm) was then pulled over the loop and heated briefly. Nail polish was used to seal the join between the heat shrink and silastic.

Animals were then anaesthetised as described in the section above, and the scalp and an area of the abdomen were shaved. The animals were fixed in the stereotactic frame and rotated so that the abdomen laid upper most. After preparation of skin with iodine (Betadine, Seton Healthcare Group plc, UK) a small abdominal incision was made. The incision was deepened, and the peritoneal cavity was entered. The abdominal radiotransmitter end of the EEG probe was placed into the abdominal cavity. A linear midline cranial incision was then made, and a hollow trocar (Data Sciences, UK) tunnelled from the abdominal to the cranial wounds subcutaneously. The EEG leads were passed though the trocar from the abdominal end and brought out through the cranial incision. The abdominal incision was closed in layers with 4.0 silk sutures. Two burrholes were drilled, 3 mm posterior to and 3 mm lateral to bregma, and in the midline 3mm posterior to Lambda overlying the cerebellum. Stainless steel screws (4mm long × 2mm diameter) were passed through loops in the EEG leads, and screwed into the burr holes drilled earlier, taking care not to pierce the underlying meninges. The white lead was always placed over the cerebellum (reference electrode) whilst the red lead was placed over the neocortex (recording electrode). The EEG leads and screws were secured with dental cement (Simplex rapid, Associated Dental products Ltd, UK).

It was ensured that bregma was clearly identifiable, and that dental cement did not extend to the coronal suture. The wound was sutured with silk, and the animals were allowed to recover on a heating blanket before being returned to their cage. Implanted animals were used one week after initial surgery.

2.4 Experimental procedures

2.4.1 Assessment of cell death.

Cell death was assessed 24 h or 48 h after striatal injections. Animals were killed by exposure to a rising concentration of carbon dioxide (CO_2) followed by cervical dislocation. The brain was rapidly removed, frozen, by immersion in isopentane (-35°C) or by standing on dry ice (-70°C) and then stored at -20°C until sectioned on a cryostat.

2.4.1.1 Tissue preparation

2.4.1.1.1 Cryostat sections

Frozen brains were placed on a cryostat chuck and covered in embedding medium, (O.T.C, Tissue-Tek, Raymond Lamb, UK). The chuck was housed in the cryostat (Bright Instruments Co, UK), and the chamber temperature was set at -20°C. The mounted brain was sectioned (20μm) in the coronal plane every 500μm throughout the damaged area, sections being mounted onto 3-aminopropylmethoxysilane (APES) coated microscope slides (Chance Propper Ltd, UK). Two sets of sections were taken at each level for each brain.

2.4.1.1.2 Cresyl violet staining

Mounted brain sections were fixed in 95% methylated spirits (IMS, Genta Medical, UK) for 2 min. The slides were rinsed in water and then immersed in a 1% cresyl violet

solution for 5 min. Excess cresyl violet was removed by washing in water, and the slides were then dehydrated by passing sequentially through an increasing concentration of IMS (5 washes in 95%, 99% and 99% IMS) and xylene (×3) prior to being cover slipped (Chance Propper Ltd, UK).

2.4.1.1.3 Fluoro-jade staining.

Fluoro-jade was obtained from Histo-Chem Inc., USA. A 0.01% solution was prepared in distilled water, and diluted to a 0.001% working solution (in 0.1% acetic acid in distilled water).

Cryostat sectioned mounted brain sections were placed in a slide rack, and transferred to a 100% ethyl alcohol solution for 3 min. Sections were then placed in distilled water (3 min) prior to being transferred to the 0.001% fluoro-jade solution for 30 min. Sections were then rinsed 3 times in distilled water for a minute each. Slides were then air-dried, passed through xyelene, and cover with cover slips as above. Sections were then examined using a microscope with a filter system suitable for visualising fluorecin.

Perfuse fixed tissue sections were mounted onto gelatin coated slides, and oven dried overnight (37°C). Sections were placed directly into the 0.001% fluoro-jade solution for 30 min. After washing (×3) in distilled water, sections were air-dried and cover slips were applied prior to examination.

2.4.1.2 Quantification of lesion size.

The lesion area was analysed using image analysis software (Northern Eclipse, Canada). The total lesion volume was calculated by summing the lesion areas (mm^3) measured for each brain and then multiplying by the interval thickness between sections. Each

brain was corrected for oedema by calculating the percentage increase in the volume of the ipsilateral compared to contralateral hemispheres and adjusting the measured volume accordingly.

2.4.2 Immunohistochemistry

2.4.2.1 Tissue preparation

2.4.1.1.1 Perfusion-fixation

At the chosen time point after striatal injections, rats were terminally anaesthetised with sodium pentobarbitone (Sagatal; Rhone Merieux, UK (intraperitoneal dose of 1mg/kg)). Once anaesthetised, a midline incision was made below the xiphoid and the peritoneal cavity exposed. The rib cage was lifted, and the exposed diaphragm was incised at its junction with the anterior abdominal wall. The incision was continued circumferentially until adequate exposure of the pleural cavity was achieved. Whilst holding the xiphiod process, a deep cut was made on both sides of the rib cage and the anterior section of the ribcage lifted upwards so as to allow access to the mediastinum. The descending aorta was clamped and the rat perfused transcardially via the left ventricle. The inferior vena cava was then cut and the animal exsanguinated. The rat was perfused with cold (4° C) 0.9% saline for 8 min (flow rate of 25 ml/min) followed by a cold (4° C) 4% paraformaldehyde (PFA) in 0.1M phosphate buffered saline solution (PBS) for 15 min at the same flow rate.

The brains were removed from the skull, placed in a 4% paraformaldehyde solution and kept overnight at 4°C. They were then washed three times in PBS and transferred to a 30% sucrose solution. The brains were removed after approximately 48 h, frozen on dry ice and stored at -20° C until they were sectioned.

2.4.2.1.2 Preparation of brain sections

Serial coronal sections (30μm) were cut on a cryostat (Bright Instrument Co.UK) for all perfuse-fixed brains (from plates 17-33) {Paxinos & Watson 1986} and transferred to a twelve-well plate containing phosphate buffered saline (PBS). Alternate sections were transferred to a separate plate. All sections were stored at 4°C until use.

2.4.2.2 Standard immunohistochemical techniques.

All immunohistochemistry was performed on free floating brain sections as prepared by methods described above. All solutions were prepared in 0.1M phosphate buffer (PB) unless stated otherwise, and all washes were performed three times.

Primary antibody	**Source**	**Dilution used**
Sheep anti rat IL-1β	NIBSC, UK	1:1000
Rabbit anti fos	Calbiochem, UK	1:1000
Mouse anti rat CD11b (MRC OX-42)	Serotec, UK	1:200
Secondary antibody	**Source**	**Dilution used**
Biotinylated donkey anti sheep	Sigma, UK	1:500
Goat anti rabbit IgG peroxidase complex	Vector, USA	1:500
FITC labelled donkey anti mouse	Vector, USA	1:200

Table 21: Antibodies used for immunohistochemistry experiments.

2.4.2.2.1 IL-1 immunohistochemistry

After incubation with hydrogen peroxide (H_2O_2) ((200μl H_2O_2 (obtained as 30% solution) in 10 ml of 0.1M PB) to quench any endogenous peroxidase activity, the

sections were washed and then immersed in blocking buffer (5% donkey serum (DS)) for 45-60 mins. After washing, sections were incubated for 48 h at 4°C in sheep anti- rat IL-1β antibody diluted 1:1000 in 0.3% Triton X (Tx), 1% DS, PB solution. After 48 h, the sections were washed, and then incubated for two hours at room temperature with the secondary antibody. The sections were washed again prior to incubation with the biotinylated horseradish peroxidase H and avidin complex (Vectastain ABC kit, Vector Labs, USA) for one hour before the signal was visualised by incubation with Diaminobenzene tetrahydrochloride (DAB) solution (0.25 mg/ml DAB, 1% H_2O_2 in PB). This reaction was followed under the microscope and terminated by rinsing in PB, following formation of a brown precipitate. Sections were subsequently mounted onto gelatin coated slides, and air-dried over night. The mounted sections were passed through xylene, covered with glass cover slips and stored at room temperature. All sections were viewed using a light microscope (Leitz Labor Lux, Leica, Germany). The observed spatial expression of IL-1 was transcribed onto pre-prepared brain maps in a blinded fashion.

2.4.2.2.2 c-fos immunohistochemistry

Perfuse-fixed brain sections (30μm) were incubated for 20-30 mins in a 20% methanol 0.2% Tx, and 1.5% H_2O_2 solution of PB. Sections were washed, incubated with blocking serum (1% normal Goat serum (NGS)) for 1 h, before being incubated overnight (4°C) with rabbit anti-fos antibody. After 24 h sections were washed, and incubated (two hours at room temperature) with a goat anti-rabbit IgG peroxidase complex. After three washes sections were washed (× 1) in a 0.1 M acetate buffer solution, and signal was visualised by incubating in a Nickel-DAB solution. This reaction was followed under the microscope and terminated by rinsing in PB, following formation of a black precipitate. Upon development of required signal, sections were

washed in 0.1M acetate buffer, and then in 0.1M PB . Sections were subsequently mounted onto gelatin coated slides, and air-dried over night. The mounted sections were passed through xylene, covered with glass cover slips, and stored at room temperature. All sections were viewed at using a light microscope (Leitz Labor Lux, Leica, Germany). The observed spatial distribution of c-fos was transcribed onto pre-prepared brain maps in a blinded fashion and then tabulated.

2.4.2.2.3 Double-labelling immunohistochemistry

Double immunohistochemistry was performed on sections in which immunoreactive IL-1 had been previously observed. Brain sections were incubated in 5% DS for 45 min prior to being incubated with sheep anti-rat IL-1β for 48 h (4° C). After three washes, sections were incubated with biotinylated donkey anti sheep antibody and signal was developed by incubation in a Texas-Red labelled avidin (Vector Labs, USA) for 2 h (diluted 2.6μl/ml). All sections from this point were protected from the light. After washing, sections were incubated with a 1: 200 dilution of mouse anti-rat (no Tx added) CD11b (microglial cell marker) for three days (4°C). Sections were subsequently washed and then incubated with fluoroscein isothiocynate (FITC) labelled donkey anti mouse antibody for 2 h at room temperature. After further washes, sections were loaded onto gelatin coated slides, air dried, mounted (Vectashield, Vector Labs, USA) and cover slips were applied. Sections were examined using a fluorescence microscope (Leitz DMR, Germany).

2.4.2.3 Immunohistochemistry controls

Specificity of anti-sera was assessed by omission of primary or secondary antibody, or by preadsorbtion of primary antibody with recombinant rat IL-1β. For preadsorbtion, equal volumes of recombinant rat IL-1β (1nmol, 10nmol, 100nmol) and primary

antibody (1:500 dilution in TBS) were incubated at 4°C for 24 h. These were centrifuged (15 min, 1000g at 4°C), and the supernatant substituted for primary antibody on brain sections taken at 16 h after injection of S-AMPA and IL-1. All other steps were followed as documented in the procedure for immunohistochemistry (**section 2.2.3.3**). Specificity of sheep anti-IL-1β had already been determined, and therefore controls concentrated for double immunoflourescence experiments concentrated on demonstrating that no cross reactivity occurred between antibodies. Accordingly, both the mouse anti-rat antibody, and its secondary label (donkey anti-mouse antibody) were omitted.

2.4.2.3 Photography

Photomicrographs were taken with digital cameras mounted on the light (colour KY-F55B Camera JVC, Japan.) and fluorescence microscopes (black and white, Hamamatsu digital camera, Japan.). Captured images were formatted using Photoshop (Adobe Photoshop 5.5, Adobe USA).

2.4.3 Seizure assessment

2.4.3.1 Behavioural assessment of seizures

After surgery, all animals were allowed to fully recover consciousness, housed individually, and filmed to record the motor expression of seizures using tripod mounted camcorders (Sony Corporation, UK) connected to cassette video recorders (Samsung Electronics, UK). Recording of the motor expression of seizures began after complete recovery of the experimental animal from the effects of surgery, and was continued for a minimum period of 8 h after striatal injection. Seizures observed in response to striatal injection of S-AMPA alone or S-AMPA with IL-1 resembled those

defined by Racine {Racine 1972} and therefore this classification was used in the present study in order to assess the motor expression of seizures {Lawrence, Allan, et al. 1998}. However, only pawing (grade 3), rearing (grade 4), or rearing and falling (grade 5) episodes were recorded as these were considered to be the only unambiguous evidence of seizure activity. Frequency, duration, intensity (grade of seizure activity observed), and temporal progression of seizure activity were recorded and analysed. For any continuous fit that comprised a mixture of seizure intensities, the seizure intensity assigned was the most intense seizure observed during that episode.

2.4.3.2 EEG recording

EEG signal was acquired using the TA11CTA-F40 (Data Sciences, USA) radiotransmitter. The signal from these transmitters is transmitted by radio frequency, which was captured through a receiver pad underneath the cage of each animal (Data Sciences, USA). This information was relayed to a computer that sampled and recorded the analogue output (Dataquest A.R.T analogue (Data Sciences, USA). Analogue data were then sent via an output matrix (Data Sciences, USA) through a data acquisition unit (CED 1401, Cambridge Electronic Design, UK). The EEG Signal was visualised and analysed using the Spike 2 software (Cambridge Electronic design, UK).

All animals were allowed to acclimatise to individual housing for 24 h. The EEG signal was recorded for 8 h during the day, and for 8 h during the night (peak activity) in all rodents. EEG was then measured continuously after striatal injections of S-AMPA or S-AMPA with IL-1. Pre-injection recordings served as controls, and all animals were simultaneously filmed for 8 h after surgery.

2.5 Data analysis

No animals were excluded from analysis. Normality tests were performed on all data prior to further statistical analysis.

2.5.1 Lesion volume and sites of cell death.

All lesion volumes were expressed as mean ± standard error of the mean (sem). The number of sites in which neuronal damage was observed was also expressed as mean ± sem. Differences between two groups was determined by an unpaired t test whilst differences between more than two groups was determined by analysis of variance (ANOVA), followed by the appropriate multiple comparison post–hoc test.

2.5.2 Immunohistochemistry analysis.

The pattern of immunoreactivity (or neuronal damage) was transcribed onto corresponding pre -prepared brain maps. For IL-1β immunohistochemistry, the number of immunoreactive cells was counted in a number of regions- stritatum, parietal cortex and frontal cortex (neocortex), the nucleus reuniens (NR), and dorsomedial thalamus (DMT). Regions were chosen on the basis of the frequency of occurrence of immunoreactivity, and upon ease of unequivocal identification of the region. For the striatum, NR, and DMT, an average count was taken by counting two sections per animal. For the neocortex, four sections were counted per animal. Cells were expressed as number of cells counted per field and each field corresponded to an area of $0.12mm^2$.

The region of interest for c-fos immunohistochemistry was limited to the neocortex, and more specifically the parietal cortex. A grid was placed over the parietal cortex on four separate sections per brain, and the number of cells seen to express c-fos were counted at high magnification (× 40) using a light microscope (Leitz Labor Lux, Leica,

Germany). Sections and site of placement was kept consistent between brains. Data were expressed as mean ± sem, and differences determined by ANOVA, followed by the appropriate multiple comparison post-test. Differences between two groups were determined by an unpaired students t test.

Data on the number of sites of IL-1β immunoreactivity (or degenerating neurones) was expressed as a percentage of animals in which IL-1β immunoreactivity (or degenerating) was observed per site per time point per treatment.

2.5.3 Seizure analysis

2.5.3.1 Behavioural analysis

All data are presented as mean ± sem for the number of animals given. Significant differences between treatment groups were determined by analysis of variance (ANOVA) followed by the Tukey's multi-comparison post-test. Differences between groups in relation to time were analysed using a multiple analysis of variance (MANOVA). Significant differences identified between treatments at different time points were further analysed by ANOVA followed by the Scheffe post-test. The Spearman correlation coefficient was calculated to determine correlation between seizures and cell death.

Chapter 3: Validation and characterisation of cell death induced by intrastriatal injection of S-AMPA ± IL-1

3.1 Introduction

In order to study the mechanism of action of IL-1 in acute neurodegeneration, a paradigm in which the end point is specific to IL-1 is ideal. Striatal injection of S-AMPA with IL-1 results in 'distant' cortical cell death in addition to the 'local' striatal cell death seen in response to S-AMPA alone. The ipsilateral cortical cell death observed, occurs only in response to co-infusion of S-AMPA with IL-1, and is not observed in response to striatal injection of S-AMPA alone {Lawrence, Allan, et al. 1998; Grundy 2000}. Furthermore, cortical cell death does not result upon intrastriatal co-infusion of other pro-inflammatory cytokines (IL-6, TNFα) with S-AMPA {Allan 2002}. These data suggest that the cortical cell death seen is IL-1 dependent, and that this paradigm, with cortical cell death as the end point, may be useful to investigate the mechanism by which IL-1 exacerbates cell death.

Cell death in this paradigm is however variable, with cortical cell death being observed in 60-80% of rats injected with S-AMPA with IL-1. Furthermore, in order to produce consistent cortical cell death, the S-AMPA concentration injected with IL-1 has needed to be varied. Therefore, the initial aim was to achieve consistent and reproducible cortical cell death in response to striatal co-infusion of S-AMPA with IL-1.

3.2 Experiment. Volume of cell death induced by striatal injection of S-AMPA vs S-AMPA with IL-1

3.2.1 Methods

Striatal injections were performed as described in **section 2.3.1.** Two doses of S-AMPA (7.5nmol or 10nmol) were used, and the dose of IL-1 was kept constant (10ng). Rats were killed 24 h or 48 h after striatal injections, and brains removed and frozen for assessment of neuronal damage **(section 2.4.1.1)**. Striatal injection of S-AMPA resulted in ipsilateral striatal cell death. As previously noted, death was also seen in the caudally adjacent thalamic region. As both striatal and thalamic damage were quantified, this is referred to as subcortical death.

3.2.2 Results

3.2.2.1 Lesion volume induced by striatal injection of S-AMPA ± IL-1 (48 h)

Striatal injection of S-AMPA resulted predominantly in subcortical cell death although cell death was also observed in the piriform or entorhinal cortex (allocortical regions) (Figure 3.1A).

Co-infusion of S-AMPA (10 nmol) with IL-1 resulted in a significant increase in subcortical (2-fold, $p<0.05$) and fronto-parietal cortical cell death (16-fold, $p<0.01$) (Figure 3.1B, 3.2). Cortical cell death was observed as an 'all or none phenomenon', and was seen in 63% (5/8) of rats injected with S-AMPA (10nmol) and IL-1. Fronto-parietal cortical cell was not observed in response to striatal injection of S-AMPA alone.

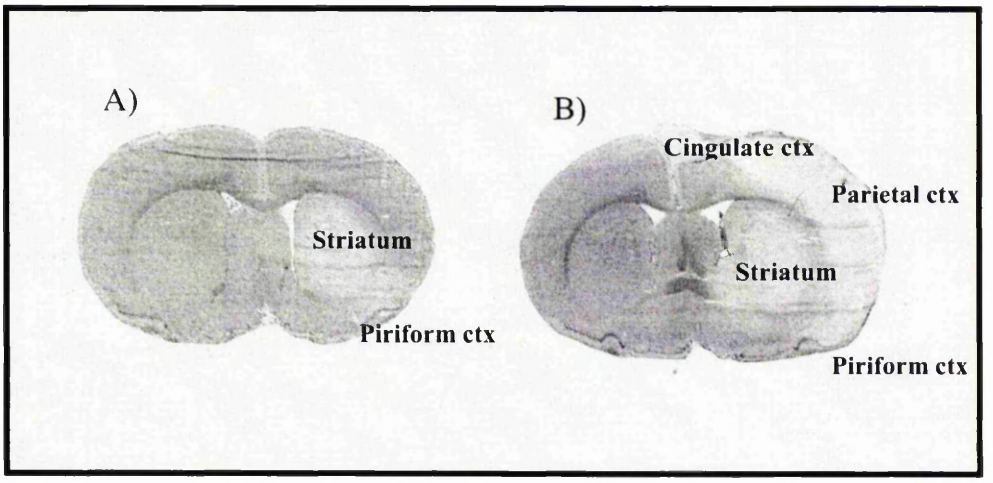

Figure 3.1: A) Representative coronal brain section at a single level (-1.00 mm from bregma) demonstrating differences in cell death induced by S-AMPA *vs* S-AMPA with IL-1. Ctx- Cortex.

Fronto-parietal cortical cell death (154 ± 29.09 mm^3) was also seen (in 71% (5/7)) in response to co-infusion of IL-1 (10ng) with a lower dose of S-AMPA (7.5nmol). No significant difference in the nature of the lesion (see Figure 3.3) or lesion volume (total lesion volume 206± 33.48; cortical lesion volume 154± 29.09; subcortical lesion volume 52.21± 8.09) was noted between rats that were injected with S-AMPA (7.5 nmol) or S-AMPA (10nmol) with IL-1 (10ng).

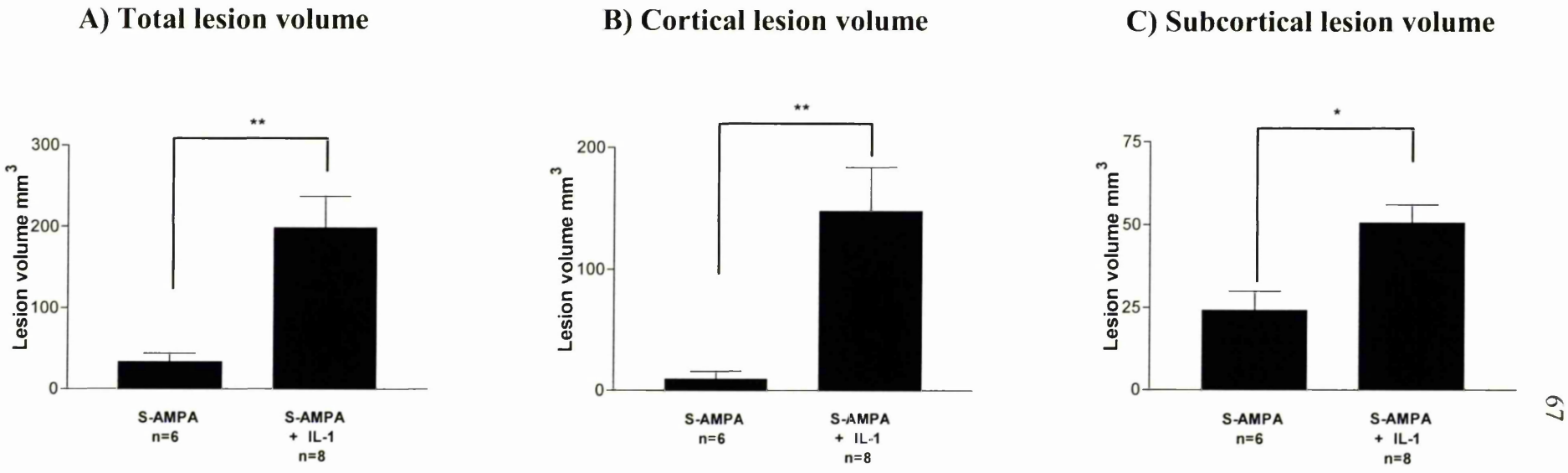

Figure 3.2: Total (A), cortical (B), and subcortical (C) lesion volumes induced 48 h after striatal injections of S-AMPA (10nmol) or S-AMPA (10nmol) with IL-1 (10ng). n= number of animals in each group. Data are expressed as mean ± SEM. **P<0.01, *P<0.05

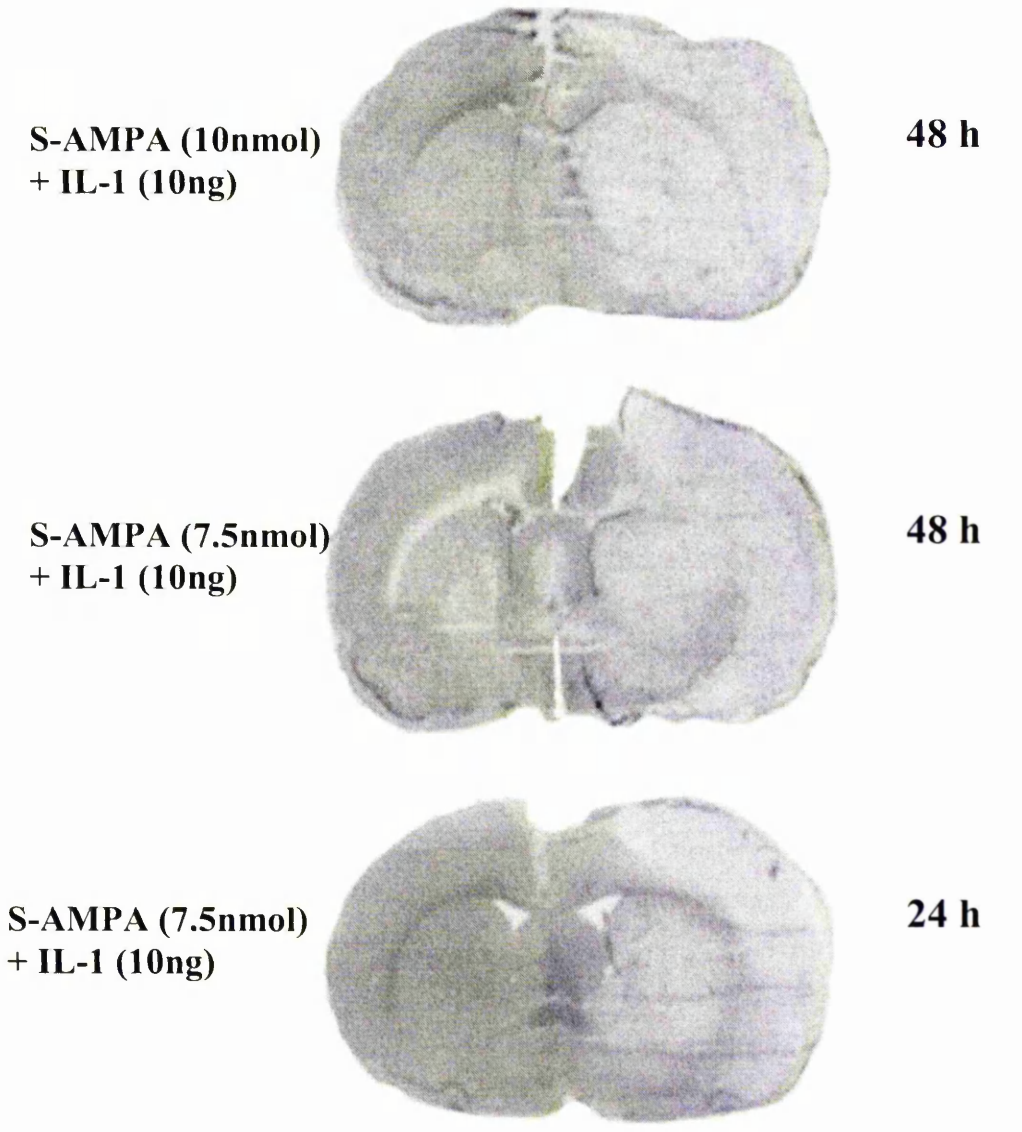

Figure 3.3: Coronal brain sections at a single level (-1.00 mm from bregma) taken 24 h and 48 h after striatal injection of S-AMPA (7.5 or 10 nmol) with IL-1 (10ng) showing similar pattern of cell death between treatments. Pale areas of staining represent regions of death.

3.2.2.1 Lesion volume induced by striatal injection of S-AMPA ± IL-1 (24 h)

Striatal injection of S-AMPA (7.5nmol) alone again resulted predominantly in subcortical cell death. Co-infusion of S-AMPA with IL-1 resulted in a 2.9-fold increase in the total lesion volume compared to S-AMPA alone (Figure 3.4). The increase in cell death volume induced by S-AMPA with IL-1, again resulted predominantly from a 8-fold increase in cortical cell death. However, co-infusion of S-AMPA with IL-1 (*vs* S-AMPA alone) also resulted in a significant increase in subcortical cell death (1.4-fold) (Figure 3.4). The percentage of rats that exhibited cortical cell death was similar between rodents sacrificed at 24 or 48 h (67% *vs* 71%) after striatal injections of S-AMPA with IL-1.

Although the lesion volume was observed to be greater in animals killed at 24 h compared to 48 h after striatal injection of S-AMPA (7.5nmol) with IL-1 the pattern of injury was similar (Figure 3.3). However, experiments were not performed to allow direct comparison of lesion volumes in animals sacrificed 24 h or 48 h after striatal injection of S-AMPA (7.5 nmol) with IL-1.

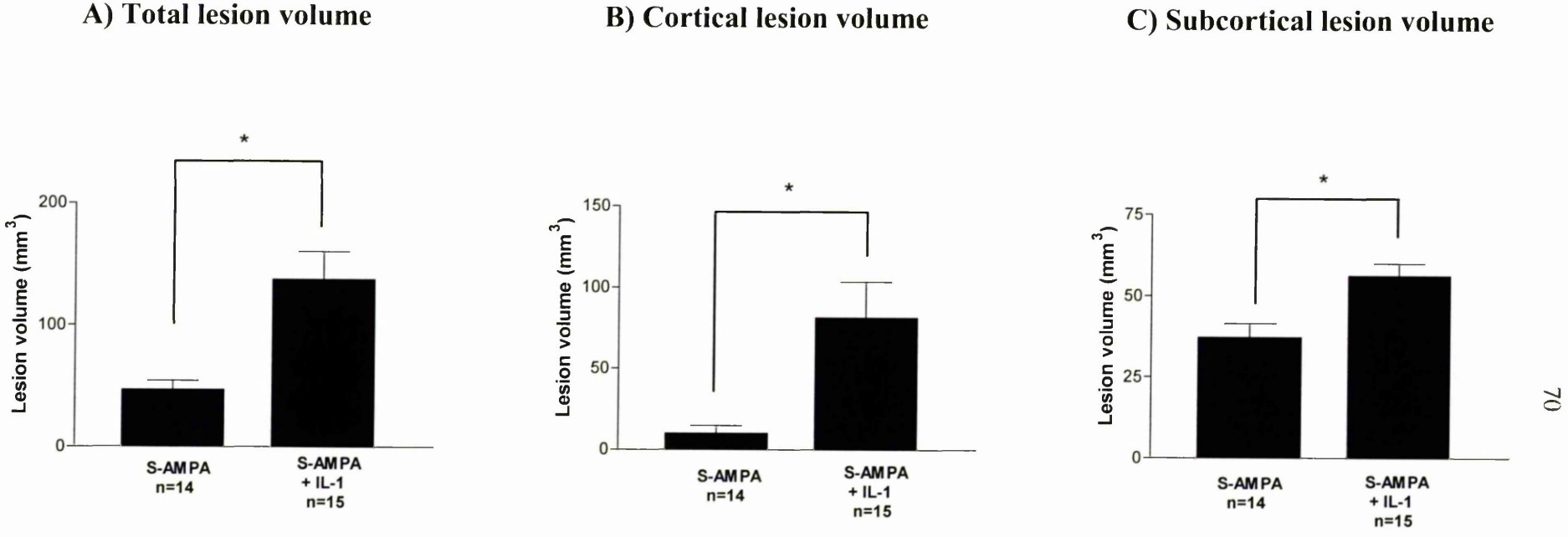

Figure 3.4: Total (A), cortical (B), and subcortical (C) lesion volumes induced 24 h after striatal injections of S-AMPA (7.5nmol) or S-AMPA (7.5nmol) with IL-1 (10ng). n= number of animals in each group. Data are expressed as mean ± SEM. *P<0.01

3.3 Experiment. Sites of neuronal degeneration in response to striatal injection of S-AMPA ± IL-1

Lawrence et al (1998) reported that striatal co-infusion of S-AMPA with IL-1, and to a lesser extent striatal injection of S-AMPA alone results in thalamic damage in addition to cell death at the site of injection in the striatum. This has not been fully documented, as detailed histological analysis was not performed on the cresyl violet or tetrazolium chloride stained brain sections used to delineate cell death. Regions of pale staining (denoting cell death) on cresyl violet stained brain sections have been seen in the nucleus reuniens (NR) and dorso-medial thalamus (DMT) in response to intrastriatal injection of S-AMPA with IL-1 in the rat (Allan, unpublished). Further, 'distant' cell death has been noted in subcortical regions (including the NR and DMT) in response to intrahippocampal injection of S-AMPA in the rat {Lees & Leong 2001}. These data suggested that 'distant' regions of neuronal death induced by intrastriatal injection of S-AMPA compared to S-AMPA with IL-1 still required documenting.

Fluoro-jade is an anionic fluoro-chrome that has recently been shown to be a more sensitive and definitive marker of neuronal degeneration than nissel type stains such as cresyl violet {Schmued, Albertson, et al. 1997}. Although the mechanism by which it labels degenerating cells is not known, it has been shown to be a reliable, sensitive, and easy to use, method for determining degenerating neurones.

Therefore, in order to further delineate neuronal damage in extrastriatal regions, fluoro-jade staining of brain sections was undertaken.

3.3.1 Methods

Additional brain sections (adjacent to those used for cresyl violet staining to determine lesion volume) were taken from the brains' of animals sacrificed 24 h after injection with S-AMPA (7.5 nmol) or S-AMPA (7.5 nmol) with IL-1 (10ng). Sections were processed and stained as outlined in **section 2.4.1.1.3**. The frequency and site of fluoro-jade staining in different brain regions in response to each treatment was noted.

3.3.2 Results

Figure 3.5 illustrates the pattern of fluoro-jade staining compared to cresyl violet staining in brain sections from rats 24 h after striatal injection of S-AMPA with IL-1 in the rat. Degenerating cells stained with fluoro-jade appear bright against a dark background (Figure 3.5). Cell death that was equivocal or considered absent on gross visual examination of cresyl violet stained brain sections (hippocampus, NR, contralateral parietal cortex) was readily and unequivocally identified on adjacent fluoro-jade stained brain sections (Figure 3.5).

Striatal cell death was consistently observed in response to both S-AMPA and S-AMPA with IL-1 24 h after striatal injections. Cell death was also observed in 17 (excluding the striatum) regions ipsilateral to the injection site (Figure 3.6). Cell death was consistently seen in sites adjacent to the striatum such as the bed nucleus of the stria terminalis (BST), substansia innominata (SI), and various thalamic nuclei (anterior, lateral and ventral). In addition, regions such as the hippocampus, amygdala, nucleus reuniens (NR), dorsomedial thalamus (DMT), which, were further removed from the striatum also exhibited cell death. Neuronal degeneration was also seen in 15 regions contralateral to the site of injection (all regions in which cell death was observed

ipsilaterally) suggesting that extrastriatal subcortical cell death was not a result of direct extension of striatal damage.

Subcortical cell death was seen in similar regions in response to S-AMPA or S-AMPA with IL-1 (Figure 3.6). Cortical cell death in response to S-AMPA was also observed, but this was limited to allocortical regions (piriform cortex, entorhinal cortex, or infralimbic/cingulate cortex). Neocortical (parietal cortex or frontal cortex) cell death, which was noted to be bilateral in 1/14 rats was only observed in response to striatal injection of S-AMPA with IL-1.

Overall, cell death was seen in more regions in total (1.5-fold), ipsilaterally (1.5-fold) and contralaterally (2-fold) in response to striatal co-infusion of S-AMPA with IL-1 *vs* S-AMPA alone (Figure 3.7).

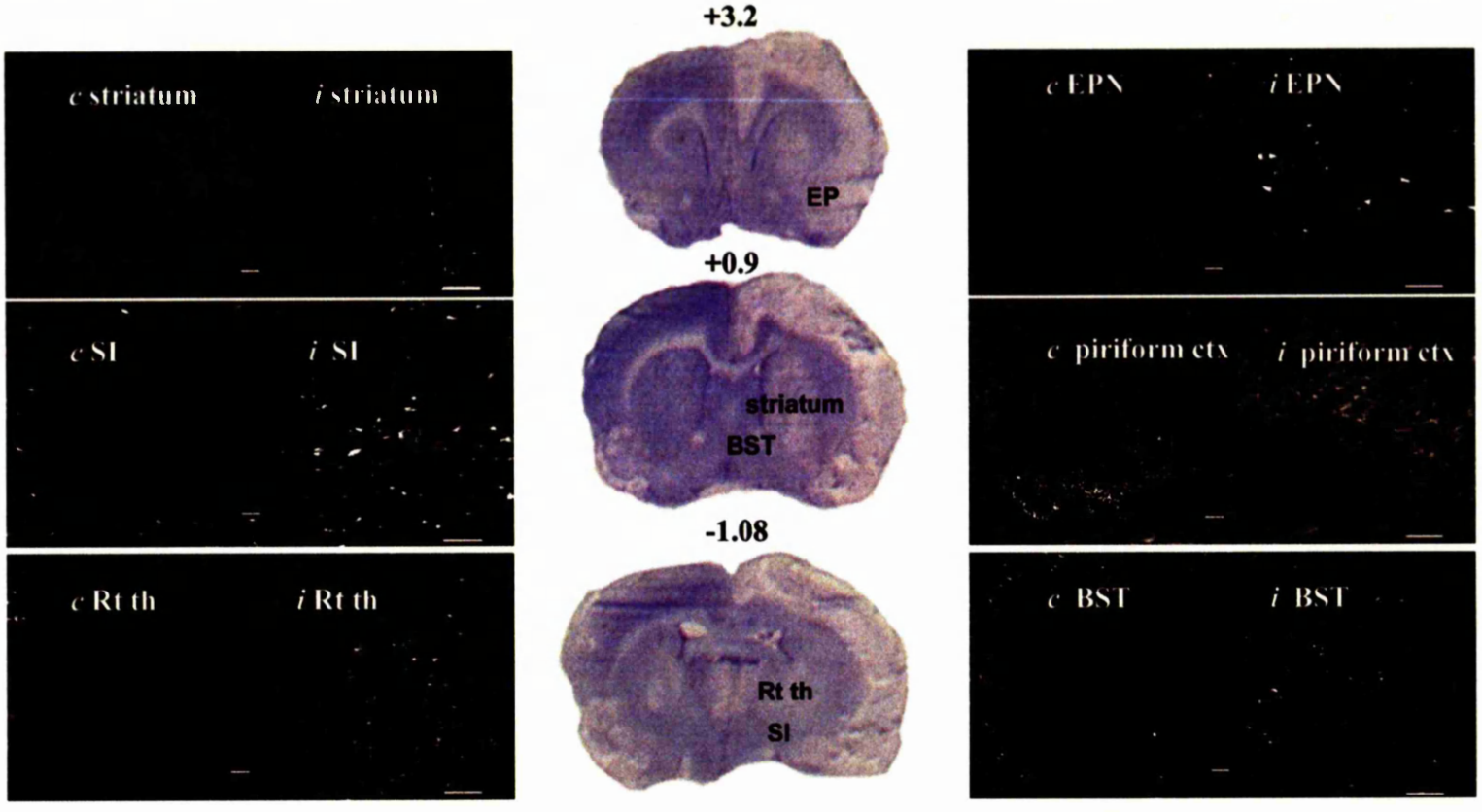
+3.2
c striatum
i striatum
EP
c EPN
i EPN
+0.9
c SI
i SI
striatum
BST
c piriform ctx
i piriform ctx
-1.08
c Rt th
i Rt th
Rt th
SI
c BST
i BST

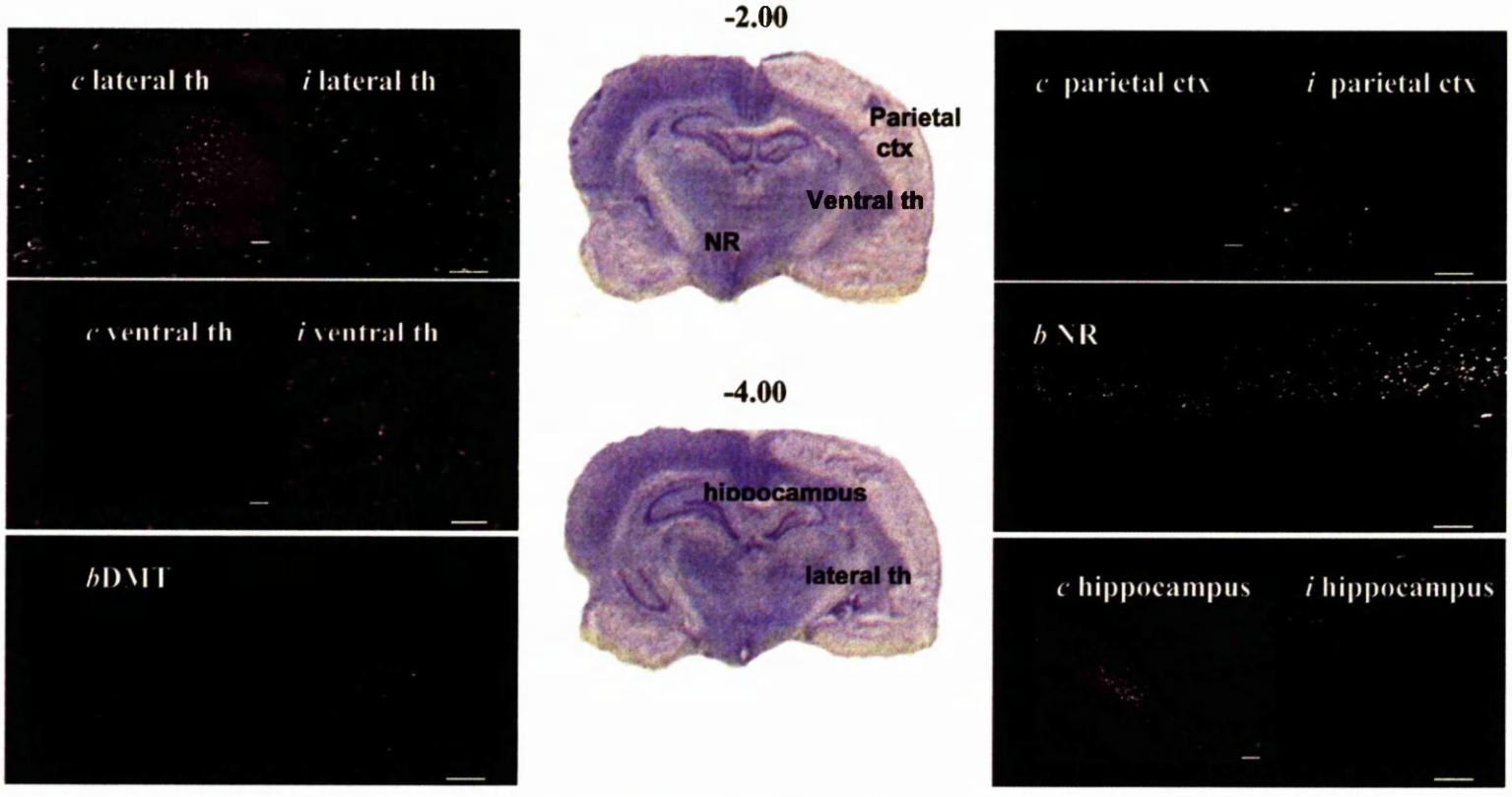

Figure 3.5: Photomicrographs of fluoro-jade stained brain sections and images of cresyl violet stained brain sections demonstrating neuronal damage observed in (*i* ipsilateral, *c* contralateral, *b* bilateral) in response to striatal injection of S-AMPA (7.5nmol) with IL-1. Fluoro-jade staining (white dots) representing degenerating neurones was observed in regions not obviously damaged on visual inspection of cresyl violet sections (NR nucleus reuniens, DMT dorsomedial thalamus, SI substansia innominata, BST bed nucleus of stria terminalis, ctx cortex, th thalamus EPN endopiriform nucleus). Scale bar for ipsilateral images = 70 µm; contralateral images and images of bilateral (*b*) NR and DMT = 140µm

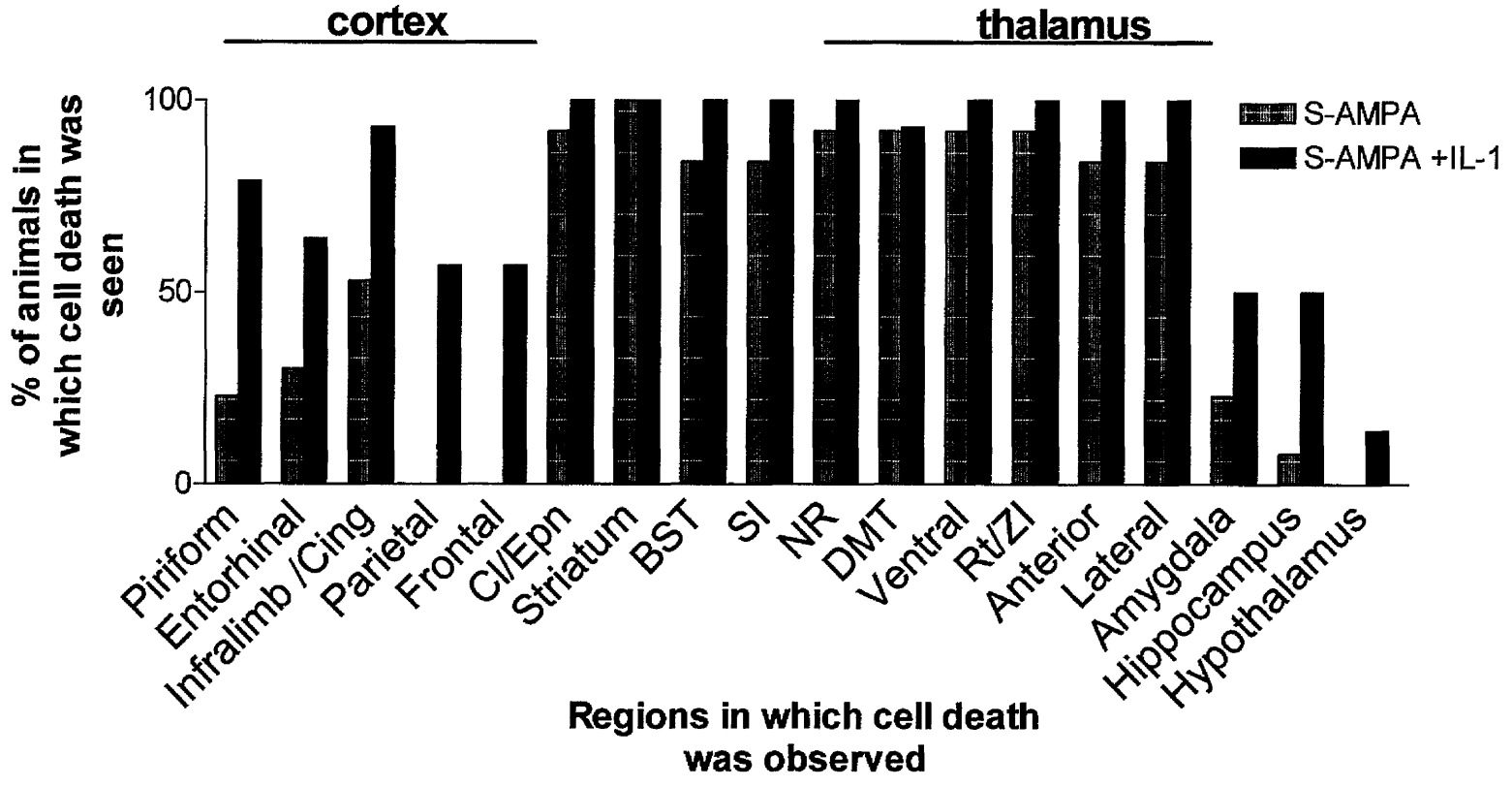

Figure 3.6: Sites in which degenerating neurones were observed 24 h after striatal injection of S-AMPA (7.5nmol) *vs* S-AMPA (7.5nmol) with IL-1. Data are expressed as the percent of animals that exhibited neuronal damage in each brain region examined.

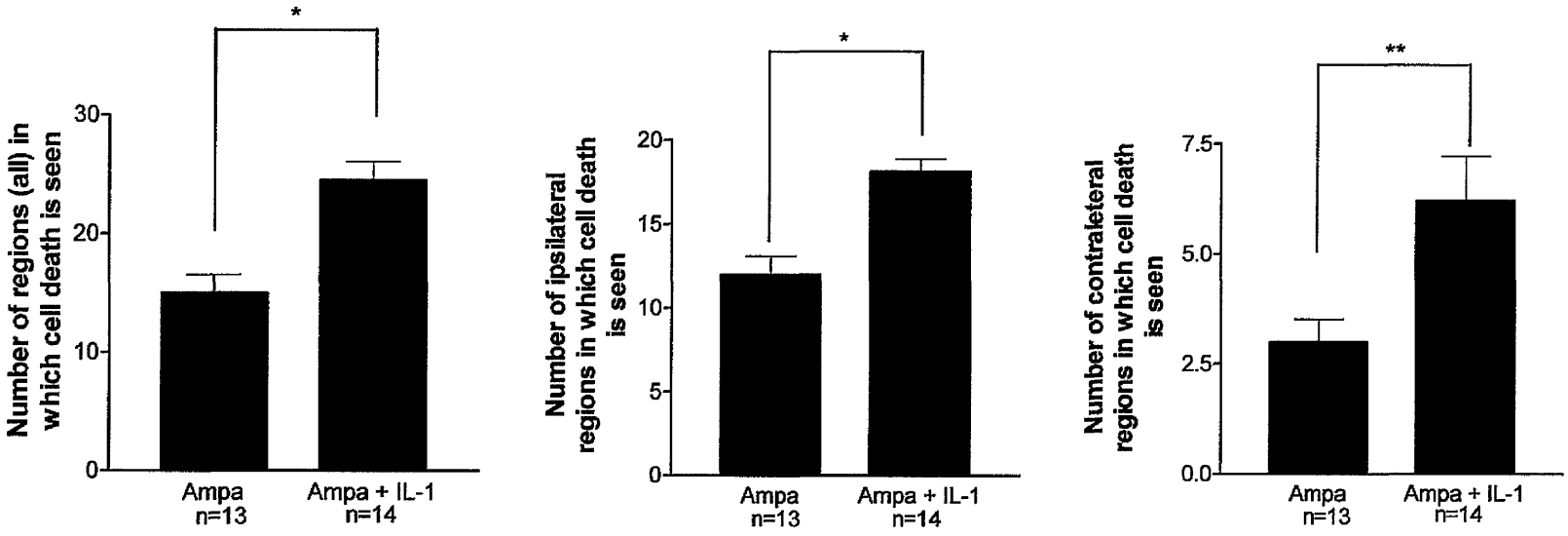

Figure 3.7: Number of sites in which cell death was observed in response to striatal injection of S-AMPA *vs* S-AMPA with IL-1. Data are expressed as mean ± sem. * P<0.001, ** P<0.05

3.4 Discussion

The aim of the experiments performed in this chapter was to validate and reproduce the cell death induced by striatal injection of S-AMPA with IL-1 and S-AMPA alone, so that the mechanism(s) by which IL-1 induces cell death may be investigated further. Accordingly, it has been demonstrated that striatal co-infusion of S-AMPA with IL-1 exacerbated cell death induced by striatal injection of S-AMPA alone as shown previously {Lawrence, Allan, et al. 1998}.

Striatal injection of S-AMPA resulted mainly in subcortical cell death although occasionally, cell death in the cortex was also seen. However, as observed previously, {Lawrence, Allan, et al. 1998; Grundy 2000} this was limited to the piriform, infralimbic and entorhinal cortices (allocortical regions), and was never observed in the parietal or frontal cortex (neocortex). 'Cortical' cell death induced by S-AMPA with IL-1 therefore refers to cortical death in the fronto-parietal (neocortical) regions. Cortical lesion volume assessment was not quantified separately as allocortical and neocortical regions throughout this thesis. However, for descriptive or discussion purposes, a distinction between allocortical and neocortical regions has been made.

Co-infusion of S-AMPA with IL-1 in the striatum in the rat exacerbated cell death induced by S-AMPA alone. As previously reported, the increase in cell death was predominantly seen as an increase in parietal and frontal (neocortical) cortical cell death {Lawrence, Allan, et al. 1998; Grundy 2000} and occurred as an 'all or nothing' phenomenon, with damage in approximately 60-80% of rats {Lawrence, Allan, et al. 1998; Grundy 2000}. A significant increase in the subcortical volume of cell death (which has not been reported previously) was also seen in response to S-AMPA with

IL-1 compared to S-AMPA alone. Furthermore, the total, cortical and subcortical lesion volumes (48 h) induced by S-AMPA with IL-1 were also greater compared to previous studies. In addition, cortical, lesion volumes (in this experiment) in response to S-AMPA (7.5nmol) with IL-1 48 h (*vs* 24 h) were also greater. Although lesion volumes at these time points were not compared directly, cortical cell death is reported to be complete by 24 h after striatal injections, and therefore, no difference was expected {Grundy 2000}.

The differences in lesion volume(s) observed between this and earlier studies may be due to a number of factors, not least inter experimental variation, and / or increased sensitivity of rodents to excitotoxin as a result of alteration in the genetic background of the rats used. Quoting increased unpredictable variability in animal response to S-AMPA, Grundy (2000) varied the doses of S-AMPA injected in order balance the need to achieve consistent cortical cell death upon co-infusion of with IL-1 *vs* minimising excitotoxin induced mortality {Grundy 2000}.

Differences in anaesthetic techniques may also account for some of the differences in lesion volumes observed. Lawrence et al (1998) used phenobarbitone, which reduces excitotoxin induced neuronal loss as compared to halothane {Lawrence, Allan, et al. 1998; Lees 1992}. However, halothane (albeit without Nitrous Oxide) was used by Grundy who also observed smaller lesion volumes (48 h) than those reported here. Grundy (2000) performed most striatal injections without the use of an infusion pump, which may have resulted in variable drug administration and therefore discrepancy in lesion volumes {Grundy 2000}. Failure to quantify the rostral thalamic damage may also contribute to some of the discrepancy observed between this and previous studies.

In later studies in this thesis, cell death was studied at 24 h after striatal injections in order to comply with British home office regulations. Despite the difference in lesion volume seen between 24 h and 48 h, significant differences in lesion volume were seen in response to S-AMPA with IL-1 *vs* S-AMPA at both points. Further, no difference in the frequency of cortical cell death was noted in response to striatal co-infusion of S-AMPA (7.5 nmol) with IL-1 (48 h (63%) *vs* 24 h (71%)) and also, no neocortical cell death was seen in response to striatal injection of S-AMPA alone. Thus, this paradigm was considered to be useful to investigate the mechanism of action of IL-1 in acute neurodegeneration.

Cresyl violet staining has been used in this and previous studies as it allowed simple rapid and clear visual assessment of cell death on frozen brain sections. However it is limited in a number of ways; neuronal shrinkage, vacuolation and hyperchromatism, all signs which can be used to infer cell death on cresyl violet sections, require careful and slow examination by a trained examiner {Garcia & Kamijioyo 1974}. Furthermore, these features may result from tissue processing and therefore lead to false positive identification of neuronal cell death {Cammermeyer 1961}. Conventional staining such as silver staining for demonstrating cell death unequivocally is disadvantaged by a long processing time. Fluoro-jade, which is an anionic fluorochrome has been compared to nissel stains, haematoxylin stains, and silver stains and has been shown to be a more sensitive marker of degenerating neurones {Schmued, Albertson, et al. 1997}. Degenerating cells are easily and unequivocally identified as they fluoresce when visualised with a fluorescence microscope using a filter system suitable for visualising fluorescein. This negates the need for long processing time (as for silver staining), and allows for quantification of regions in which neuronal degeneration is not obvious without histological expertise {Schmued, Albertson, et al. 1997}.

Degenerating cells (on fluoro-jade stained sections) were observed in similar sites 'distant' to site of injection of S-AMPA or S-AMPA with IL-1 although no degenerating cells were observed in the neocortex in response to S-AMPA alone. A similar spatial pattern of 'distant' cell death is also seen in response to intrahippocampal injection of S-AMPA (2 nmol) in the rat {Lees & Leong 2001}. The pattern of neuronal degeneration in response to intrastriatal injection of S-AMPA, S-AMPA with IL-1, or intrahippocampal S-AMPA is also similar to that induced by kainic acid or bicuculline administration in the rat, with degenerating neurones being observed in the hippocampus, amygdala, and thalamus {Ben-Ari, Tremblay, et al. 1980; Ben Ari, Tremblay, et al. 1981; Ben Ari 1985}. Interestingly, neocortical cell death is also observed (although variably) in response to kainic acid or bicuculline {Ben-Ari, Tremblay, et al. 1980; Ben Ari, Tremblay, et al. 1981; Ben Ari 1985}. 'Distant' cell death in response to kainic acid correlates with extent and duration of seizure activity, with cell death being observed in regions of increased metabolic activity {Ben Ari 1985}. Furthermore, 'distant' cell death is reduced by anticonvulsants, suggesting also that these lesions are related to seizures {Ben Ari, Tremblay, et al. 1979; Ben-Ari, Tremblay, et al. 1980; Ben Ari 1985}. Lees et al (2001), have used the extent of 'distant' cell death as a measure of seizure activity, and devised a scale using the sites of cell death to test the effects of various drugs on seizure activity{Lees & Leong 2001}.

Sites in which degenerating neurones were observed in response to S-AMPA *vs* S-AMPA with IL-1 were graphed and compared. The scoring system used by Lees at al (2001) was modified to reflect differences in regions of cell death seen. It was used primarily used to visualise differences between groups rather than as a measure of seizure activity.

In summary, previous reports showing that co-infusion of S-AMPA with IL-1 results in 'distant' cortical death in addition to 'local' striatal death observed with S-AMPA alone have been reproduced. The increased sensitivity, and ease of identification of degenerating neurones on flouro-jade stained sections has significantly extended the observations made by Grundy, Allan and others in the paradigm of brain injury described in this chapter. The use of the anionic dye flouro-jade has allowed the observation that 'distant' cell death is seen in many similar subcortical and allocortical regions in response to striatal injection of S-AMPA with IL-1 and S-AMPA alone in the rat to be made. These data suggest that 'distant' cell death is an S-AMPA dependent process, and that 'distant' neocortical death is a result of the effects of IL-1 on an S-AMPA dependent process.

Chapter 4: IL-1 expression and cell death induced by striatal injection of S-AMPA ±IL-1 in the rat.

4.1 Introduction

Co-infusion of IL-1 with the excitotoxin S-AMPA (*vs* S-AMPA alone) results in the exacerbation of neuronal cell death in the rat {Lawrence, Allan, et al. 1998; Allan, Parker, et al. 2000; Grundy 2000}. This exacerbation is predominantly seen as an increase in ipsilateral neocortical cell death, and is reproduced and described further in chapter 3. The mechanism(s) by which IL-1 increases the volume of neocortical cell death in this paradigm of brain injury however is not known.

Hypothalamic expression of immunoreactive IL-1 protein is significantly increased by 8 h after striatal injection of S-AMPA with IL-1 *vs* S-AMPA alone, and this precedes the cell death in the neocortex which is seen first around 12 h (on cresyl violet stained brain sections) after injection {Allan, Parker, et al. 2000}. IL-1 protein expression in the hypothalamus is also significantly increased in response to striatal injection of IL-1 alone (*vs* S-AMPA or vehicle), 8 h after striatal injection, and administration of intra-hypothalamic IL-1ra significantly reduces the increased neocortical cell death induced by striatal injection of S-AMPA with IL-1{Allan, Parker, et al. 2000}. In addition, neocortical lesion volumes and the proportion of animals that exhibit neocortical damage appear to be dependent on the site of infusion of S-AMPA with IL-1, as the frequency and volume of cortical cell death are increased if the S-AMPA and IL-1 is infused into the ventral *vs* the dorsal striatum; or into the nucleus accumbens shell *vs* core {Grundy, Rothwell, et al. 2002}. Furthermore, no increase in cell death volume is seen after cortical injection of S-AMPA *vs* cortical injection of S-AMPA with IL-1 {Lawrence, Allan, et al. 1998}. These observations have led to the hypothesis that IL-1 exacerbates excitotoxin induced neuronal cell death by activating neuronal pathways

through specific sites in the brain that include the striatum and hypothalamus {Allan, Parker, et al. 2000; Grundy, Rothwell, et al. 2002}.

The aim of this study was to determine the temporal progression of IL-1 expression in response to striatal injection of S-AMPA *vs* S-AMPA with IL-1, in order to identify other potential sites of action of IL-1, so that a putative 'pathway for IL-1' action could be identified.

4.2 Experiment: Temporal progression of immunoreactive IL-1β (irIL-1β) in response to striatal injection of vehicle, IL-1, S-AMPA or S-AMPA with IL-1 in the rat

4.2.1 Method

Striatal injections of vehicle, IL-1 (10ng), S-AMPA (7.5nmol) or S-AMPA (7.5nmol) with IL-1 (10ng) were performed as described in **section 2.3.1**. Brains from these animals were removed (4 h, 8 h, or 16 h after striatal treatments) after transcardial perfusion with 4% PFA under terminal anaesthesia (**see section 2.4.2**). The perfuse-fixed brains were sectioned (30μm) on a cryostat. Multiple coronal sections were taken at each level of forebrain sectioned. (**see section 2.4.2.1.2**).

One set of sections from each animal was processed for IL-1β immunohistochemisty **(section 2.4.2.2)** to determine the location and progression of irIL-1β expression in response to striatal treatments.

Specificity for IL-1 staining was determined by examining brain sections for the presence of irIL-1β after 1) omission of primary antibody (sheep anti-rat IL-1β

antibody), 2) omission of secondary antibody (biotinylated donkey anti-sheep antibody) and, 3) incubation with supernatant from samples in which equal volumes of the primary antibody had been incubated (for 24 h at 4 °C) with varying concentrations of recombinant rat IL-1β (preadsorbtion) (**section 2.4.2.3**).

4.2.2 Results

4.2.2.1 Specificity of staining for irIL-1β

Omission of the primary or secondary antibody completely abolished immunostaining for irIL-1β (Figure 4.1 A, B). Substitution of primary antibody with supernatant from pre-adsorbed antibody preparation (100nM) also completely abolished IL-1β immunostaining (Figure 4.1D). The clarity and intensity of IL-1β immunostaining increased in inverse proportion to the concentration of rat IL-1β (1nM or 10nM) used for preadsorption (Figure 4.1 E, F).

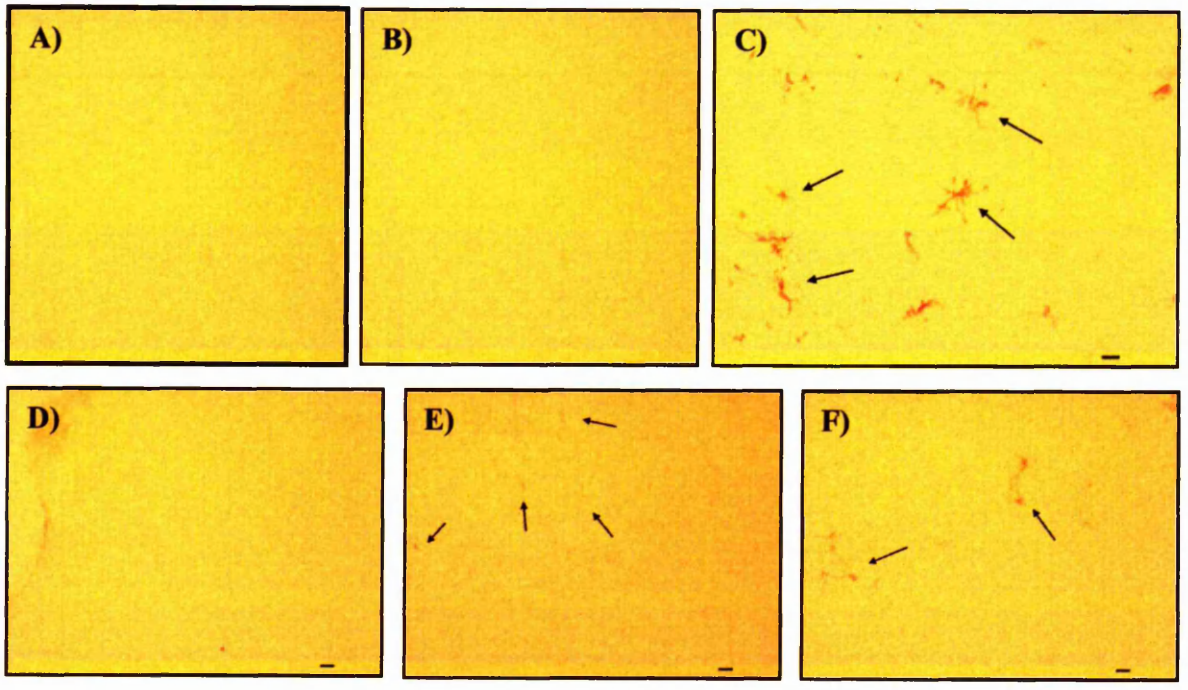

Figure 4.1: Photomicrographs of brain sections (parietal cortex) 8 h after striatal injection of S-AMPA with IL-1 in the rat. Abolition of immunoreactive staining with omission of primary (A) or secondary antibody (B) *vs* control (C), and increase in intensity and clarity of IL-1β immunostaining in proportion with a decrease in the concentration of the rat IL-1β (100 nM (D),10 nM (E) or 1 nM (F)) used for preadsorption. Arrows denote IL-1β immunoreactive cell. Scale bar = 20μm

4.2.2.2 Local irIL-1β expression in response to striatal injections

IL-1β immunoreactivity in response to striatal injection of vehicle or IL-1 was observed from 4 h after striatal injections. This was limited to the site of mechanical injury induced by the injection needle in the striatum and the injection tract (Figure 4.2).

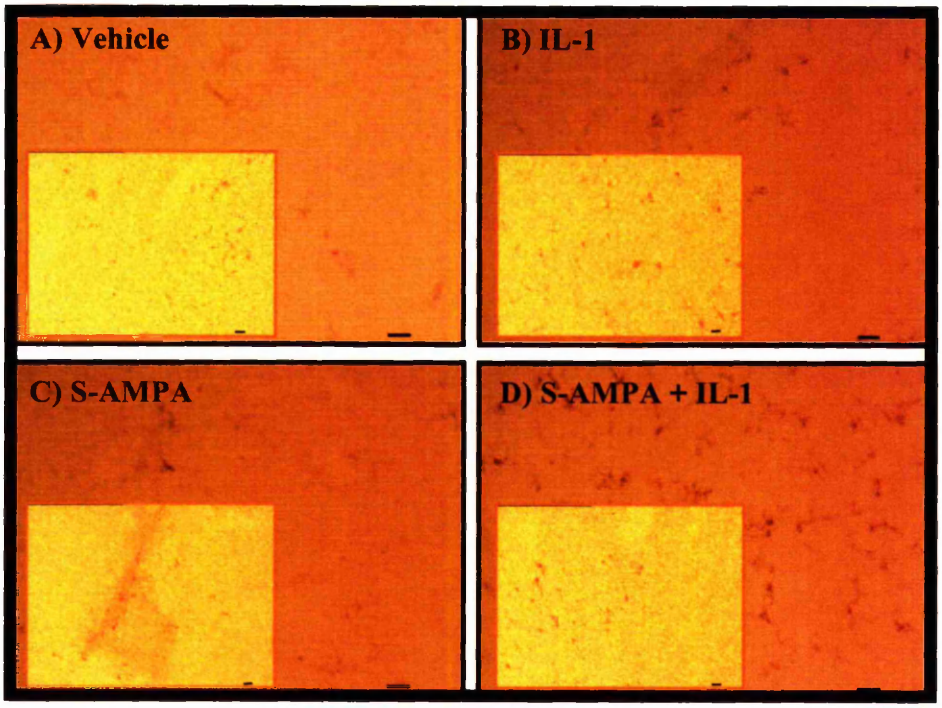

Figure 4.2: Photomicrographs showing irIL-1β in the striatum and cortex (inset) around site of injection 4h after striatal injections of vehicle, IL-1, S-AMPA and S-AMPA + IL-1 in the rat. Scale bar = 20 μm.

No difference in the number of irIL-1β cells in the striatum was seen between vehicle, IL-1, S-AMPA or S-AMPA with IL-1 treated rats, 4 h after striatal injection (Figure 4.3). The number of irIL-1β cells counted in the striatum in response to all treatments, was maximal 8 h after striatal injections (Figure 4.3). IrIL-1β cells in animals infused with S-AMPA alone were limited to the striatum and injection tract. No difference in

the number of irIL-1β cells was observed in the striatum between S-AMPA *vs* S-AMPA with IL-1β treated brains at any of the time points (Figure 4.3).

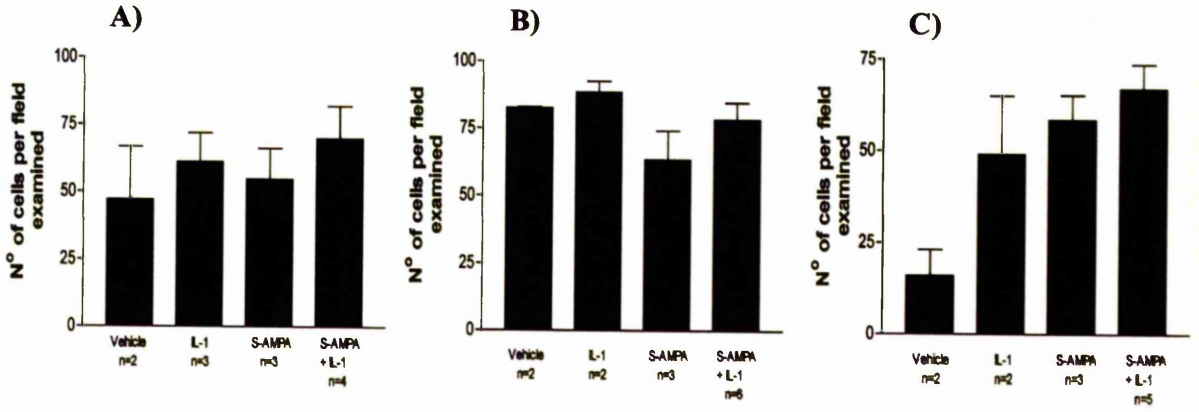

Figure 4.3: Graph represents the number of irIL-1β cells counted in the striatum A) 4 h, B) 8 h and C)16 h after striatal treatments. Data are expressed as mean ± SEM.

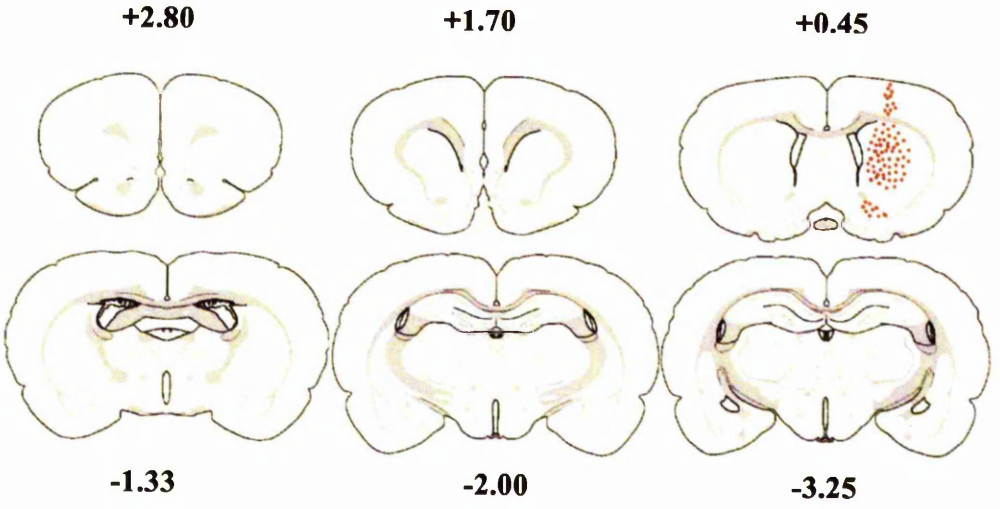

Figure 4.4: Diagram representing spatial distribution of irIL-1β observed 4 h after S-AMPA + IL-1 in the rat. Dots indicate the regional distribution of irIL-1β observed. Numbers represent distance from bregma (mm)

4.2.2.3 Remote irIL-1β expression 4 h after striatal injections of S-AMPA ±IL-1 in the rat.

Although only seen in one out of four rats, irIL-1β was observed in the substansia innominata (SI), reticular thalamus/ zona incerta (Rt/ZI), and anterior thalamus in addition to the striatum in response to striatal injection of S-AMPA with IL-1 (Figure 4.4, 4.5A).

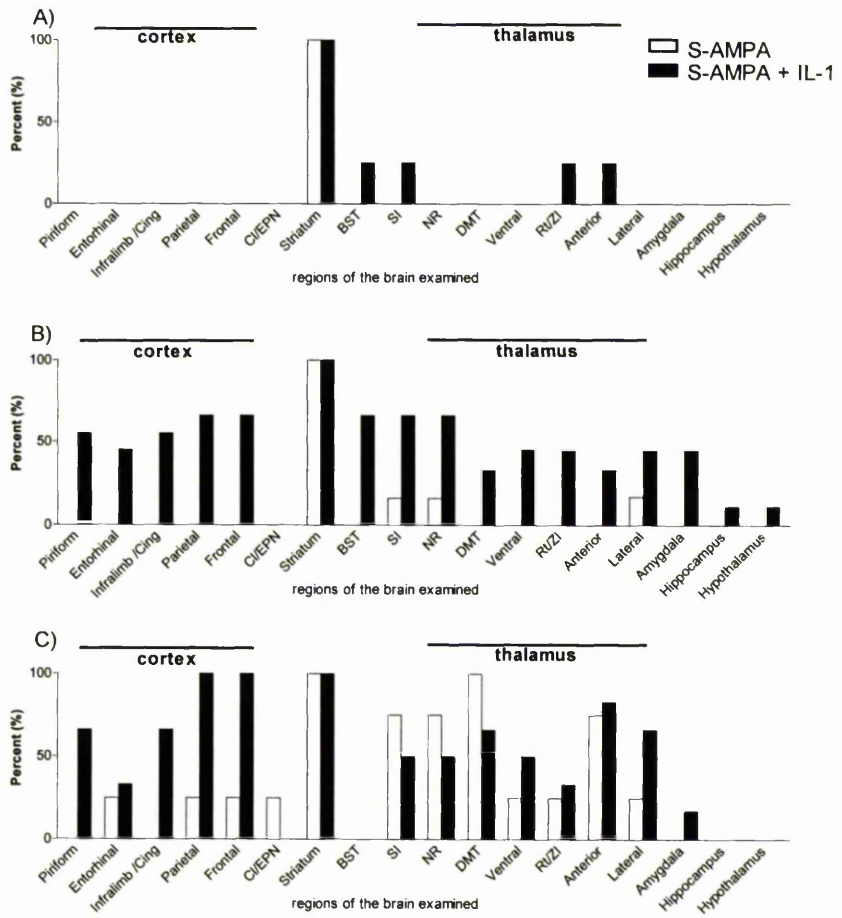

Figure 4.5: Sites of expression of irIL-1β observed 4 h (A), 8 h (B) and 16 h (C) after striatal injection of S-AMPA or S-AMPA + IL-1 in the rat . Data are expressed as the percent of animals noted to have damage in particular areas per treatment per time point (EPN Enteropiriform nucleus, SI substansia innominata, BST bed nucleus of stria terminalis, NR nucleus reuniens, DMT dorsomedial thalamus, Rt/ZI reticular thalamus/zona incerta, Infralimb/cing infralimbic/cingulate) (n=4-8).

4.2.2.4 Remote irIL-1β expression 8 h after striatal injections of S-AMPA ± IL-1 in the rat

Although irIL-1β cells (in response to striatal injection of S-AMPA alone) were seen in the SI, nucleus reuniens (NR), and lateral thalamus in one out of six rats, the majority of staining was again limited to the striatum, similar to that 4 h after striatal injection of S-AMPA (Figures 4.5B, 4.6).

Striatal co-injection of S-AMPA with IL-1 resulted in a marked increase in the number of sites at which irIL-1β cells were seen compared to S-AMPA alone (Figure 4.7). In addition to the striatum, irIL-1β cells were seen consistently in the neocortex (parietal cortex (6 out of 9 animals (6/9)) frontal cortex (6/9)), the allocortex (piriform cortex (5/9), entorhinal cortex (4/9), infralimbic/cingulate cortex (5/9)), various thalamic nuclei (NR (6/9), dorsomedial thalamus (DMT) (3/9), and ventral thalamus (4/9)) (Figure 4.5, 4.6, 4.8). Furthermore, contralateral staining was also noted in the DMT (3/12), ZI/Rt (7/12), and NR (6/12).

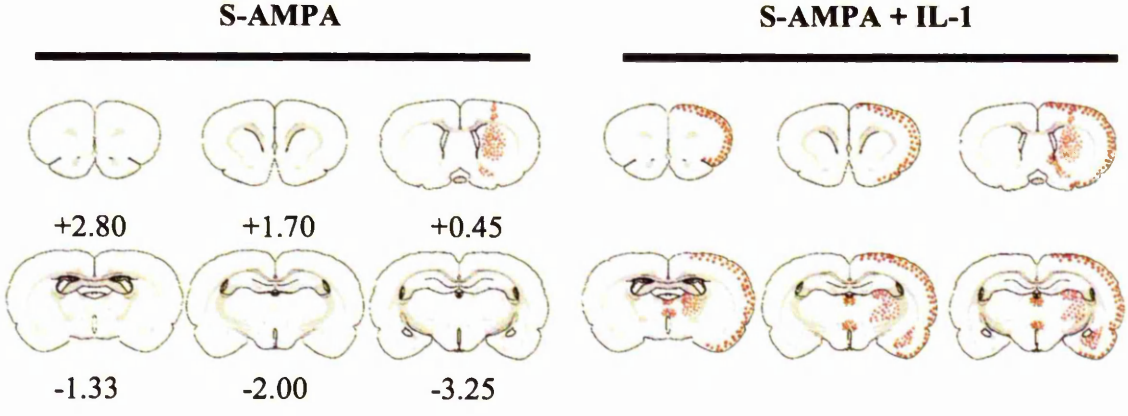

Figure 4.6: Diagram representing spatial distribution of irIL-1β observed 8 h after striatal injection of S-AMPA ± IL-1. Dots represent regions in which irIL-1β was observed. Numbers represent distance of sections from bregma (mm).

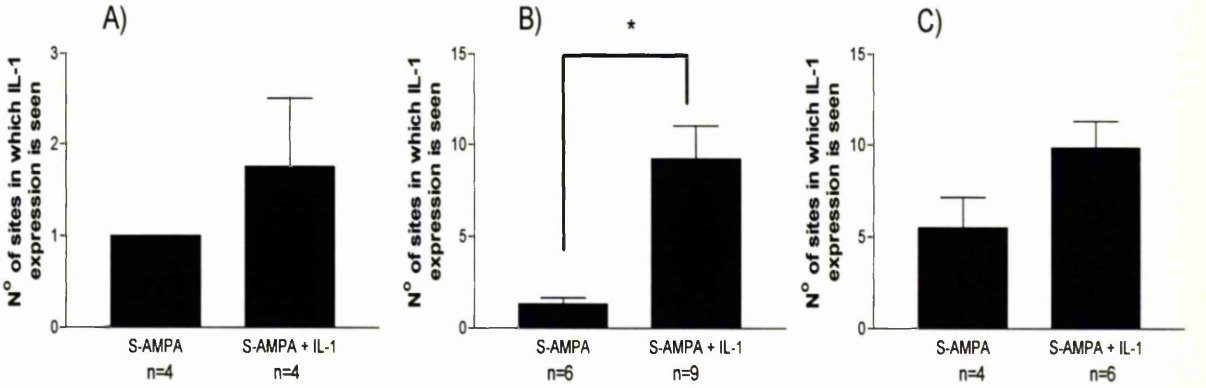

Figure 4.7: Number of sites in which irIL-1β cells were observed 4 h (A) 8 h (B) and 16 h (C) after striatal injection of S-AMPA or S-AMPA with IL-1. Data are expressed as mean ± SEM *P<0.003

The number of cells expressing irIL-1β in the neocortex, NR (7.6 fold), and DMT (2.8 fold) were also greater in the group of rats injected with S-AMPA with IL-1 compared to those that received S-AMPA alone (Figure 4.9). Only one rat (1/9) was noted to have immunoreactive cells in the hypothalamus (Figure 4.5B).

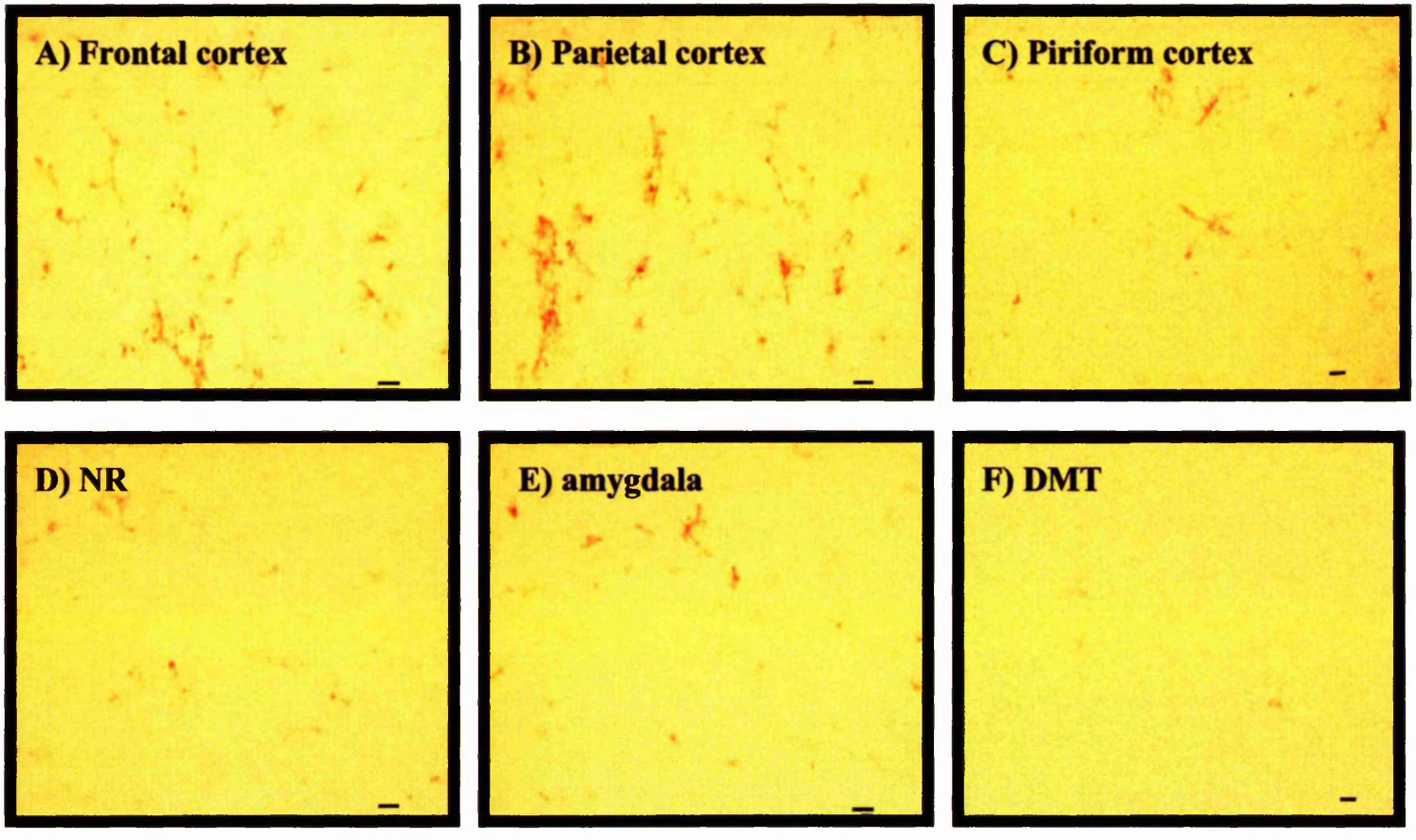

Figure 4.8: Photomicrographs of selected regions in which irIL-1 cells were observed 8 h after striatal injection of S-AMPA with IL-1. Scale bar = 20µm.

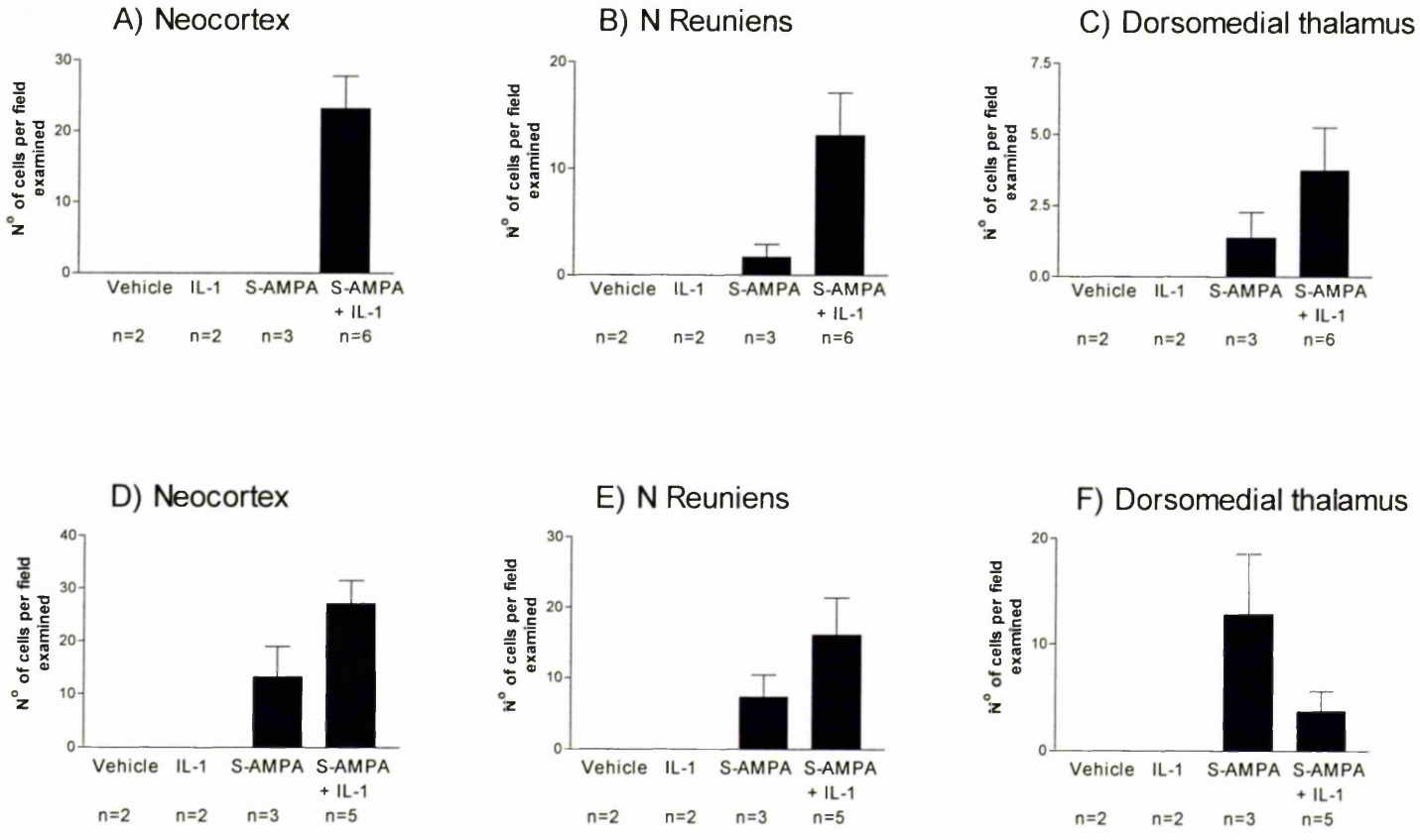

Figure 4.9: Number (N^O) of irIL-1β cells counted in 2 fields (4 fields for neocortex) per selected region in response to striatal injections of vehicle, IL-1, S-AMPA, or S-AMPA with IL-1, 8 h (A-C) and 16 h (D-F) after surgery. Data are expressed as mean ± SEM.

4.2.2.5 Remote irIL-1β expression 16 h after striatal injections of S-AMPA ±IL-1 in the rat

By 16 h there was no significant difference in the number of sites in which irIL-1β was observed between S-AMPA *vs* S-AMPA with IL-1 treated rats (Figure 4.7).

IrIL-1β cells were seen in similar regions in response to S-AMPA or S-AMPA with IL-1 treated rodents (Figures 4.5 C, 4.10). IrIL-1β cells were also noted in the neocortex in response to striatal injection of S-AMPA alone (1 out of 4 rats) although the frequency with which this was observed was less than that induced by striatal injection of S-AMPA with IL-1 (5 out of 8 rats) (Figure 4.5 C).

The number of immunoreactive cells counted was variable between regions; being greater in the cortex and NR, less in the DMT, and similar in the striatum in S-AMPA with IL-1 *vs* S-AMPA treated rats (Figure 4.9). These differences however were not significant.

There was also no difference in the number, or spatial distribution of sites in which irIL-1β positive cells were observed 8 h *vs* 16 h after striatal injection of S-AMPA with IL-1 (Figures 4.5-4.8,4.10,4.11). A difference in the spatial distribution of irIL-1β cells within the neocortex was however observed in response to striatal injection of S-AMPA with IL-1 8 h *vs* 16 h after surgery. Immunoreactive cells were limited to the outer layers (I and II) of the neocortex at 8 h (Figure 4.6) after surgery, whilst by 16 h, irIL-1β positive cells were observed through out the ipsilateral neocortex (Figure 4.10). The distribution of irIL-lβ positive cells seen in the neocortex in response to S-AMPA (16 h)

was similar to the distribution seen in response to S-AMPA with IL-1 at 8h (Figures 4.6, 4.10).

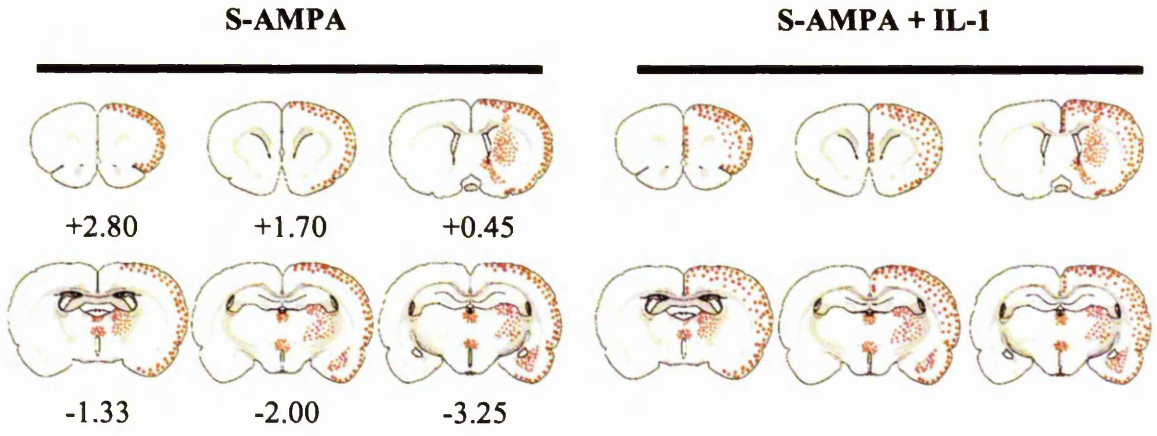

Figure 4.10: Diagram representing spatial distribution of irIL-1β observed 16 h after striatal injection of S-AMPA ± IL-1. Dots represent regions in which irIL-1β was observed. Numbers represent distance of sections from bregma (mm).

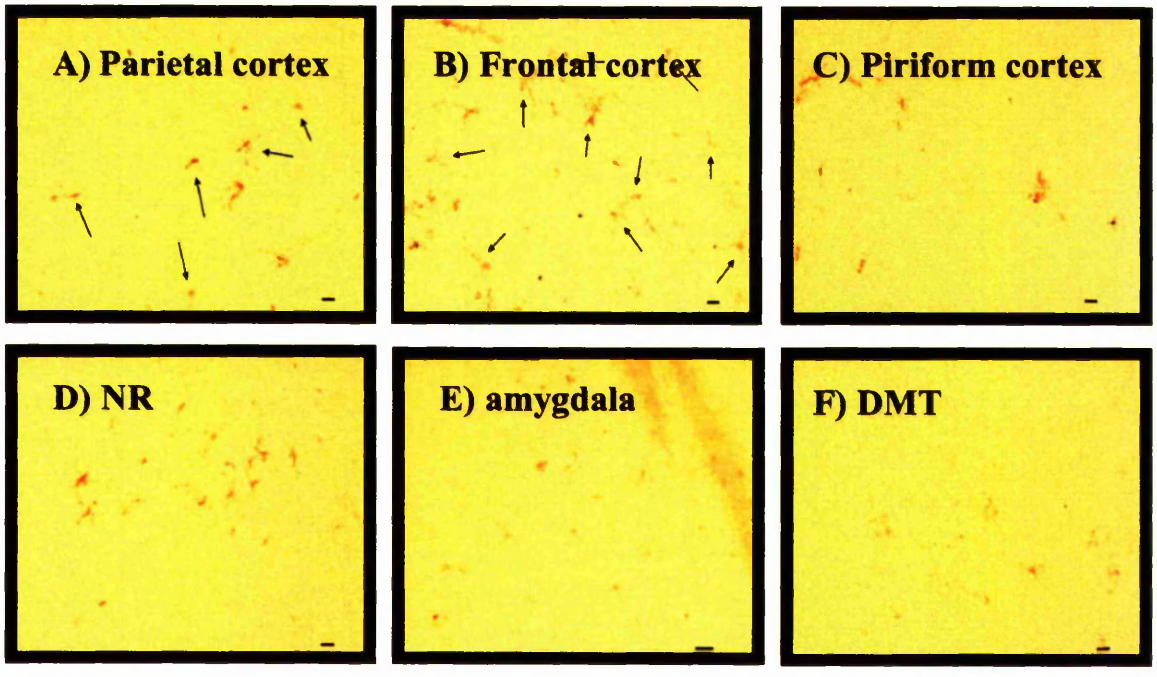

Figure 4.11: Photomicrographs of selected regions in which irIL-1 cells were observed 16 h after striatal injection of S-AMPA with IL-1. Arrows represent the predominant cell morphology observed. Scale bar = 20μm.

4.2.2.6 Cellular source of irIL-1β

Cells of a similar morphology were observed in most regions in which irIL-1β was observed (Figures 4.8,4.11,4.12). IrIL-1β positive cells were typically seen to have a small, irregular cell body with short cellular processes emanating from each pole (Figures 4.8,4.11,4.12), and in this respect resembled microglia. However, cells with a rounded cell body and retracted cellular process were also observed at later time points particularly in the parietal cortex and striatum 16 h after striatal injection of S-AMPA with IL-1 (see Figure 4.8 A *vs* B and 4.11B).

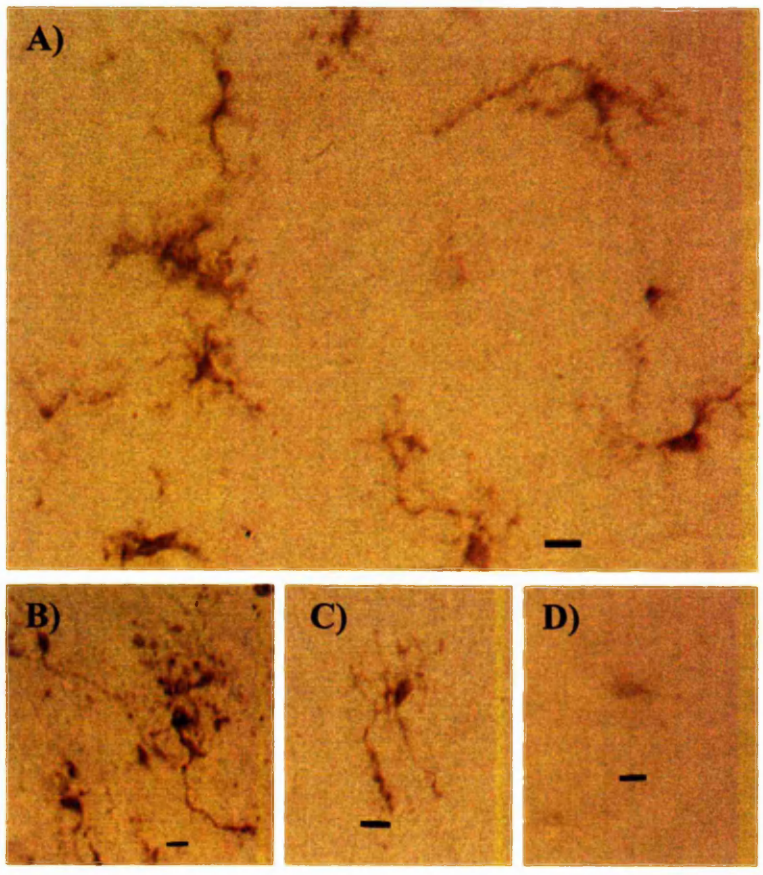

Figure 4.12: Photomicrographs of irIL-1 cells observed in the frontal cortex (A), parietal cortex (B), NR (C), and DMT (D) 16 hours after striatal injection of S-AMPA with IL-1 in the rat. Scale bar = 100μm

To show that microglia were the main cells in which irIL-1β was observed, double immunohistochemistry was performed on brain sections 16 h after striatal injection of S-AMPA with IL-1 using antibodies for the microglial marker OX-42 and the sheep anti-rat IL-1β antibody used previously (**section 2.4.2.2.3**). Double-fluorescence immunohistochemistry demonstrated that irIL-1β positive cells also stained with the microglial marker OX-42 (Figure 4.13 A-D). OX-42 positive cells were seen through out the entire brain (including contralateral cortex Figure 4.13 E) and therefore, not all OX-42 positive cells were irIL-1β positive (Figure 4.13 A-E).

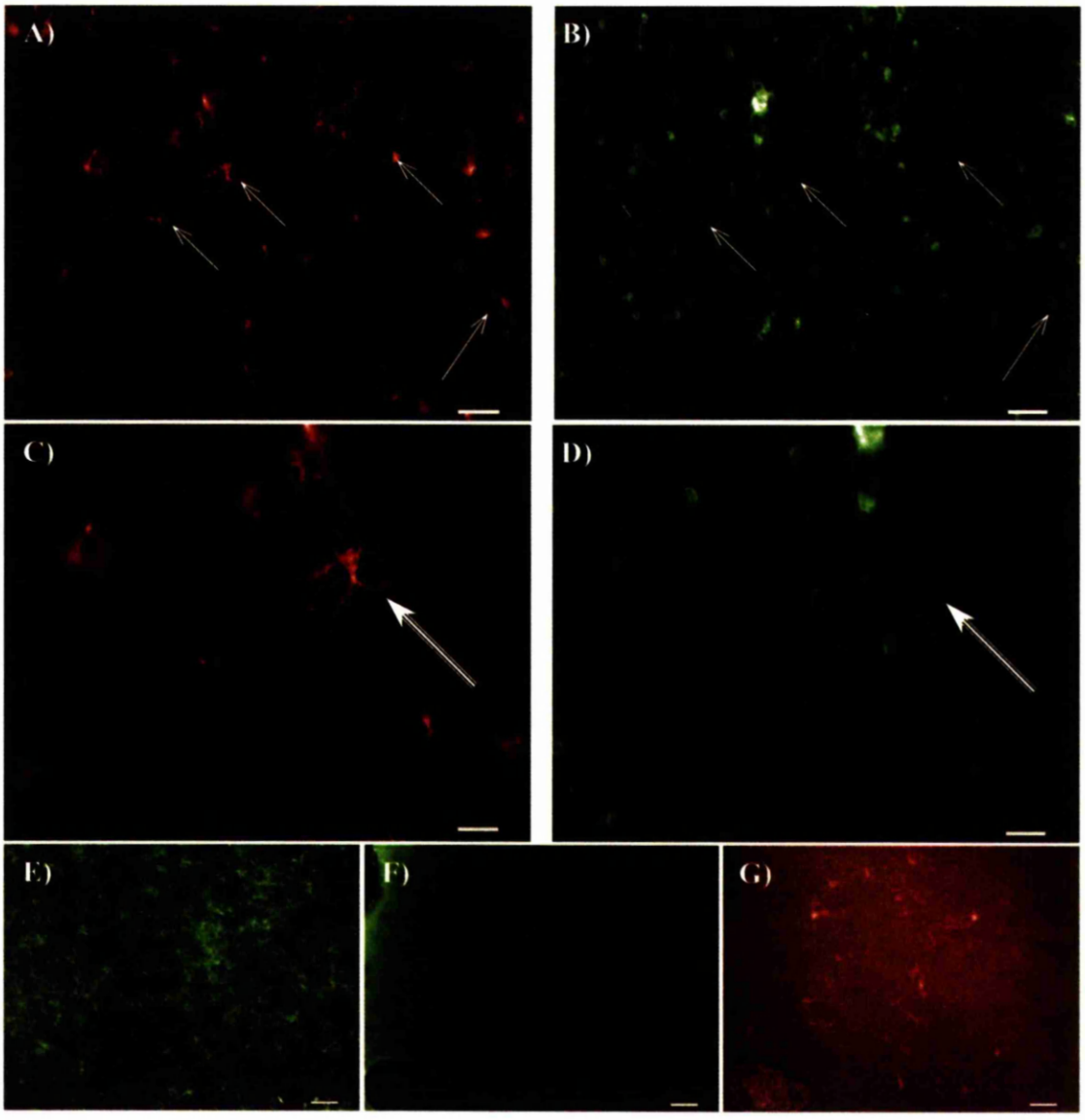

Figure 4.13: Immunohistochemical staining for IL-1β (A, C) and OX-42 (B, D) of the frontal cortex 16 h after striatal injection of S-AMPA + IL-1 in the rat. Sections reveal co-localisation of staining for irIL-1β and the microglial cell marker OX-42 (complete arrows). Not all OX-42 positive cells expressed irIL-1β (incomplete arrows). E)-G) control sections demonstrating OX-42 expression in the contralateral cortex (E), and staining for OX-42 (F) and irIL-1β(G) after omission of OX-42 antibody. Scale bar = 70μm (A, B, G-F), 35 μm (C, D).

4.3 Experiment: Temporal progression of cell death

Expression of IL-1 (mRNA or protein) in the brain may be induced by a number of stimuli / mechanisms; including peripheral or central inflammation or infection, seizures or cellular injury {Hopkins & Rothwell 1995; Davies, Loddick, et al. 1999; Pearson, Rothwell, et al. 1999; Vezzani, Conti, et al. 1999; de Simoni, Perego, et al. 2000}. IrIL-1β positive cells are observed in response to injury induced by intrastriatal injection of the NMDA receptor agonist methanoglutamate (Mglu) in the rat {Pearson, Rothwell, et al. 1999}. IrIL-1β is seen at the edge of the lesion 8 h after striatal injury, in regions that subsequently die 16 h later. Therefore, in this paradigm expression of irIL-1β appears to precede cell death. IrIL-1β in response to intrastriatal injection of S-AMPA or S-AMPA with IL-1 in the rat has also been observed in many regions that are seen to die 24 h after striatal injection of S-AMPA or S-AMPA with IL-1 in the rat **(section 4.2)**. In addition, degenerating neurones (as seen on fluoro-jade stained brain sections) in response to striatal injection of S-AMPA alone or S-AMPA with IL-1 were observed in subcortical areas distant to the site of injection (striatum) (chapter 3). However, as cell death and irIL-1β has not been co-localised in individual brains after striatal injections of S-AMPA or S-AMPA with IL-1, the true relationship between neuronal degeneration and irIL-1β is not known. Therefore, the temporal progression of neuronal damage was studied after striatal injection of vehicle, IL-1, S-AMPA, and S-AMPA with IL-1 and correlated to irIL-1β expression to determine whether irIL-1β preceded or followed cell death.

4.3.1 Method

Regions of neuronal degeneration were determined by examining fluoro-jade stained brain sections (30μm) 4 h, 8 h and 16 h after striatal injections of S-AMPA or S-AMPA

with IL-1. Additional sections taken from brains on which immunohistochemistry for IL-1 was performed were stained with fluoro-jade as previously described **(section 2.4.1.1.3)**. The sites of neuronal damage were noted, tabulated and compared (where applicable) with the distribution of irIL-1β cells.

4.3.2 Results

4.3.2.1 Neuronal degeneration induced by striatal injection of vehicle or IL-1

Degenerating neurones in response to striatal injection of vehicle or IL-1 were observed in the peri-injection tract region in the cortex and the striatum from 4 h after striatal injections, and did not change over time (Figure 4.14).

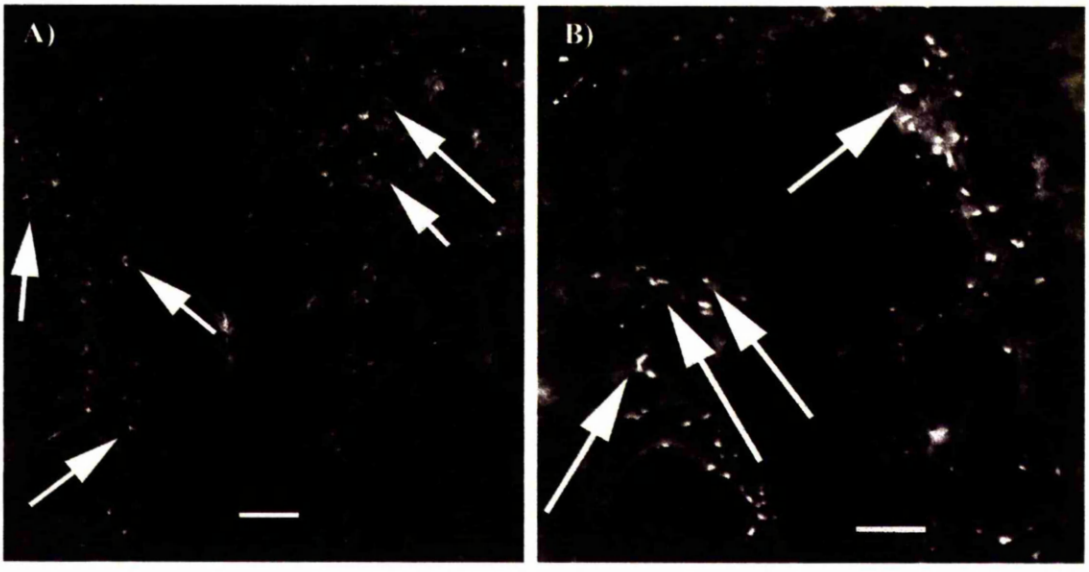

Figure 4.14: Photomicrographs of brain sections stained with fluoro-jade showing degenerating neurones around the injection tract in the rat striatum 8 h after injection of vehicle (A) or IL-1 (B) Arrows denote cells that are stained with fluoro-jade. Scale bar =70μm.

4.5.2.2 Neuronal degeneration in response to striatal injection of S-AMPA vs S-AMPA with IL-1 in the rat

The number of regions of the brain in which degenerating neurones were observed in response to striatal injection of S-AMPA, or S-AMPA with IL-1 increased with time (Figure 4.15). Whilst no significant differences were seen 4 h after striatal injection of S-AMPA with IL-1 *vs* S-AMPA alone, significant increases in the total number of sites in which degenerating neurones were observed 8 h (2-fold) and 16 h (1.25-fold) after striatal treatments (Figure 4.15, 4.16, 4.17).

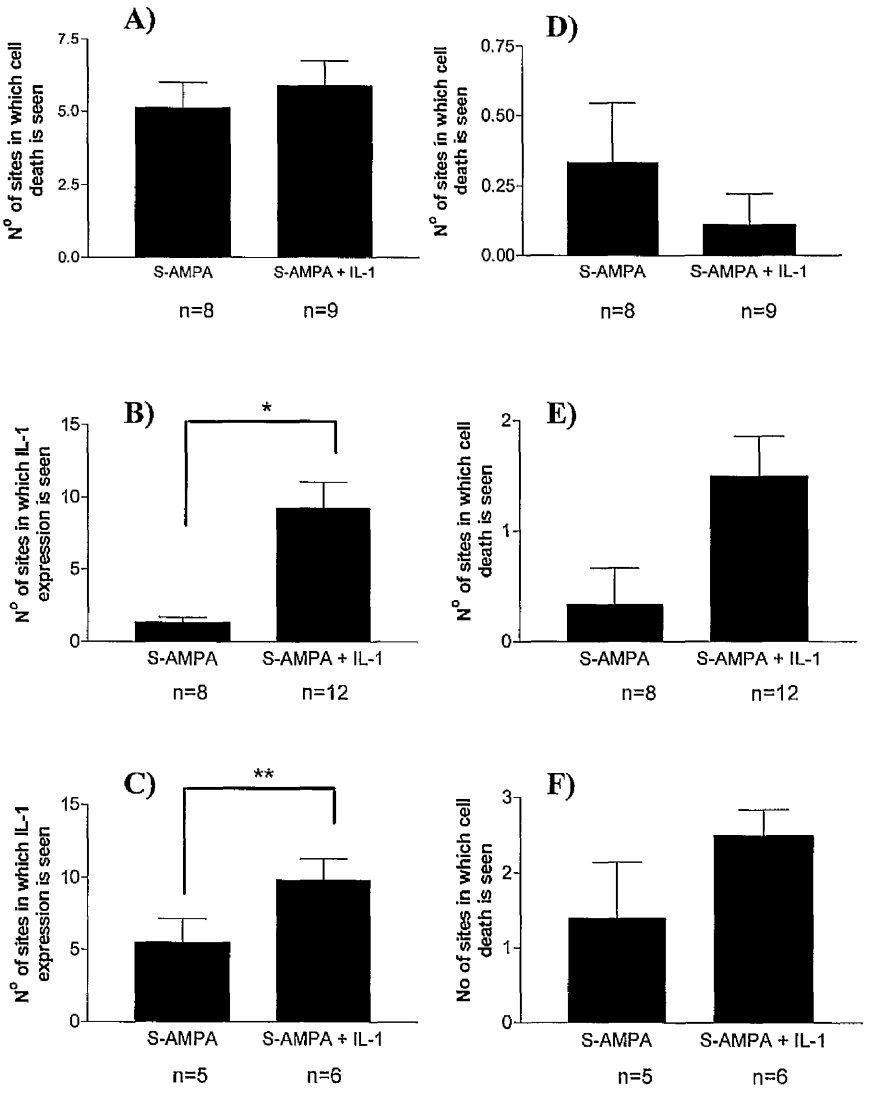

Figure 4.15: A-C) Total number of sites in which degenerating neurones were observed 4 h (A) 8 h (B) and 16 h (C) after striatal injection of S-AMPA or S-AMPA with IL-1. D-E) number of regions of contralateral neuronal damage in response to striatal injection of S-AMPA or S-AMPA with IL-1 4 h (D) 8 h (E) and 16 h (F) after surgery. Data are expressed as mean ± SEM *P<0.005, **P<0.05.

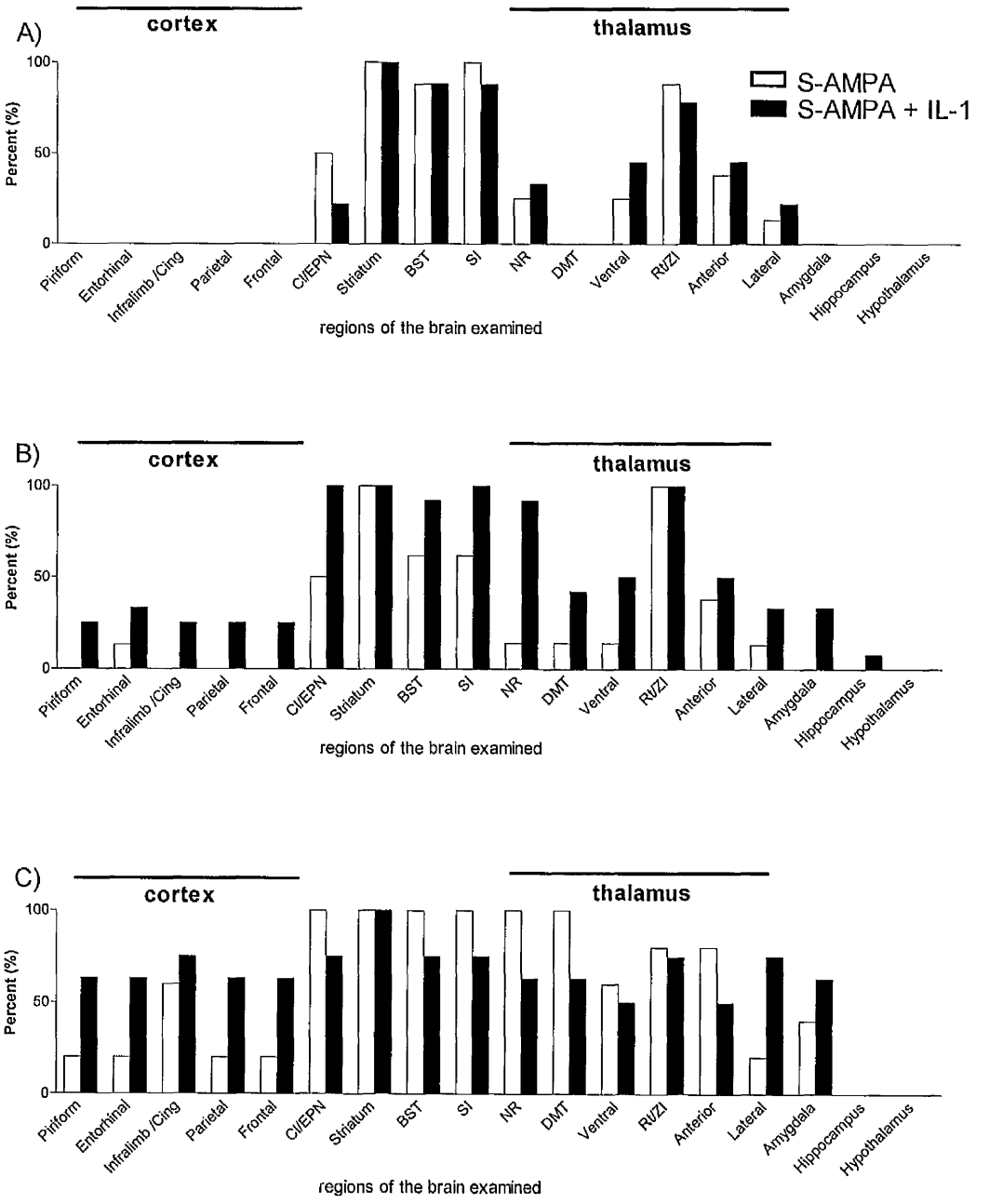

Figure 4.16: Sites in which degenerating neurones were observed in response to striatal injection of S-AMPA or S-AMPA with IL-1 4 h (A), 8 h (B) and 16 h (C) after striatal treatments in the rat. Data are expressed as the percent of animals noted to have damage per region specified (n=5-12).

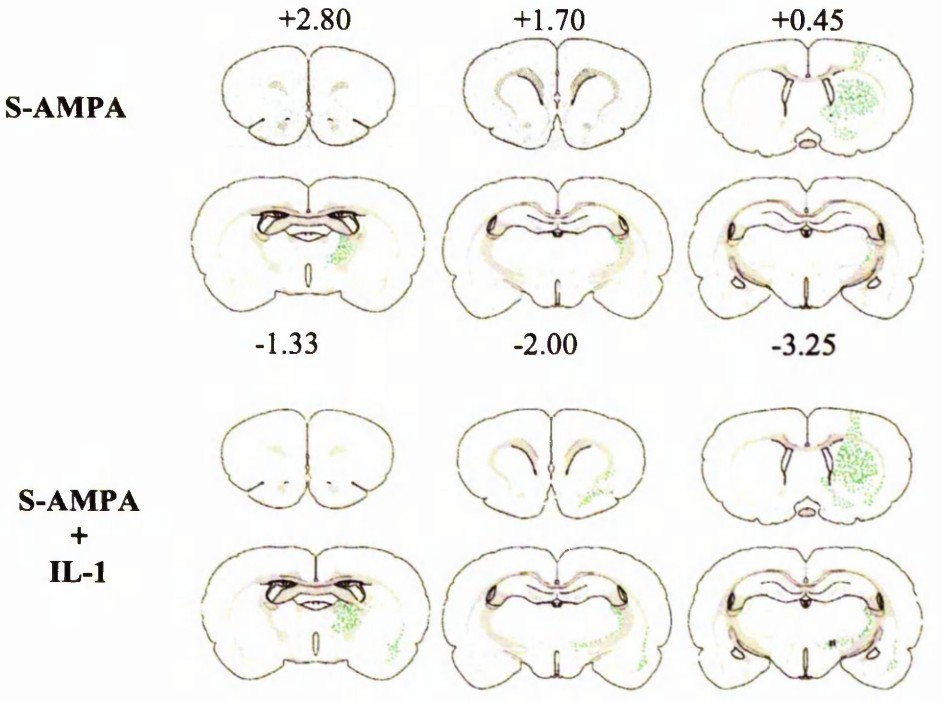

Figure 4.17: Representative diagram of the temporo-spatial progression of neuronal degeneration in response to intrastriatal injection of S-AMPA *vs* S-AMPA with IL-1 4 h after striatal injections Green dots represent regions of incomplete cell death.

Neuronal degeneration induced by S-AMPA alone was observed in similar regions (including the neocortex) as those seen in response to striatal injection of S-AMPA with IL-1 (Figures 4.16,4.18,4.19). However, the neuronal damage in response to S-AMPA with IL-1 (*vs* S-AMPA alone) occurred earlier (neocortical cell death was first observed 8 h after striatal injection of S-AMPA with IL-1 compared to 16 h in response to S-AMPA alone), and more frequently (neocortical cell death 16 h after striatal injection of S-AMPA (1/4 rats) *vs* S-AMPA with IL-1 (6/8 rats) (Figure 4.16,4.18,4.19).

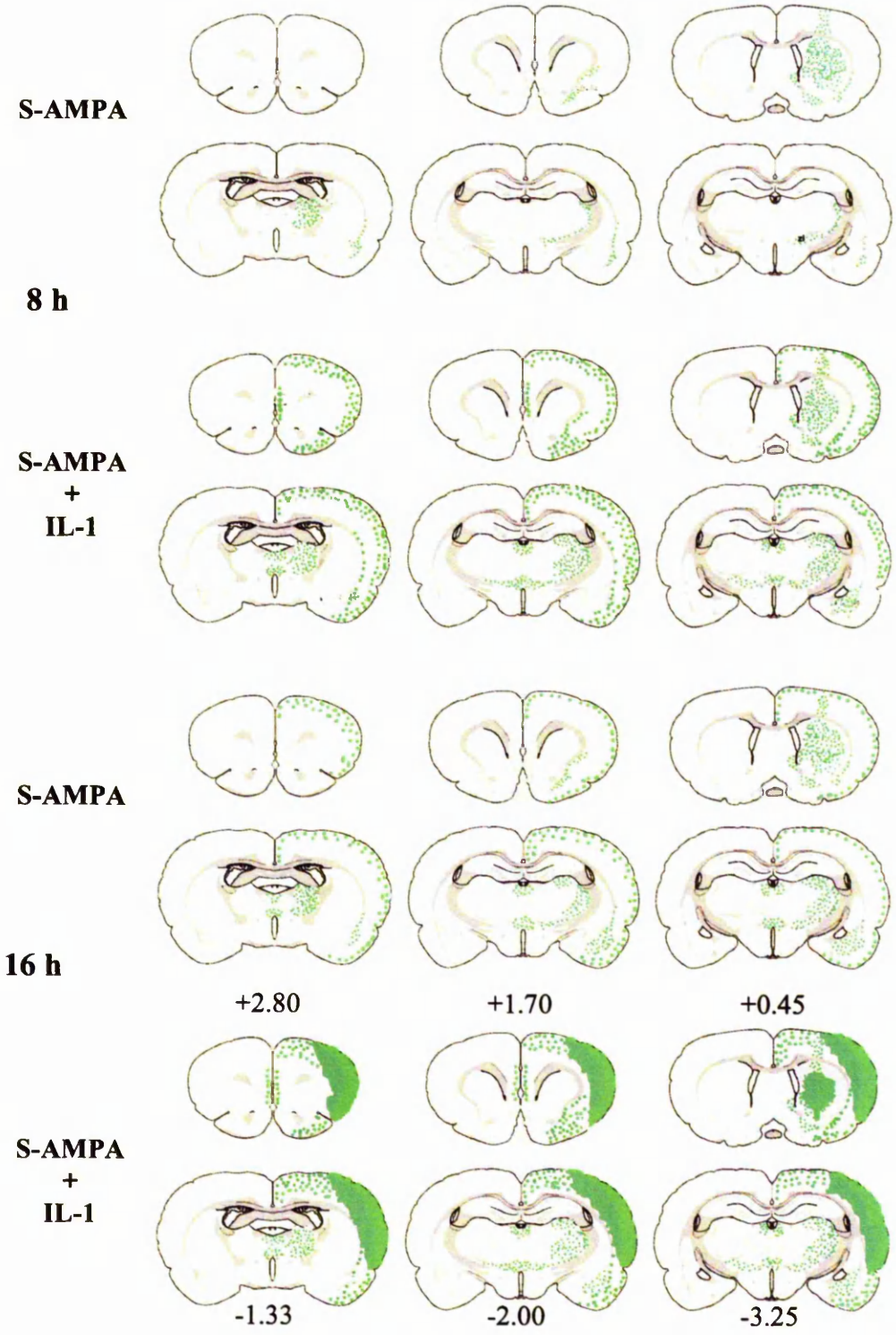

Figure 4.18: Representative diagram of the temporo-spatial progression of neuronal degeneration in response to intrastriatal injection of S-AMPA *vs* S-AMPA with IL-1 8 h and 16 h after striatal injections Green dots represent regions of incomplete cell death while filled areas represent regions of complete neuronal loss. Numbers represent distance of sections from bregma (mm).

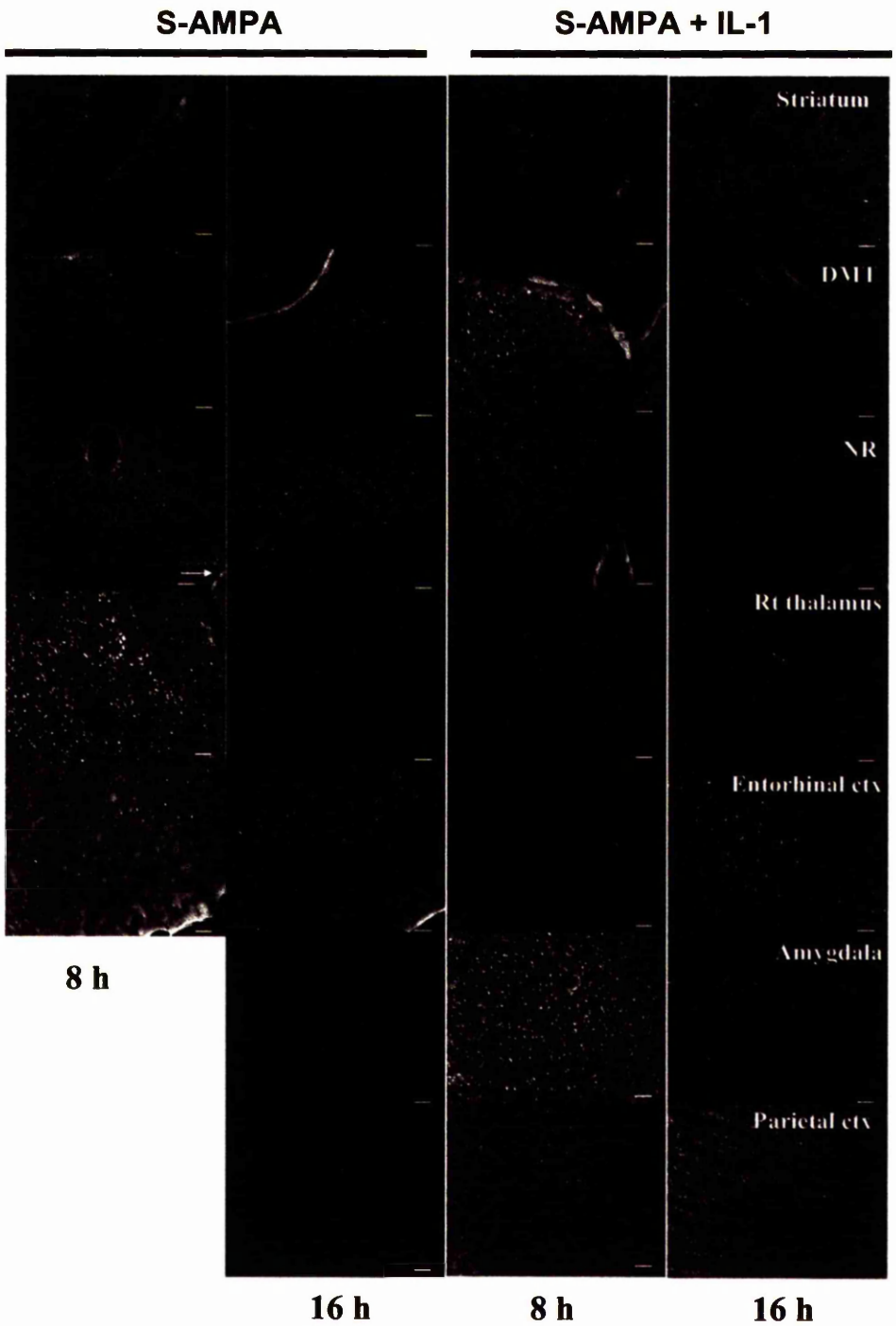

Figure 4.19: Photomicrographs demonstrating regions in which degenerating neurones were observed 8 h and 16 h after striatal injection of S-AMPA or S-AMPA with IL-1 in the rat. White dots represent degenerating neurones. Scale bar =70µm

Degenerating neurones were also observed in the contralateral NR (1/5) and DMT (1/5) in response to S-AMPA (8 h), and in the NR (7/12)), DMT (3/12), BST (1/12) and Rt/ZI (6/12) in response to S-AMPA with IL-1 (8 h). By 16 h post injection, contralateral neuronal damage in response to S-AMPA increased and was also observed in the Rt/ ZI.

The temporal or spatial progression of neuronal damage in subcortical or allocortical regions was not consistent. In the neocortex however, neuronal degeneration did progress uniformly, with the area of death spreading inwards from the outer (I and II) to deeper layers with time (Figure 4.18).

4.5.2.3 Neuronal damage and irIL-1β expression

Compared to irIL-1β, degenerating neurones were seen in more regions of the brain in response to S-AMPA or S-AMPA with IL-1 (Figure 4.20).

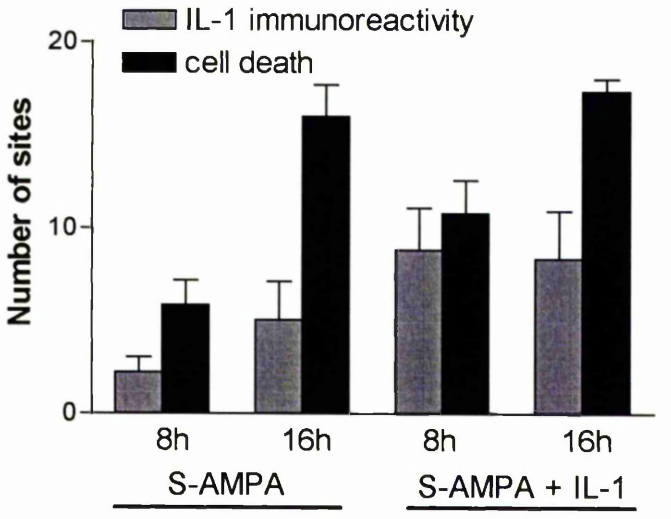

Figure 4.20: Number of sites in which neuronal damage and irIL-1β was observed 8 h or 16 h after intrastriatal injection of S-AMPA or S-AMPA with IL-1 (n=3-5).

IrIL-1β cells were not always seen in regions that stained for fluoro-jade, and equally irIL-1β expression was noted in the absence of neuronal damage (Figure 4.21,4.22). IrIL-1β expression in the absence of degenerating neurones was most notable in the neocortex in rodents 8 h after injection of S-AMPA with IL-1, suggesting that irIL-1β expression precedes neuronal damage in the neocortex (Figure 4.21,4.22). In addition, with the exception of rare irIL-1β cells seen in the hypothalamus (in 1/5 animals in response to S-AMPA with IL-1 (8 h)) irIL-1β positive cells were observed only in regions that subsequently died 16 h after striatal injection of S-AMPA with IL-1.

The progression of irIL-1β in the neocortex mirrored that of the progression of neuronal degeneration, and both phenomenon progressed inwards from the outer layers of the neocortex (Figure 4.6, 4.10, 4.18).

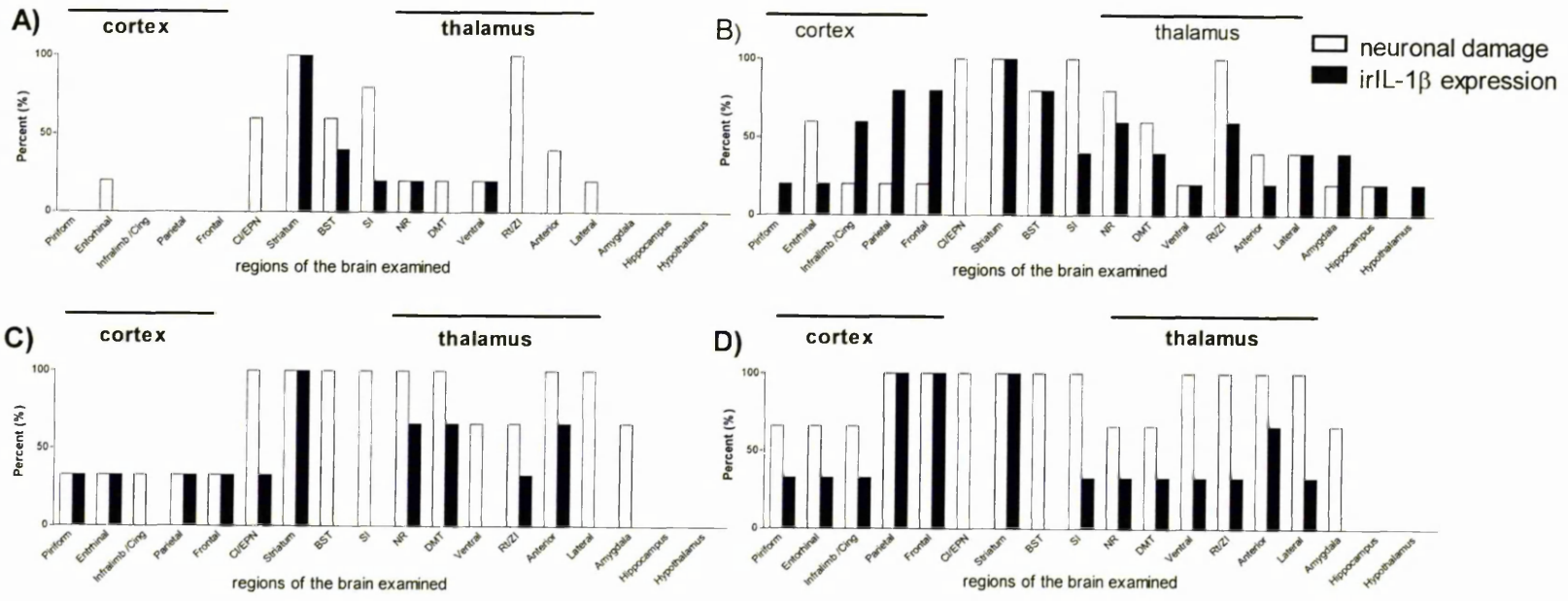

Figure 4.21: Regions of the brain in which neuronal damage and cell death and irIL-1β were observed in response to striatal injection of S-AMPA (A,C), or S-AMPA with IL-1 (B,D) 8 h (A,B) and 16 h (C,D) after striatal injection. Data are expressed as the percent of animals in which irIL-1β or neuronal damage was observed per site per time point (n=3-5).

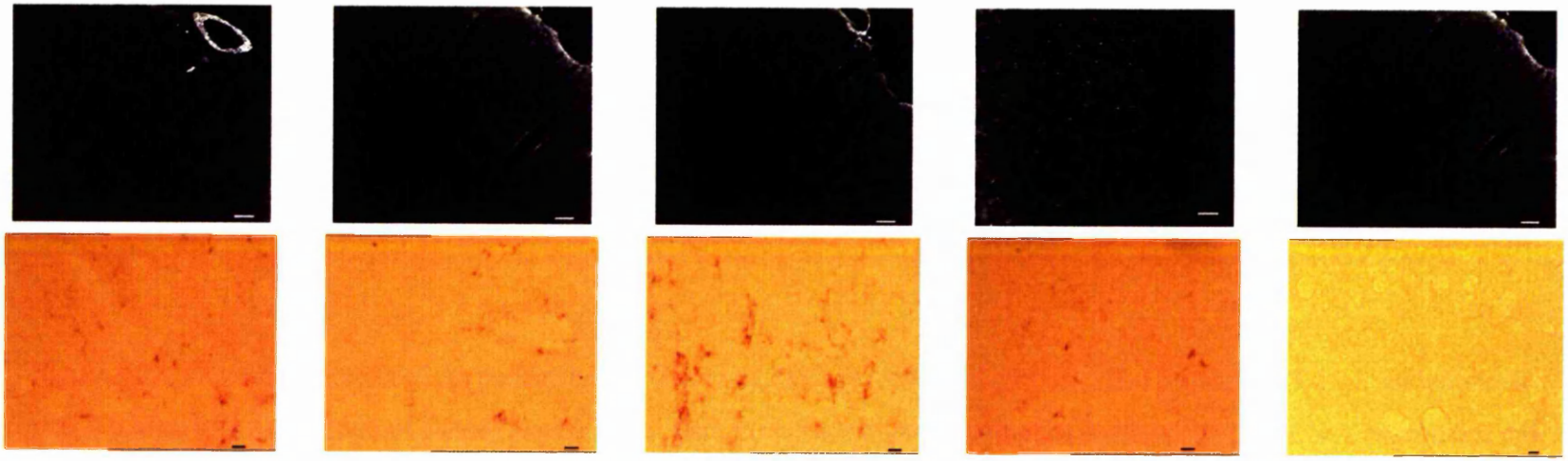

Figure 4.22: Photomicrographs of the parietal cortex (neuronal damage (A-E) and cortical irIL-1β staining (F-J)) from individual rats, 8 h after striatal injection of S-AMPA with IL-1. Data from these photomicrographs demonstrate that; irIL-1 expression was not observed in all rodents (J); that neuronal damge and irIL-1 may coexist (D, I); and that irIL-1 was observed in the absence of cortical degenerating neurones (A-C compared to F-H). Scale bar A-E=35μm, F-J=20μm.

4.4 Discussion

The results obtained in this chapter demonstrated that the temporal and spatial progression of irIL-1β in response to S-AMPA or S-AMPA with IL-1 was variable. IrIL-1β was expressed in similar regions in response to S-AMPA or S-AMPA with IL-1β, and hypothalamic irIL-1β noted in only 1/9 rats injected with S-AMPA with IL-1. The temporo-spatial progression of neuronal damage in response to S-AMPA or S-AMPA with IL-1 was also variable. IrIL-1β in the neocortex in response to S-AMPA with IL-1 was however consistently observed 8 h after striatal injections (in 4/5 rats; Figure 4.22). Neuronal damage in the neocortex induced by intrastriatal S-AMPA with IL-1 (8 h), in contrast was observed in only 1/5 rats, suggesting that irIL-1β expression preceded neuronal damage in the neocortex in this paradigm. These observations allow a number of points to be addressed.

4.4.1 Methods used.

The anti-rat IL-1β antibody used to localize irIL-1β in this study is a polyclonal antibody that recognizes multiple epitopes in the mature IL-1β peptide. As the pro-IL-1β fragment contains the full-length mature peptide, the antibody is unable to differentiate between pro and mature IL-1β, and results reported have to be interpreted with this in mind. Demonstration of the relative expression of pro or mature peptide could be determined by Western blot analysis of cortical brain homogenates. However, thus far, western blots on brain homogenates for IL-1β has not been successful largely due to high background. Therefore, this technique was not used in the present series of experiments to differentiate the nature of the IL-β protein.

Neuronal degeneration was studied in response to striatal treatments in this paradigm since cell death is a potent stimulus for irIL-1β induction, and this allows the temporo-spatial relationship between neuronal damage and irIL-1β to be documented. Degenerating neurones were localised using fluoro-jade staining of perfuse-fixed sections. The advantage of this technique over the use of cresyl violet staining has been discussed previously {Schmued, Albertson, et al. 1997} (Chapter 3).

The time points (4 h, 8 h, 16 h) chosen to study irIL-1β and neuronal damage were based on previous observations (Allan, unpublished). Neocortical cell death in response to S-AMPA with IL-1 is first observed 12 h after striatal injections, and becomes established at 16 h post injection on cresyl violet brain sections. IrIL-1β in the hypothalamus and striatum are observed 8 h after striatal injection of S-AMPA with IL-1, and irIL-1β expression in the hypothalamus precedes neocortical cell death {Allan, Parker, et al. 2000}. The 8 h time point was therefore chosen as the critical time point for this study since neocortical cell death is not reportedly present, while irIL-1β is up-regulated at sites considered important in the putative pathway for IL-1 action in acute neurodegeneration. IrIL-1β expression was also studied at time points before (4 h) and after (16 h) neocortical cell death is observed.

Finally, the aim of this study was to identify sites of irIL-1β induction in response to intrastriatal injection of S-AMPA *vs* S-AMPA with IL-1 using immunohistochemistry to map the 'putative pathway' of action of IL-1 in the brain in acute neurodegeneration in the rat. Immunohistochemistry was used to study irIL-1β expression because of its spatial and temporal sensitivity. In addition, whilst immunohistochemistry cannot

quantify the magnitude of a response compared to ELISA, counting of immunopositive cells in a standardised fashion, can allow for comparisons between treatment groups.

4.4.2 Site specific hypothesis

The main aim of this study was to identify brain regions through which IL-1 may act to exacerbate acute brain injury, according to the 'site specific action of IL-1' hypothesis {Allan, Parker, et al. 2000 ; Allan & Rothwell 2001}. This was based on the observations that (i) a significant increase in hypothalamic IL-1 is seen in response to S-AMPA with IL-1 and IL-1 alone (*vs* S-AMPA or vehicle), (ii) that IL-1 protein expression in the hypothalamus (8 h) precedes cell death in the neocortex (first observed 12 h after surgery) in response to striatal injection of S-AMPA with IL-1{Allan & Rothwell 2001} and (iii) that intra hypothalamic injection of IL-1ra reduces this cell death (see **section 1.10.1**). On this basis, the hypothalamus was considered to be critical in mediating the effects of IL-1 in acute neurodegeneration {Allan, Parker, et al. 2000}. The hypothalamus is an important site of action of IL-1, as IL-1 effects on host tissue defence responses to peripheral infection, inflammation, and injury are mediated through this region {see Hopkins & Rothwell 1995; Rothwell & Hopkins 1995} The pyrogenic effects of IL-1 in particular are mediated through specific sites in the hypothalamus {Cartmell, Luheshi, et al. 1999; Cartmell, Luheshi, et al. 2001}. In addition, it is a rare site at which the IL-1R1 has been localized to the brain parenchyma {Ericsson, Liu, et al. 1995}. These observations all support a role for actions of IL-1 in the hypothalamus.

However in contrast to the observation obtained by Allan et al, in this experiment, no irIL-1β was observed in the hypothalamus in response to striatal injection of IL-1 at any time point. In addition only in 1 animal (out of 9) was hypothalamic irIL-1β observed in

response to striatal injection of S-AMPA with IL-1 (8 h). The reason for this discrepancy in results is not clear, but it may relate to the antigen presentation, accessibility, and/or recognition property differences between ELISA and immunohistochemical techniques. The concentration of irIL-1β (pg of IL-1) induced by striatal injection of S-AMPA with IL-1 or IL-1 alone was 4-fold greater in the hypothalamus (8 h after injection) *vs* the striatum (4 h) {Allan, Parker, et al. 2000}. In this study, irIL-1β was readily visible 4 h after striatal treatments, and therefore differences in the sensitivity between techniques used for detection of irIL-1β are unlikely.

Intraparenchymal injection of IL-1 in the rat CNS induces an intense myelomonocytic infiltrate into the choroid plexus, meninges, and ventricular system, and infiltrating cells strongly express IL-1 {Andersson, Perry, et al. 1992; Proescholdt, Chakravarty, et al. 2002}. Brain regions that were labelled as hypothalamus in the study by Allan et al 2000, included parts of the ventral third ventricle, midline thalamic nuclei, and possibly meninges {Allan, Parker, et al. 2000}. Therefore, contamination of hypothalamic brain samples with tissue from these regions is more likely to account for the increased IL-1 protein observed in the hypothalamus in response to S-AMPA with IL-1 or IL-1 alone {Garabedian, Lemaigre-Dubreuil, et al. 2000; Allan, Parker, et al. 2000}.

Although hypothalamic irIL-1β was not observed, widespread subcortical irIL-1β expression was observed. This was observed in similar regions in response to S-AMPA with IL-1 or S-AMPA alone. These data suggest that subcortical irIL-1β was induced by an S-AMPA dependent process, and that neocortical cell death is not dependent on the site of subcortical irIL-1β expression.

'Distant' neocortical cell death has been reported previously only in response to co-infusion of S-AMPA with IL-1 {Lawrence, Allan, et al. 1998; Grundy 2000}, and has never been reported in response to S-AMPA alone. Neocortical cell death is therefore proposed to be IL-1 dependent. Neocortical cell death in this set of experiments however, was induced by intrastriatal S-AMPA alone (in 1 out of 4 rats) 16 h after surgery (see Figure 4.18)). This was the first time that cell death in the neocortex was observed in response to S-AMPA alone. However, this observation, has since been verified independently by others in the lab. This observation suggests that cell death may actually be driven by an S-AMPA dependent process rather by an IL-1 dependent process as previously thought {Allan, Parker, et al. 2000}.

Neocortical cell death in this paradigm has previously been referred to as 'distant' cell death. 'Distant' death although predominantly limited to subcortical regions was observed in response to S-AMPA alone as well as S-AMPA with IL-1 in these experiments (**section 4.5.2.2**). 'Distant' subcortical cell death is also reported to occur in response to intrahippocampal S-AMPA or kainic acid in the rat {Sperk 1994; Lees & Leong 2001}, and 'distant' neocortical cell death occurs in response to kainic acid administration alone{Ben Ari, Tremblay, et al. 1980}. These data further support the postulate that 'distant' neocortical cell death is dependent on an S-AMPA phenomenon rather than due to an IL-1 specific process as previously thought.

Finally, it has recently been demonstrated that intracortical injection of IL-1ra reduces neocortical cell death induced by S-AMPA with IL-1. Taken together, these data all argue against the hypothesis that IL-1 mediates acute brain injury by acting through an IL-1 specific pathway in the brain.

Whilst data presented in this chapter have suggested that 'distant' cell death is an S-AMPA dependent process, it is important to note that increasing the dose of S-AMPA does not result in an increased frequency of 'distant' neocortical cell death {Grundy 2000}. Further, observations that neocortical cell death occurs with greater frequency when S-AMPA with IL-1 is injected into the shell *vs* the core of the nucleus accumbens, or into the ventral *vs* the dorsal striatum does suggest that the site of injection of S-AMPA with IL-1 is important. Combined with the observations from this study that suggest that 'distant' cell death was dependent on an S-AMPA phenomenon, and that IL-1ra in the cortex reduces neocortical cell death (Allan unpublished), the dependency of neocortical cell death on site of injection, may actually be related to the site at which S-AMPA (rather than IL-1) is injected. The effect of site of injection of S-AMPA alone on distant' cell death has not been investigated.

4.4.3 IL-1 immunoreactivity and cell death

Neuronal damage was studied because cell death is a potent stimulus for irIL-1β expression {Davies, Loddick, et al. 1999; Pearson, Rothwell, et al. 1999}. In addition, irIL-1β expression was observed in similar regions (**section 4.2.2.4 and 4.2.2.5**) to those in which neuronal damage was observed in response to intrastriatal injection of S-AMPA with IL-1 24 h after injection (chapter 3). However, the temporo-spatial progression of both neuronal damage and irIL-1β expression observed were variable. In addition, irIL-1β and neuronal damage were poorly co-localised in most brain regions in response to S-AMPA or S-AMPA with IL-1 (**section 4.5.2.2**). Neuronal degeneration was however only seen in regions in which irIL-1β was observed. Conversely, irIL-1β was observed only in sites that died 16 h or 24 h (chapter 3) after striatal injection of S-AMPA with IL-1 (with the exception of the one animal in which irIL-1β was seen in the

hypothalamus). These data suggest that neuronal degeneration and irIL-1β expression are related, although it is not clear how.

In most experimental models of acute neuronal degeneration in the rat, the temporo-spatial progression of irIL-1β expression parallels cell death. Further, irIL-1β expression in response to cell death induced by either MCAO, or intrastriatal injection of excitotoxin is greatest at the boundary of the region, with low / absent irIL-1β cells being observed in regions of complete neuronal loss {Davies, Loddick, et al. 1999; Pearson, Rothwell, et al. 1999}. The variability of irIL-1β expression (particularly in regions in which neuronal damage was observed in the absence of irIL-1β) may be therefore be related to the magnitude of neuronal damage as suggested by Pearson (1999) and Davies (1999) {Davies, Loddick, et al. 1999; Pearson, Rothwell, et al. 1999}. However, this is unlikely as irIL-1β expression was still seen in regions in which complete neuronal loss was observed (striatum, neocortex). Interestingly, irIL-1β in the study by Davies et al was only observed at times when neuronal damage was well established. In the present experiment, irIL-1β was often observed in the absence of neuronal damage suggesting that irIL-1β expression in this paradigm was not induced by death alone.

Whilst irIL-1β distant to the site of injury is seen in response to cerebral ischaemia induced by MCAO in the rat, this is seen late (48 h after onset of cerebral ischaemia), and in regions which do not subsequently die {Davies, Loddick, et al. 1999}. 'Distant' irIL-1β expression is also seen in response to peripheral kainic acid injection in the rat. In addition, 'distant' irIL-1β expression in response to kainic acid is observed in similar regions to those in which irIL-1β was observed in response to S-AMPA or S-AMPA

with IL-1 described (this chapter). However, in contrast with the findings reported in this chapter, spatial distribution of irIL-1β expression was not variable, and well correlated with neuronal damage {Eriksson, Van Dam, et al. 1999}. The reason for this discrepancy is again not clear. Cell death in response to kainic acid is well reported to be variable, and lack of variability reported by Eriksson et al (1999) may be due to the fact that they described pooled data rather than data on an individual animal basis.

The problems of variability in irIL-1β expression or neuronal damage observed were however limited to subcortical regions in this experiment. A clearer relationship between irIL-1β and neuronal damage was observed in the neocortex. IrIL-1β in the neocortex was consistently induced (4/5 rats) 8 h after intrastriatal injection of S-AMPA with IL-1. In contrast, neuronal damage 8 h after striatal injections was only seen in 1/5 of these rats. At 16 h after striatal injection of S-AMPA with IL-1, irIL-1β and neuronal degeneration was seen in all animals. This suggests that irIL-1β precedes neuronal degeneration in the rat neocortex in response to S-AMPA with IL-1. IrIL-1β reportedly precedes cell death in response to striatal injection of the NMDA agonist methanoglutamate (Mglu) {Pearson, Rothwell, et al. 1999}. IrIL-1β positive cells are localized to the lesion 4 h after intrastriatal injection of Mglu, although by 8 h irIL-1β cells are seen in the regions observed to die at 24 h {Pearson, Rothwell, et al. 1999}. In this paradigm cell death was identified by paucity of staining on cresyl violet brain sections and therefore, the margin of cell death may have been underestimated. Neuronal degeneration in the present study was determined on fluoro-jade staining and therefore was unequivocal and required no specialized histopathology skills to enable the recognition of dead/dying cells {Schmued, Albertson, et al. 1997}. The data presented here in which irIL-1β was seen in 3/5 rodents in the absence of cell death (on

brain sections from the same animal) suggests unequivocally that irIL-1β preceded cell death in the neocortex 8 h after intrastriatal co-infusion of S-AMPA with IL-1. This is the first time that irIL-1β has been reported to precede cell death in the neocortex in the rat. In addition, the observation that intracortical injection of IL-1ra reduces cell death in the neocortex in response to S-AMPA with IL-1, suggests that IL-1 is a primary mediator of cell death in the neocortex in this paradigm.

4.4.4 How does IL-1 induce 'distant' cell death in this paradigm?

Data obtained from this experiment argues against IL-1 mediating its effects on neurodegeneration through specific sites in the brain. However, data obtained here demonstrated that irIL-1β and neuronal damage was observed in 'distant' sites in response to S-AMPA or S-AMPA with IL-1, and this suggested that 'distant' neuronal damage and irIL-1β expression were a result of an S-AMPA dependent process. Increased sites of irIL-1β and neuronal damage were seen in response to S-AMPA with IL-1 compared to S-AMPA alone, suggesting that IL-1 increased the S-AMPA mediated process responsible for inducing distant irIL-1β and neuronal damage. 'Distant' neocortical cell death induced by striatal injection of S-AMPA with IL-1 and 'distant' death induced by intrahippocampal injection of S-AMPA or kainic acid can both be reduced by NMDA antagonists in the rat, suggesting that 'distant' cell death (neocortical or subcortical) is induced by a similar mechanisms.

The number of sites in which distant cell death is observed correlates with seizure duration, and is reduced by anticonvulsants {Lees & Leong 1994; Lees & Leong 2001} IL-1 is rapidly up-regulated by bicuculline-induced seizures, and IL-1 increases kainic acid induced seizures{Vezzani, Conti, et al. 1999}. Therefore, it is hypothesized that IL-1 exacerbates excitotoxin induced cell death by increasing seizures (see chapter 5).

Chapter 5: IL-1 seizures and cell death

5.1 Introduction

The mechanism(s) by which the cytokine IL-1 exacerbates excitotoxic brain injury remain unclear. Co-infusion of S-AMPA with IL-1 (*vs* S-AMPA alone) exacerbates cell death. This exacerbation, results predominantly from an increase in 'distant' ipsilateral neocortical cell death. It has been suggested that this neocortical cell death is mediated by IL-1 acting through the hypothalamus {Allan, Parker, et al. 2000}.

However in the studies performed in this thesis, 'distant' ipsilateral neocortical cell death was observed in response to intrastriatal injection of S-AMPA alone, and no consistent hypothalamic IL-1 expression was observed in response to intrastriatal injection of S-AMPA with IL-1 or IL-1 as suggested previously (chapter 4) {Allan, Parker, et al. 2000}. Furthermore, 'distant' cell death was also observed in subcortical regions in response to intrastriatal injection of S-AMPA and S-AMPA with IL-1 in the rat (chapters 3 and 4). These data suggest that the 'distant' cell death in the experimental paradigm used here is an S-AMPA dependent process. Since neuronal degeneration is observed in more 'distant' sites, and that neocortical cell death occurs earlier and more frequently in response to S-AMPA with IL-1 compared to S-AMPA alone, this suggests that IL-1 exacerbates cell death by potentiating an S-AMPA dependent process.

'Distant' cell death (most commonly in subcortical regions) has also been observed in response to intraparenchymal, intracerebroventicular (icv), and peripheral injection of kainic acid as well as in response to intrahippocampal injection of S-AMPA in rats {Ben Ari 1985; Lees & Leong 2001}. The 'distant' cell death induced by kainic acid or intrahippocampal S-AMPA is reduced by administration of anticonvulsants and is therefore thought to be dependent on seizure activity {Ben Ari, Lagowska, et al. 1978}.

IL-1 has recently been implicated in seizure activity. IL-1 expression increases rapidly in the rat hippocampus in response to bicuculline or kainic acid induced seizures, {Vezzani, Conti, et al. 1999; de Simoni, Perego, et al. 2000} and exogenous administration of IL-1 significantly increases the duration of kainic acid induced seizures in the rat, whilst administration of the selective IL-1 receptor antagonist, IL-1ra, significantly reduces the latency to onset and duration of motor seizures in response to bicuculline induced epilepsy in the mouse {Vezzani, Conti, et al. 1999; Vezzani, Moneta, et al. 2000}.

Therefore the objective of this chapter was to test the hypothesis that IL-1 exacerbates excitotoxin (S-AMPA) induced seizure activity and that this seizure activity contributes directly to cortical cell death induced by intrastriatal injection of S-AMPA with IL-1.

5.2 Experiment: Effect of the anticonvulsant diazepam, on seizures and cell death induced by intrastriatal injection of S-AMPA or S-AMPA with IL-1

5.2.1 Method

Striatal injections of vehicle, IL-1 (10ng), S-AMPA (7.5nmol) or S-AMPA (7.5nmol) with IL-1 (10ng) were performed as described in **section 2.3.1.** Animals were divided into four different treatment groups which received either: vehicle (i.p) and striatal injection of S-AMPA (7.5 nmol) with IL-1 (10ng) (n=18); vehicle (i.p) and striatal injection of S-AMPA (7.5 nmol) with 0.1%BSA/saline (n=13); diazepam (i.p) and striatal injection of S-AMPA (7.5 nmol) with IL-1 (10ng) (n=15); or diazepam (i.p) and striatal injection of S-AMPA with 0.1%BSA/saline (n=12). Diazepam (5mg/kg i.p) or

the equivalent volume of vehicle was administered 30 min before striatal injections and then hourly for a further 5 h.

After surgery, all animals were allowed to recover, housed individually, and filmed to record the motor expression of seizures using tripod mounted camcorders (Sony Corporation, UK) connected to cassette video recorders (Samsung Electronics, UK). Recording of the motor expression of seizures began after complete recovery from the effects of surgery, and was continued for a minimum period of 8 hours after striatal injection.

Twenty-four hours after striatal treatments, the animals were killed by exposure to increasing levels of carbon dioxide, and the brains were removed and frozen on dry ice. The volume of cell death, and number of sites of neuronal degeneration was determined from coronal cryostat sections stained with cresyl fast violet or fluoro-jade respectively as described previously **(section 2.4.1).** Seizures were scored according to the scale described in (**section 2.4.3.1**). Seizure frequency and duration were observed and recorded for an 8 h period after striatal injections.

5.2.2 Results

5.2.2.1 Cell death

The volume of damage induced by striatal injection of S-AMPA was limited predominantly to subcortical regions. Co-infusion of S-AMPA with IL-1 into the striatum significantly increased the total volume of cell death (260%, $P<0.001$) over that induced by striatal injection of S-AMPA alone (Figure 5.1). This increased damage was due mainly to a 7.5-fold increase in the extent of cortical cell death ($P<0.001$)

(Figure 5.1). No significant difference in subcortical cell death was seen between rats that received intrastriatal S-AMPA with IL-1, or S-AMPA alone (Figure 5.1).

Diazepam administration had no significant effect on the lesion volume induced by striatal injection of S-AMPA alone (Figure 5.1). However, the increased cell death resulting from co-infusion of IL-1 with S-AMPA was significantly reduced by the anticonvulsant diazepam ($P< 0.001$). Diazepam also significantly reduced both the cortical (82%, $P<0.001$) and subcortical cell death (32%, $P<0.05$) observed in response to striatal injection of S-AMPA with IL-1.

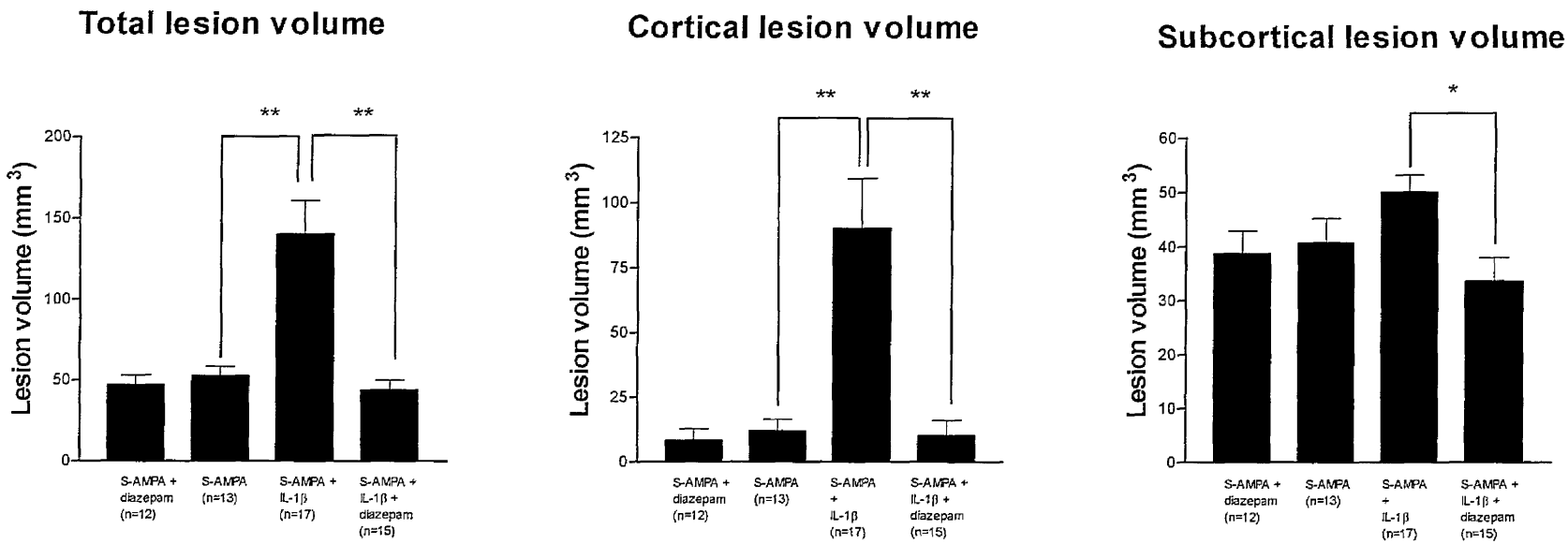

Figure 5.1: Volume of damage induced by striatal injection of S-AMPA with IL-1 ± diazepam (i.p) or S-AMPA ± diazepam. n = number of animals in each experimental group. All data are expressed as mean ± SEM. (F values: Total lesion volume ($F=13.67$, $P<0.001$), Cortical lesion volume ($F=11.75$ $P<0.001$), Subcortical lesion volume ($F=3.258$, $P<0.05$)) (* $P<0.05$, ** $P<0.001$).

Consistent with the observations in Chapter 3 & 4, cell death was seen in similar regions in response to intrastriatal injection of S-AMPA with IL-1 as with S-AMPA alone. Co-infusion of S-AMPA with IL-1 increased (2-fold) the number of sites in which cell death was seen compared to intrastriatal injection of S-AMPA alone (Figure 5.2). Diazepam reduced the number of sites of cell death induced by S-AMPA (20%) and by S-AMPA with IL-1 (40% P<0.001) (Figure 5.2).

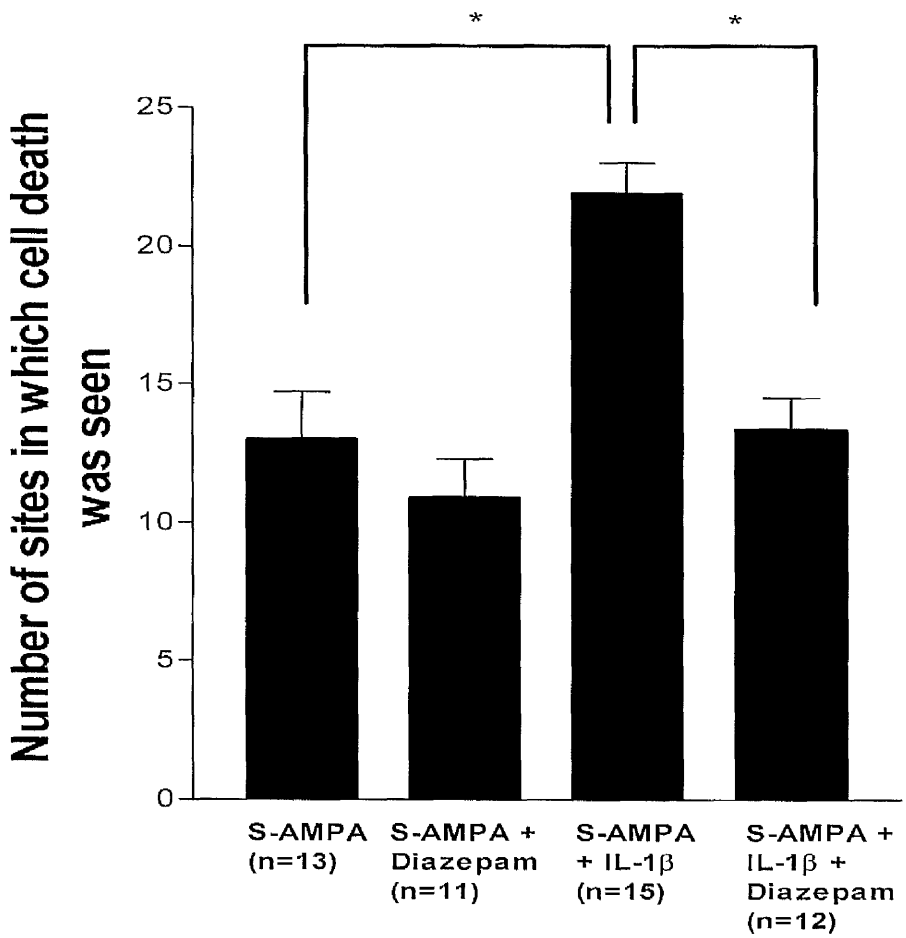

Figure 5.2: Number of sites in which cell death was seen in response to striatal injection of S-AMPA with IL-1 ± diazepam (i.p) or S-AMPA ± diazepam. n = number of animals in each experimental group. Bar represents median value for each group (F =13.78, P<0.001) (*P<0.001).

Whilst no neocortical cell death was observed in rats injected with diazepam and S-AMPA, neocortical cell death was seen in 2/13 (15%) of rats that received striatal injections of S-AMPA alone. In contrast, neocortical cell death was observed in 11/17

(64%) of rats injected with S-AMPA and IL-1, but in only 1/15 (7%) of rats that received diazepam (i.p) and a co-infusion of S-AMPA with IL-1.

5.2.2.2 Seizure duration and frequency

Epileptiform movements such as wet dog shakes, masticatory movements, facial twitching, and head nodding were all observed in response to intrastriatal injection of S-AMPA or S-AMPA with IL-1. However, only pawing, rearing, and rearing and falling behaviours were recorded, as these were considered to be the only behaviours that could be unequivocally identifiable and related to seizures. Seizures observed were similar to those seen in response to kainic acid, and therefore resembled 'limbic' seizures {Racine 1972}.

Intrastriatal injection of IL-1 failed to induce any detectable seizures (data not shown). After intrastriatal injection of S-AMPA, rats displayed an average of 119 fits, and spent an average of 1415 seconds fitting in the first 8 hours (Figure 5.3, 5.4). Co-infusion of S-AMPA with IL-1 increased seizure frequency by 1.5 fold ($P<0.05$) compared to striatal injection of S-AMPA alone (Figure 5.3).

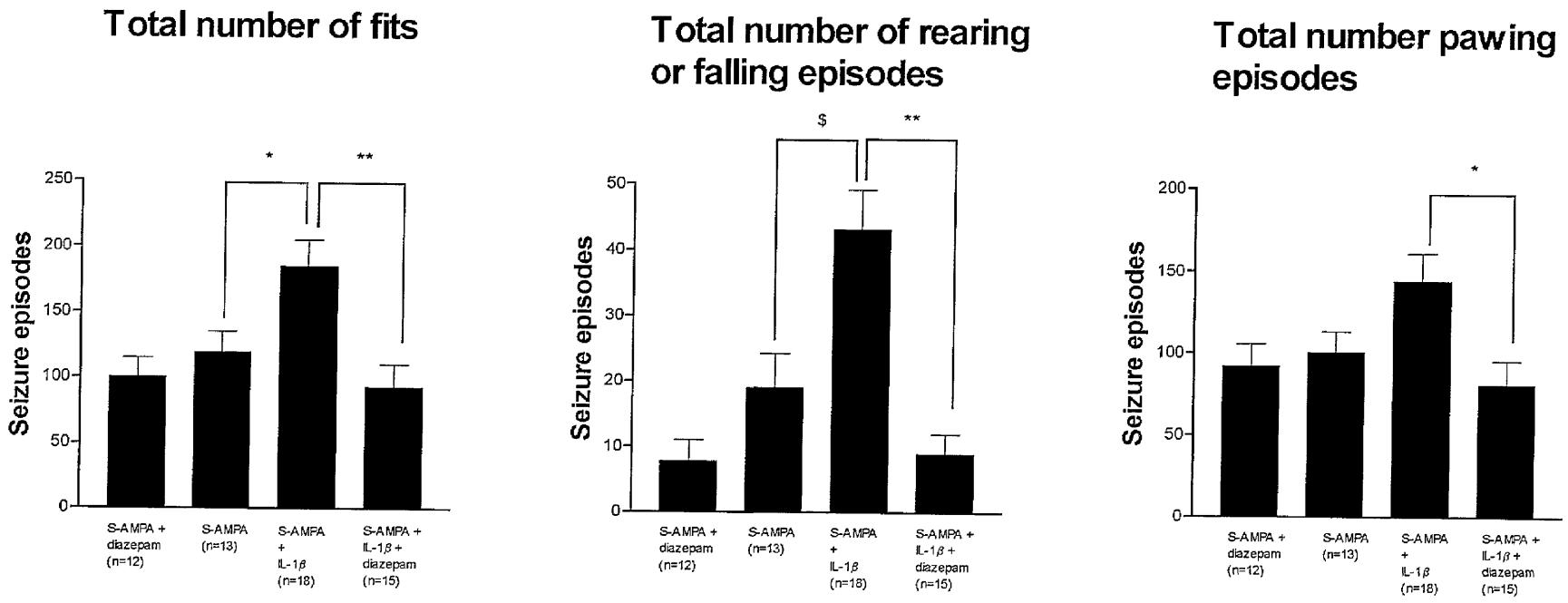

Figure 5.3: Number of fits observed (in an 8 h period) in response to in response to striatal injection of S-AMPA with IL-1 ± diazepam (i.p) or S-AMPA ± diazepam. n = number of animals in each experimental group. All data are expressed as mean ± SEM (F values: Total number of fits ($F=6.227$, $P<0.01$), rearing, or rearing and falling episodes ($F=12.62$, $P<0.01$), pawing episodes ($F=3.679$, $P<0.05$)) (* $P<0.05$, $P<0.01$ ** $P<0.001$).

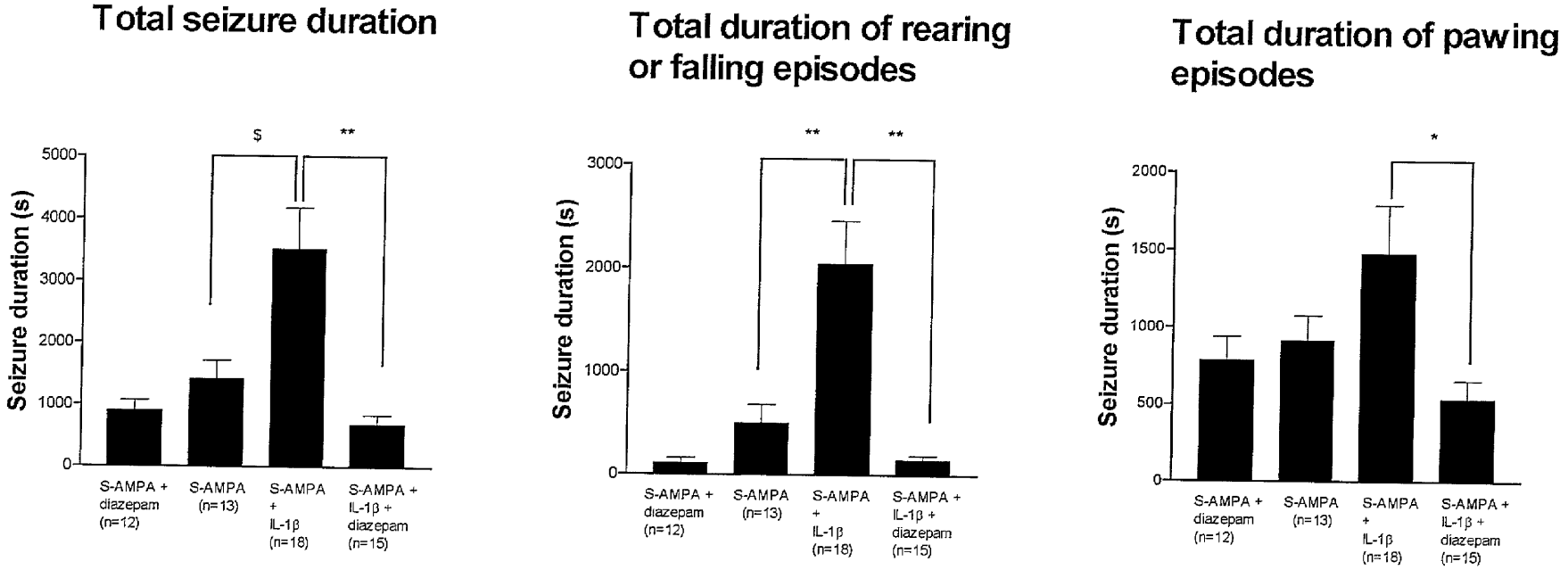

Figure 5.4: Duration of fits observed (in an 8 h period) in response to striatal injection of S-AMPA with IL-1 ± diazepam (i.p) or S-AMPA ± diazepam. n = number of animals in each experimental group. All data are expressed as mean ± SEM. (F values: Total seizure duration ($F=9.619$, $P<0.0001$), rearing, or rearing and falling duration ($F=12.60$, $P<0.0001$), pawing duration ($F=3.664$, $P<0.05$)) (* $P<0.05$, \$$P<0.01$, ** $P<0.001$).

Co-infusion of S-AMPA with IL-1 into the rat striatum also increased the total duration of seizures (over 0- 8 h period) by 2.5-fold compared to striatal injection of S-AMPA alone ($P<0.01$, Figure 5.4). Co-infusion of S-AMPA with IL-1 *vs* S-AMPA alone resulted in a two-fold increase in duration of stage 3 seizures, but this did not reach significance ($P>0.05$). The cumulative duration of the 'more intense' stage 4 or stage 5 seizures was increased four-fold ($P<0.01$) in response striatal co-infusion of S-AMPA with IL-1 *vs* S-AMPA alone (Figure 5.4).

A peak in seizure frequency in response to S-AMPA and S-AMPA with IL-1 was seen 3 h after striatal injections (Figure 5.5). A second peak in seizure frequency was observed 7 h after intrastriatal co-infusion of S-AMPA with IL-1. This was mainly due to an increase frequency of stage 4 or 5 seizure activity (Figure 5.5). Differences in fit frequency in response to intrastriatal injection of S-AMPA with IL-1 (*vs* S-AMPA) were seen late in the observation period (6-8 h), and resulted predominantly from an increase in the frequency of the 'more intense' stage 4 and stage 5 seizures (Figure 5.5).

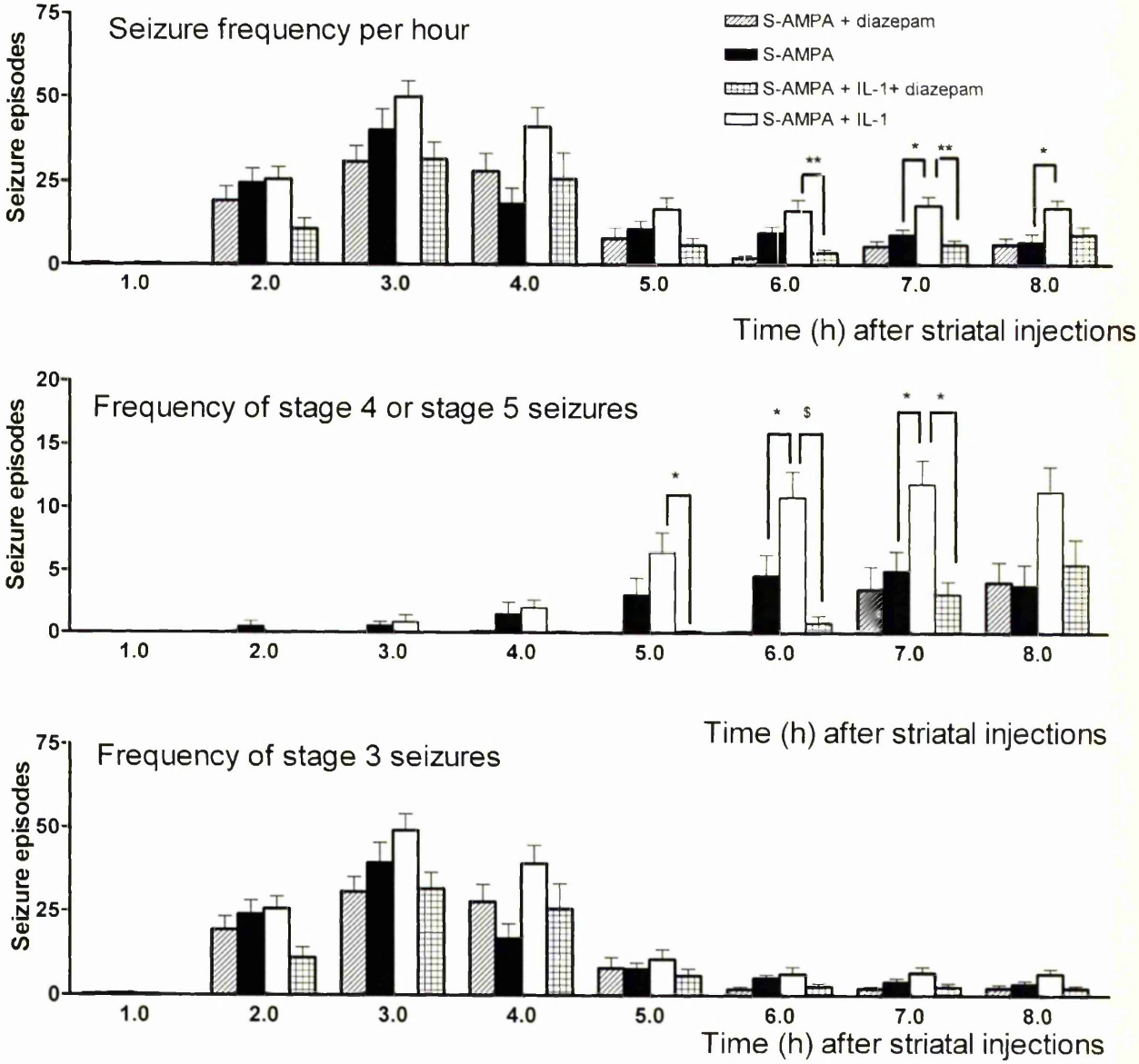

Figure 5.5: Fit frequency in response to striatal injection of S-AMPA with IL-1 ± diazepam (i.p.) or S-AMPA ± diazepam. a) total number of fits per hour, b) total number of stage 4 or 5 seizures per hour, c) total number of stage 3 seizures per hour. All data are presented as mean ± SEM. (*P<0.05, **P<0.005, $P<0.001).

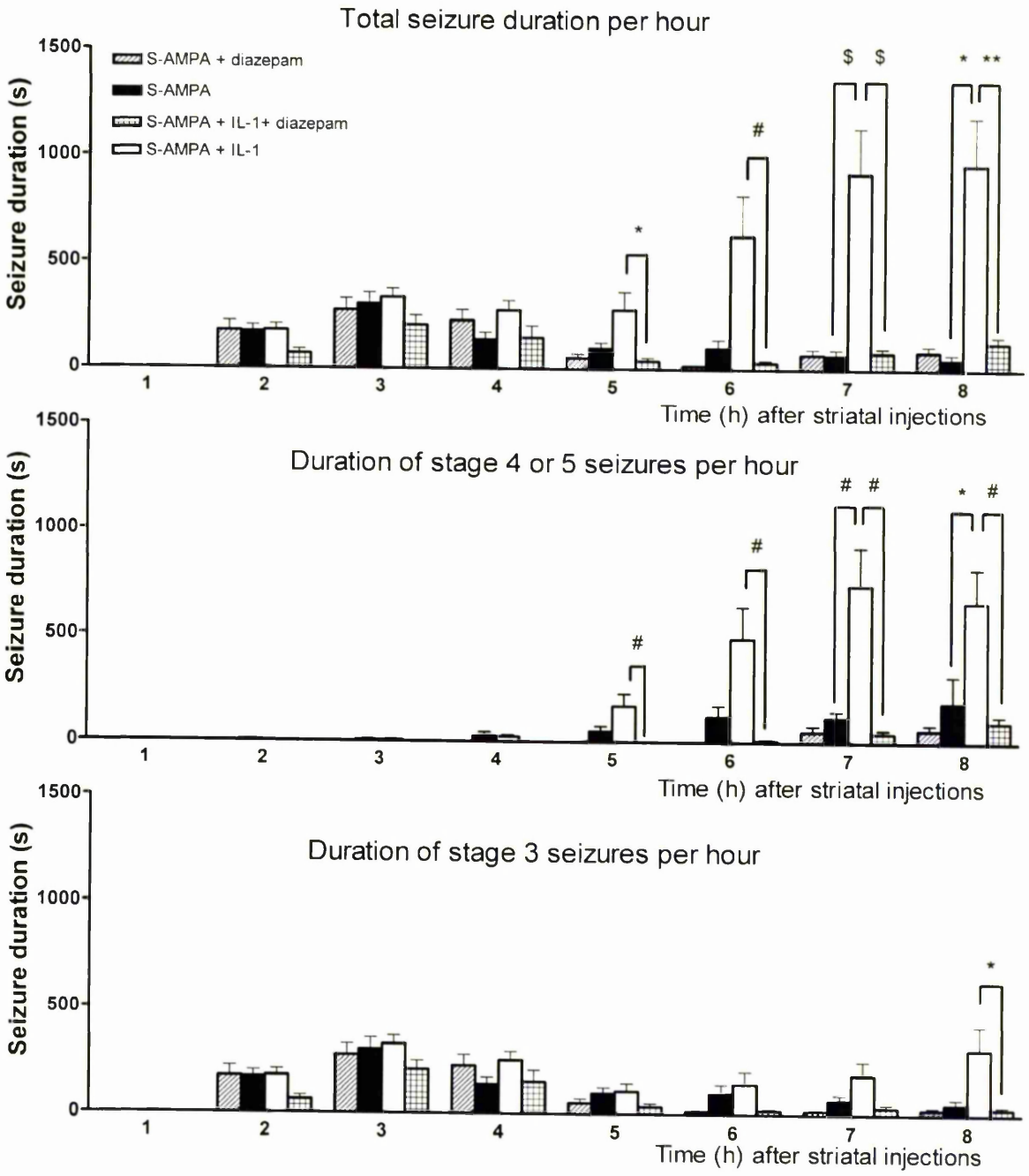

Figure 5.6: Seizure duration in response to striatal injection of S-AMPA with IL-1 ± diazepam (i.p.) or S-AMPA ± diazepam. a) total time spent fitting per hour, b) total duration of stage 4 or 5 seizures per hour, c) total duration of stage 3 seizures per hour. All data are presented as mean ± SEM. (*P<0.05, # P<0.01, **P<0.005, $P<0.001).

The difference in seizure duration between the S-AMPA alone, and S-AMPA with IL-1 treatment groups was also noted late in the observation period. Significant differences in duration of seizures were observed seven hours ($P<0.001$), and eight hours ($P<0.05$) after treatment (Figure 5.6). Differences in duration of stage 4 or 5 seizures between S-AMPA injected and S-AMPA with IL-1 injected rodents were also greatest in the seventh ($P<0.01$), and eighth ($P< 0.05$) hours after treatment (Figure 5.6).

Diazepam had no effect on the frequency or duration of seizures induced by S-AMPA alone. However, diazepam reduced both the total duration (by 82%, $P<0.001$) and frequency (by 50%, $P<0.01$) of seizure activity induced by striatal co-infusion of S-AMPA with IL-1 (Figure 5.3,5.4). Diazepam had the greatest effect on the duration (by 92%, $P<0.001$) and frequency (by 80%, $P<0.001$) of stage 4 and stage 5 seizures induced by S-AMPA and IL-1, although a significant reduction in the duration (63%, $P<0.05$) and frequency (44%, $P<0.05$) of stage 3 seizures was also observed (Figure 5.3,5.4). This reduction in seizure duration, intensity, and frequency occurred late in the seizure observation period (Figure 5.5,5.6).

A significant positive correlation was observed between seizure duration and total lesion volume (Figure 5.7).

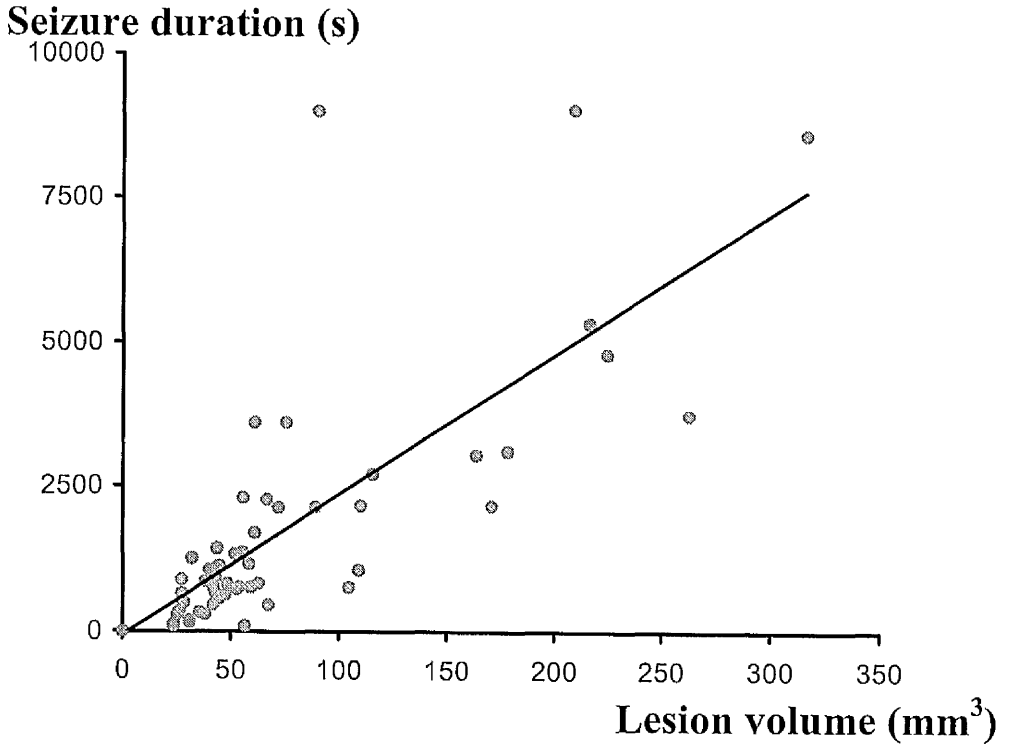

Figure 5.7: Relationship between seizure duration and total lesion volume in response to striatal injections of S-AMPA ± diazepam or S-AMPA with IL-1 ± diazepam (r^2= 0.58; P< 0.001).

5.3 Discussion

The present study demonstrated that co-infusion of S-AMPA with IL-1 into the rat striatum increased the duration, intensity and frequency of S-AMPA induced seizures. The anticonvulsant diazepam reduced both the late increase (observed 7-8 h after striatal injections) in seizure activity (duration, intensity, and frequency) and the increased cell death induced by striatal co-infusion of S-AMPA with IL-1. A significant, positive correlation between cell death volume and seizure duration was also observed. These data suggest that IL-1 exacerbates S-AMPA induced cell death by increasing the duration and intensity of seizures.

Whilst diazepam reduced seizures induced by S-AMPA with IL-1, diazepam did not reduce duration or frequency of seizures induced by intrastriatal injection of S-AMPA alone. However, diazepam did disproportionately reduce stage 4 and 5 (reduced by 70%) *vs* stage 3 (reduced by 15%) S-AMPA induced seizures. A similar disproportionate reduction was seen in seizure duration in response to S-AMPA with IL-1, and therefore, the anticonvulsant action of diazepam may be specific to the type of seizures induced.

Part of the seizure behaviour pattern that was scored was barrel rolling. This was scored as seizure behaviour as it was normally accompanied by pawing. However, this behaviour has been related to increased dopaminergic activity in the striatum and barrel-rolling can be induced by the injection of a variety of substances (somatostatin and vasopressin) in to the brain {Boakes, Ednie, et al. 1985; Mazzari S, Aldinio, et al. 1986; Diamant & de Weid 1993}. Furthermore, barrel rolling is not seen in response to kainic acid or bicuculline used to induce 'limbic' epilepsy {Ben Ari, Tremblay, et al. 1980; Ben Ari, Tremblay, et al. 1981; Ben Ari 1985; Turski, Cavalheiro, et al. 1985}.

Therefore barrel rolling may not be seizure activity, and therefore not reduced by diazepam. However, stage 3 (pawing) seizures induced by S-AMPA with IL-1 were reduced by diazepam. Barrel rolling was observed only in the first few hours after striatal treatments, and the late increase in stage 3 seizures (pawing) observed in response to intrastriatal S-AMPA with IL-1 was not associated with barrel rolling (Figure 5.6). The reduction in overall duration of pawing by diazepam on S-AMPA with IL-1 induced stage 3 seizures may therefore be reflective of the reduction in duration of stage 3 seizures that occurred late (Figure 5.4,5.6).

The volume of cell death that resulted from intrastriatal injection of S-AMPA or S-AMPA with IL-1 was similar to that observed in chapter 3. A similar percentage of neocortical cell death was also seen in both experiments (64% *vs* 71%). However in the present study, no significant difference in subcortical lesion volume was observed in response to striatal injection of S-AMPA with IL-1 *vs* S-AMPA alone. Furthermore, diazepam failed to reduce cell death in response to S-AMPA alone whilst subcortical cell death induced by S-AMPA with IL-1 was reduced by 32%. Although the reason for the lack of difference in subcortical lesion volume (S-AMPA with IL-1 *vs* S-AMPA) is not clear, variability in lesion volumes has been noted previously in this paradigm {Grundy 2000}. Seizures, and thereby seizure related cell death in response to kainic acid is also variable with full seizure pattern, (and cell death) being observed in approximately 60-70% of rodents which is consistent with the frequency of observation of neocortical cell death described here {Sperk 1994}.

Diazepam does not reduce the 'local' toxicity of S-AMPA or kainic acid, but does reduce their related 'distant' death as observed here {Ben Ari, Lagowska, et al. 1978 ; Lees & Leong 2001}. Subcortical cell death in this paradigm is made up of thalamic

('distant') and striatal (local) cell death. The proportion of cell death due to spread of injected excitotoxin to regions adjacent to the striatum however is unclear. Whilst data from chapter 3 and 4 in which neuronal degeneration was seen in contralateral regions such as the BST and SI (regions adjacent to the striatum) may suggest that ipsilateral cell death is part of the 'distant' cell death process, data from intrastriatal injection of excitotoxin in the rat suggests that excitotoxin diffusion (which is variable) is important in causing surrounding striatal death {Zaczek, Simonton, et al. 1980}. Therefore discrepancies in lesion volumes observed in Figure 5.1 may be due to a combination of variability of seizure activity, and proportion of cell death induced by seizures ('distant' death) *vs* direct excitotoxic damage ('local' cell death). Furthermore, subcortical cell death is incomplete 24 h after striatal injections in response to S-AMPA or S-AMPA with IL-1 {Grundy 2000}. Therefore analysis of lesion volume 48 h after striatal injections (when subcortical death is complete) may allow for better differentiation of whether cell death observed is seizure related or due to excitotoxicty.

Cell death induced by sustained seizure activity has been observed previously and is commonly reported with kainic acid or bicuculline induced 'limbic' seizures. Although this is observed mostly in, limbic, subcortical and allocortical regions, early studies on kainic acid induced seizures in the rat as well as some recent studies using more sensitive markers of neuronal damage have reported the occurrence 'distant' of neocortical cell death similar to that reported in this thesis {Ben Ari, Tremblay, et al. 1980; Turski, Cavalheiro, et al. 1985; Hopkins, Wang, et al. 2000}. Cell death at sites distant to administration of kainic acid occurs after the onset of seizures, and is reduced by administration of diazepam or the NMDA receptor antagonist MK801 {Ben Ari 1985; Lees & Leong 1992}. This 'distant' cell death in response to kainic acid is observed mainly in synaptically connected regions exhibiting high metabolic and

electrographic activity {Ben Ari, Tremblay, et al. 1980; Turski, Cavalheiro, et al. 1985}. These data support the fact that the kainic acid-induced remote cell death is related to seizure propagation and intensity. In the present study neocortical cell death in response to striatal injection of S-AMPA with IL-1 was also observed after the onset of intense seizure activity (8 h after striatal injections, chapter 4). In addition, it is reduced by peripheral or intracerebral treatment with NMDA-receptor antagonists {Lawrence, Allan, et al. 1998; Allan & Rothwell 2000}, and data from this chapter have demonstrated that it is also reduced by diazepam treatment. Similarities between the effects of intrastriatal administration of S-AMPA with IL-1, and those seen in response to kainic acid further support our hypothesis that the 'distant' cortical cell death induced by the former treatment is a result of increased seizure duration.

In addition to seizure intensity related neuronal cell death observed in synaptically connected regions, cell death induced by kainic acid has also been described in some non-synaptically connected regions. This cell death in non-synaptically connected regions has been related to venous infarction resultant from compression of the cerebral draining veins by seizure induced cytotoxic oedema {Ben Ari 1985; Sperk 1994}. Neutrophil dependent early disruption of the blood brain barrier and subsequent vasogenic and cytotoxic oedema has been reported in response to IL-1β in rodents {Anthony, Bolton, et al. 1997}. Therefore, IL-1 may mediate exacerbate seizure related death by increasing brain oedema.

Exogenous application of IL-1 increases the duration of seizures induced by intrahippocampal injection of kainic acid in the rat {Vezzani, Conti, et al. 1999}. Exogenous IL-1 also increases tonic and clonic seizure duration, and IL-1ra reduces the duration of tonic and clonic seizures induced by intrahippocampal injection of

bicuculline in mice {Vezzani, Moneta, et al. 2000}. These results are consistent with the observations from this chapter of increased duration of S-AMPA induced seizures by exogenous application of IL-1. This is the first time however, that, IL-1 has been reported to increase the intensity of excitotoxin induced seizures.

The cellular mechanism by which IL-1 exacerbates seizures remains unknown. Seizure activity in the brain is generally thought to result from an imbalance between excitatory and inhibitory signals {Bradford 1995}. Some investigators have suggested that IL-1 enhances seizures through the facilitation of glutamatergic function {Ye & Sontheimer 1996} particularly as the enhancement of seizures by IL-1 on kainate induced epilepsy are blocked by a selective NMDA antagonist {Vezzani, Conti, et al. 1999}. This may be due to an IL-1 induced reduction of glutamate uptake by astrocytes {Yamasaki, Matsuura, et al. 1995}. However, IL-1 also has inhibitory actions in the CNS since it has been shown to enhance GABA-dependent chloride uptake in rat cortical synaptosomes {Miller, Galpern, et al. 1991}, and induce long lasting potentiation of GABA induced currents in cultured cortical neurones.

Exogenous IL-1 fails to alter the latency to onset of kainic acid seizures in the rat {Vezzani, Conti, et al. 1999}, and IL-1ra does not modify bicuculline-induced interictal spiking in the mouse hippocampus, suggesting that IL-1 does not influence focal neuronal excitability or influence the mechanisms of seizure generation. However, the observation that the bicuculline-induced bilateral, neocortical c-fos expression is reduced or absent in mice over expressing IL-1ra (*vs* wild-type mice), suggests that IL-1 influences seizure generalisation {Vezzani, Moneta, et al. 2000}. Racine stage 4 and 5 seizures may represent 'generalised' seizures {de Simoni, Perego, et al. 2000}, and

therefore data presented here would also support the proposal that IL-1 is involved in the generalisation of seizures.

This data demonstrates that IL-1 increases seizures induced by striatal injection of S-AMPA. Good co-relation with seizure duration and lesion volume was also observed, and neocortical cell death in response to striatal injection of S-AMPA with IL-1 was reduced by the anticonvulsant diazepam. These data support the hypothesis that IL-1 exacerbates cell death by increasing seizure activity.

It remains to be seen however, whether increased neuronal activity is observed in the neocortex - the region that dies, in response to S-AMPA with IL-1. In addition, it remains to be confirmed whether behaviours quantified as the motor expression of seizures in this chapter correlate with electroencephalographic changes consistent with seizures.

Chapter 6: Neuronal activity in response to S-AMPA ± IL-1

6.1 Introduction

The results in chapter 5 demonstrated that IL-1 increased the duration and frequency of S-AMPA induced seizures. It was also demonstrated that the anticonvulsant diazepam reduced seizure duration and frequency as well as the neocortical cell death induced by S-AMPA with IL-1. These data suggest that neocortical cell death induced by striatal injection of S-AMPA with IL-1 is related to seizure activity.

However, the striatum is not a site commonly associated with epileptogenesis {Goddard, McIntyre, et al. 1969}. Further, it has been suggested that behaviours quantified as seizure activity in chapter 5 are not related to seizure activity. This is particularly because barrel rolling, which was observed with pawing episodes and which was quantified as seizure activity, can be induced by a number of non epileptogenic stimuli {Boakes, Ednie, et al. 1985; Mazzari S, Aldinio, et al. 1986}. In addition, it has been questioned whether increased neuronal activity consistent with seizure activity is seen in the region of the neocortex which dies in response to S-AMPA with IL-1.

Therefore, the aims of this study were to determine a) whether intrastriatal injection of S-AMPA or S-AMPA with IL-1 activated the same brain regions as common convulsants, b) if increased neocortical neuronal activity is observed in response to intrastriatal injection of S-AMPA with IL-1 compared to S-AMPA and c) whether behaviours induced in response to S-AMPA or S-AMPA with IL-1 and quantified as seizure activity in chapter 5 are associated with electroencephalographic changes consistent with seizure activity.

6.2 Methods

6.2.1 Pathways of neuronal activation

Neuronal activation was determined by studying the spatial distribution of the protein product of the immediate early gene *c-Fos* at 4 h or 8 h after striatal injection of S-AMPA and S-AMPA with IL-1 in the rat. Immunohistochemistry for c-Fos was performed on perfuse-fixed (**see section 2.4.1.1.1**) free-floating brain sections (30μm) as described in **section 2.4.2.2.2**.

6.2.2 EEG recording

EEG recordings were performed as described in **section 2.4.3.2** in rats that were injected with S-AMPA or S-AMPA with IL-1 (**section 2.3.1**). All rats were filmed to allow comparison of the motor expression of seizures (as described in chapter 5) to EEG activity. EEG recordings and videos were subsequently synchronised in time. The EEG recordings were visually analysed and correlated to corresponding video recorded convulsive behaviour.

6.3 Results

6.3.1 Immunoreactive c-Fos induced by intrastriatal injection of vehicle or IL-1

Scattered c-Fos positive cells were observed throughout the brain in response to intrastriatal injection of vehicle or IL-1. However, consistent and intense c-Fos staining was seen only in the ipsilateral striatum (at 4 h and 8 h) and around the region of injury induced by the injection needle in response to vehicle (n=2) (Figure 6.1). In addition to the striatum and injection tract, c-Fos was observed bilaterally in the paraventricular nucleus of the hypothalamus 4 h and 8 h after injection of IL-1 (n=2) (Figure 6.1).

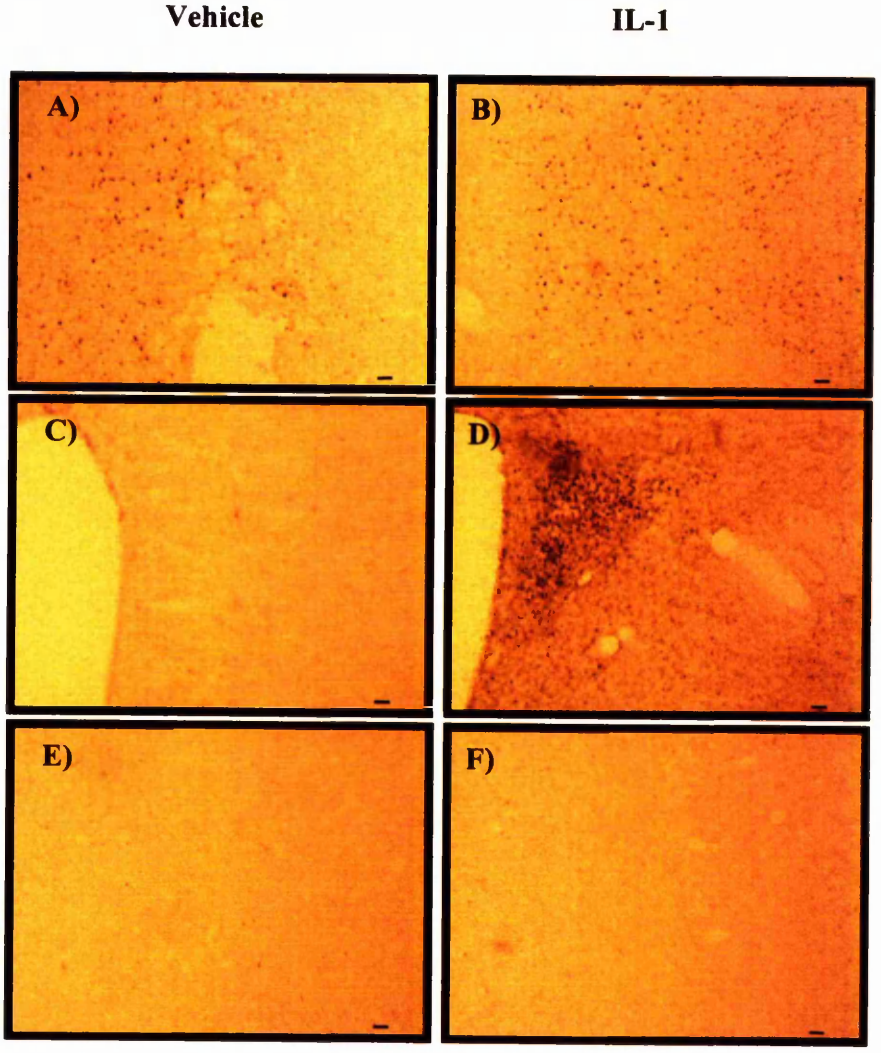

Figure 6.1: C-Fos observed in the striatum (A, B) paraventricular nucleus of the hypothalamus (C, D), and the ipsilateral cortex (E, F) in response to vehicle or IL-1. Regions of dark staining (black spots) represent c-Fos cells. Scale bar = 50μm.

6.3.2 C-Fos induced 4 h after intrastriatal injection of S-AMPA ± IL-1

C-Fos expression was seen in response to intrastriatal injection of S-AMPA or S-AMPA with IL-1 in similar limbic/limbic associated (BST, amygdala, SI, septum, medial thalamus, DMT, NR) and neocortical regions. A greater proportion of rats, exhibiting a greater number of c-Fos cells in the ipsilateral neocortex, hippocampus, and amygdala, were observed in response to intrastriatal injection of S-AMPA with IL-1 compared to

S-AMPA alone (Table 6.1). Contralateral c-Fos was also seen in a greater number of regions (including the neocortex) in a greater proportion of rats in response to S-AMPA with IL-1 *vs* S-AMPA.

	Ipsilateral		*Contralateral*	
Brain regions	**S-AMPA**	**S-AMPA + IL-1**	**S-AMPA**	**S-AMPA + IL-1**
Cortex				
Parietal	++ (2/4)	+++ (5/5)	--	+ (2/5)
Frontal	++ (2/4)	+++ (5/5)	--	+ (2/5)
Piriform	+++ (4/4)	+++ (5/5)	++ (1/4)	++ (2/5)
Entorhinal	++ (3/4)	+++ (5/5)	++ (1/4)	++ (2/5)
IL/cing	++ (4/4)	++ (5/5)	+ (1/4)	+ (4/5)
Striatum	--	--	--	--
Epn/Cl	+ (4/4)	+/- (4/5)	--	--
BST	+ (3/4)	++ (4/5)	--	--
SI	+ (3/4)	++ (4/5)	--	--
septum	+ (4/4)	+ (4/5)	--	+ (2/5)
Thalamus				
DMT	++ (4/4)	++ (5/5)	+ (2/4)	++ (3/5)
Anterior	++ (4/4)	++ (5/5)	--	--
Ventral	--	++ (5/5)	--	--
Lateral	--	++ (5/5)	--	--
Medial	+ (3/4)	+ (5/5)		+ (1/5)
Reticular	--	--	--	--
NR	+ (4/4)	+ (5/5)	--	+ (2/5)
Hippocampus				
CA1	--	+/- (2/5)	--	+/- (2/5)
CA2	--	+/- (2/5)	--	+/- (2/5)
CA3	--	+/- (2/5)	--	+/- (2/5)
dentate gyrus	--	++ (2/5)	--	++ (2/5)
Amygdala	+ (1/4)	+ (4/5)	--	+ (2/5)

Table 6.1. Brain regions in which c-Fos was observed in response to S-AMPA ± IL-1 4 h after striatal injections in the rat. Numbers in brackets represent number of rats expressing c-Fos, and (--) = no cells, (+/-) = scattered cells, (+) = low number of cells, (++) low / medium number of cells, (+++) medium number of cells, (++++) high number of cells. (IL/Cing, Infralimbic/cingulated cortex; Epn/Cl, enteropiriform cortex/claustrum, BST, bed nucleus of stria terminalis; SI, substansia innominata; DMT, dorsomedial thalamus; NR, nucleus reuniens.

6.3.3 C-Fos induced 8 h after intrastriatal injection of S-AMPA ± IL-1

C-Fos was observed in the neocortex and in limbic/ limbic associated regions (as seen at 4 h) in response to both S-AMPA and S-AMPA with IL-1 (Table 6.2, Figure 6.2, 6.3) No obvious increase in the magnitude of c-Fos was observed in the neocortex or thalamus between rats killed at 4 h or 8 h after striatal injection of S-AMPA. However, compared to earlier, c-Fos cells were observed in the hippocampus 8 h after striatal injection of S-AMPA (Table 6.1, 6.2).

There was a 2-fold ($P<0.05$) increase in the number of c-Fos cells in the ipsilateral neocortex 8 h (148 ± 38) compared to that seen 4 h (69 ± 18) after striatal injection of S-AMPA with IL-1. A significant (3-fold) increase in the number of c-Fos cells in the neocortex was also observed in rats injected with S-AMPA with IL-1 compared to S-AMPA alone at 8 h (Figure 6.2, 6.4)

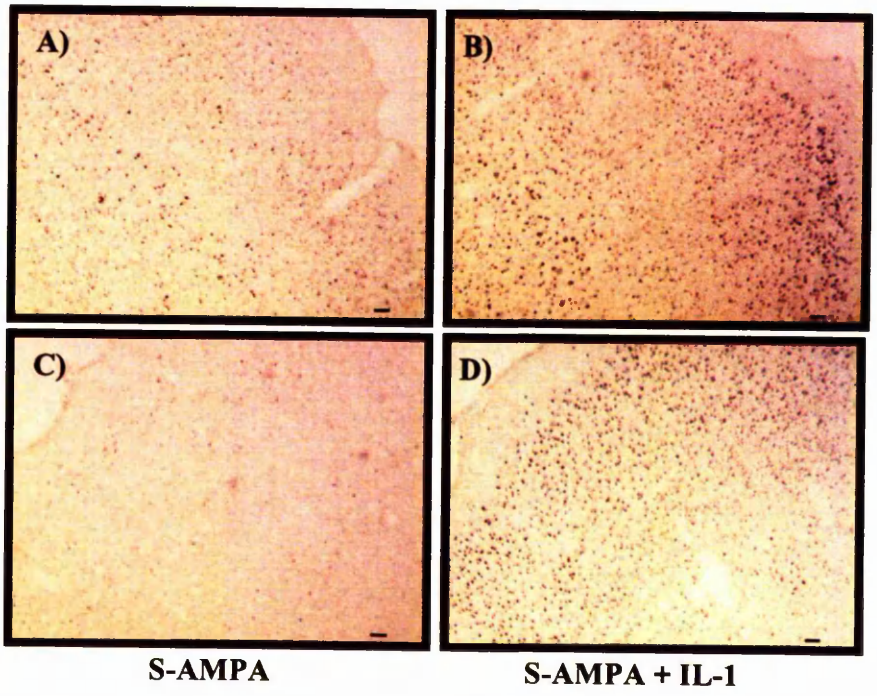

Figure 6.2: Photomicrographs of c-Fos was observed in the ipsilateral (A, B), and contralateral (C, D) parietal cortex 8 h after striatal injection of S-AMPA or S-AMPA with IL-1. Regions of dark staining (black spots) represents c-Fos. Scale bar = 50µm.

C-Fos was also observed in the ipsilateral hippocampus and contralateral neocortex in a greater proportion of rats treated with S-AMPA with IL-1 compared to those injected with S-AMPA alone (Table 6.2)

	Ipsilateral		*Contralateral*	
Brain regions	**S-AMPA**	**S-AMPA + IL-1**	**S-AMPA**	**S-AMPA + IL-1**
Cortex				
Parietal	++ (4/4)	++++ (6/6)	+ (1/4)	++ (4/6)
Frontal	++ (4/4)	++++ (6/6)	+ (1/4)	++ (4/6)
Piriform	+++ (4/4)	+++ (6/6)	++ (1/4)	++ (4/6)
Entorhinal	++ (4/4)	+++ (6/6)	++ (1/4)	++ (4/6)
IL/cing	++ (4/4)	++ (6/6)	++ (1/4)	++ (4/6)
Striatum	--	--	--	--
Epn/Cl	+ (4/4)	--	--	--
BST	+++ (3/4)	+++ (6/6)	+ (1/4)	+ (4/6)
SI	++ (3/4)	++ (6/6)	+ (1/4)	+ (4/6)
septum	+ (3/4)	+ (4/6)	+ (2/4)	+ (5/6)
Thalamus				
DMT	++ (4/4)	++ (6/6)	+ (2/4)	++ (6/6)
Anterior	++ (3/4)	++ (6/6)	--	--
Ventral	+/- (1/4)	+ (6/6)	--	--
Lateral	+ (3/4)	+ (6/6)	--	--
Medial	+ (1/4)	+ (6/6)	--	+ (3/6)
Reticular	--	--	--	--
NR	+ (3/4)	+ (6/6)	+ (2/4)	+ (3/6)
Hippocampus				
CA1	+ (2/4)	+ (6/6)	+ (2/4)	+ (5/6)
CA2	+ (2/4)	+ (6/6)	+ (2/4)	+ (5/6)
CA3	+ (2/4)	+ (6/6)	+ (2/4)	+ (5/6)
dentate gyrus	++ (2/4)	+++ (6/6)	++ (2/4)	+++ (5/6)
Amygdala	++ (2/4)	++ (6/6)	+ (2/4)	++ (5/6)

Table 6.2. Brain regions in which c-Fos was observed in response to S-AMPA ± IL-1 8 h after striatal injections in the rat. Numbers in brackets represent number of rats expressing c-Fos, and (--) = no cells, (+/-) = scattered cells, (+) = low number of cells, (++) low / medium number of cells, (+++) medium number of cells, (++++) high number of cells.

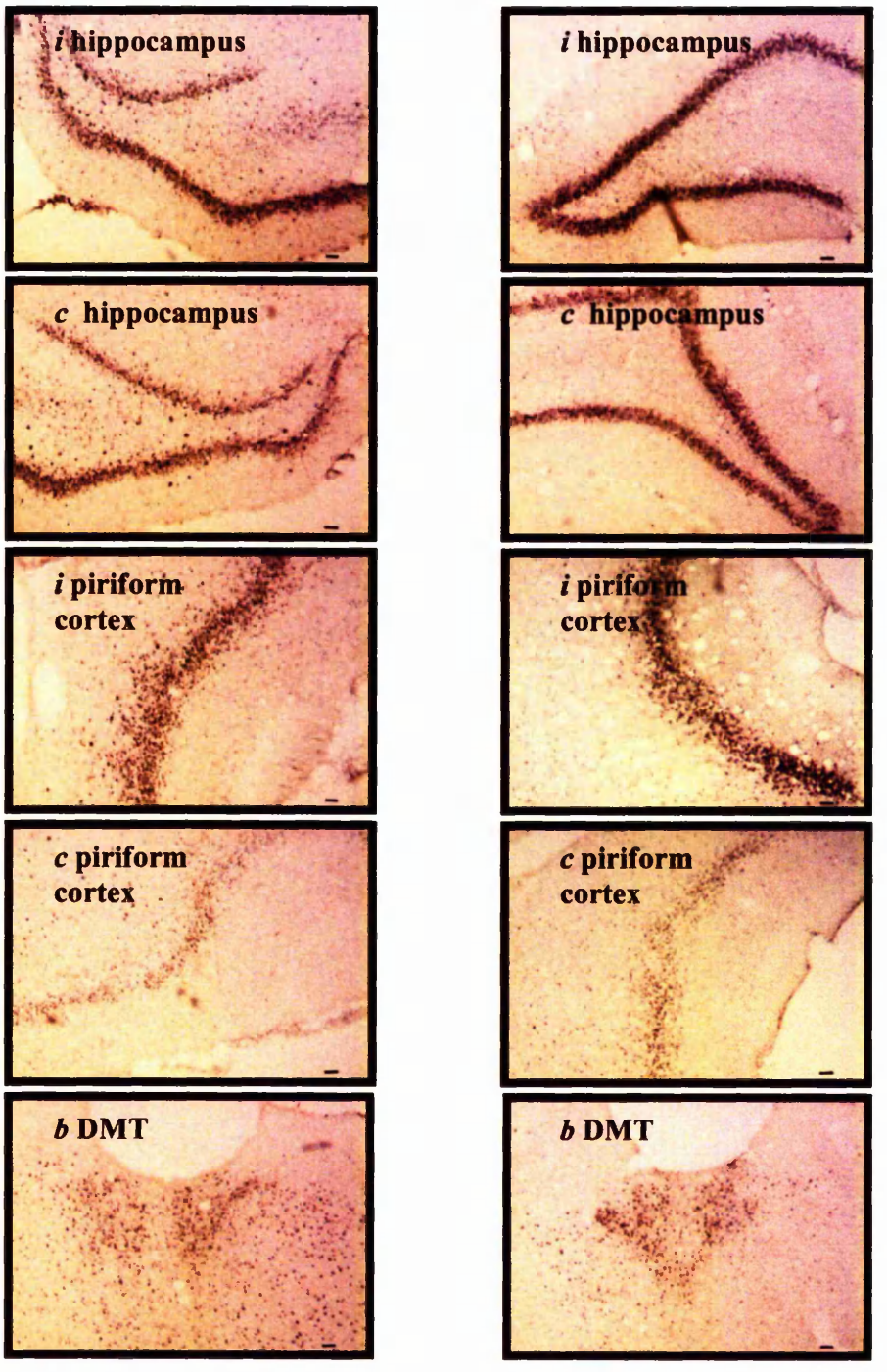

Figure 6.3: Photomicrographs of ipsilateral (*i*), contralateral (*c*) or bilateral (*b*) regions in which c-Fos was observed 8 h after striatal injection of S-AMPA or S-AMPA with IL-1. Regions of dark staining (black spots) represents c-Fos. Scale bar = 50μm.

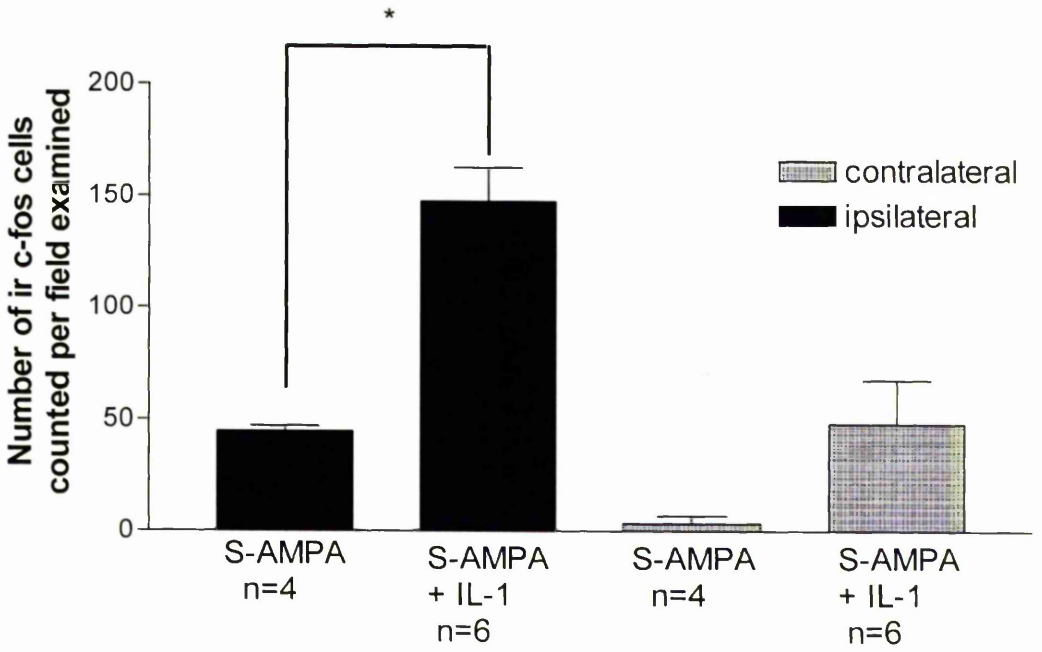

Figure 6.4: Number of c-Fos cells counted in the contralateral and ipsilateral parietal cortex 8 h after striatal treatments in the rat. Data are expressed as mean ± sem. *P<0.001.

6.3.4 EEG and motor expression of seizures

Occasional high frequency activity was observed in response to intrastriatal injection of IL-1 and in control animals (Figure 6.5). Some high frequency episodes in response to intrastriatal injection of IL-1 were associated with scratching movements. Correlation of all high frequency episodes seen in response to IL-1 or during control recordings was not performed.

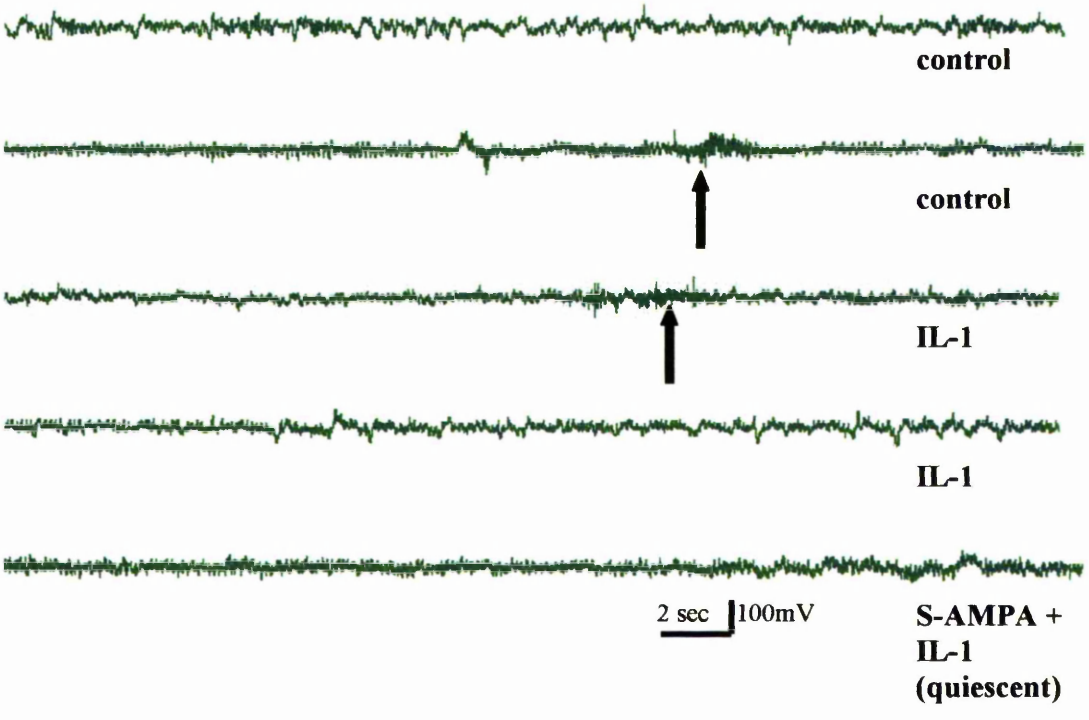

Figure 6.5. Sections of EEG traces recorded from rats, prior to surgery (control), in response to intrastriatal injection of IL-1, and in response to S-AMPA with IL-1 during a period of quiescence. Arrows denote high frequency episodes observed.

Pawing in response to S-AMPA with IL-1 or S-AMPA was associated with high frequency high amplitude EEG activity compared to, control EEG activity or EEG activity whilst the experimental rats were noted to be quiescent (Figure 6.6). In the previous chapter barrel rolling was quantified with pawing, as both behaviours were invariably seen together and these episodes were difficult to separate temporally during each episode. However, EEG changes corresponding with barrel rolling were distinct from pawing episodes. Barrel rolling was associated with a higher frequency and lower amplitude waveform compared to that seen with pawing. EEG traces therefore, allowed for the differentiation between the two behaviours.

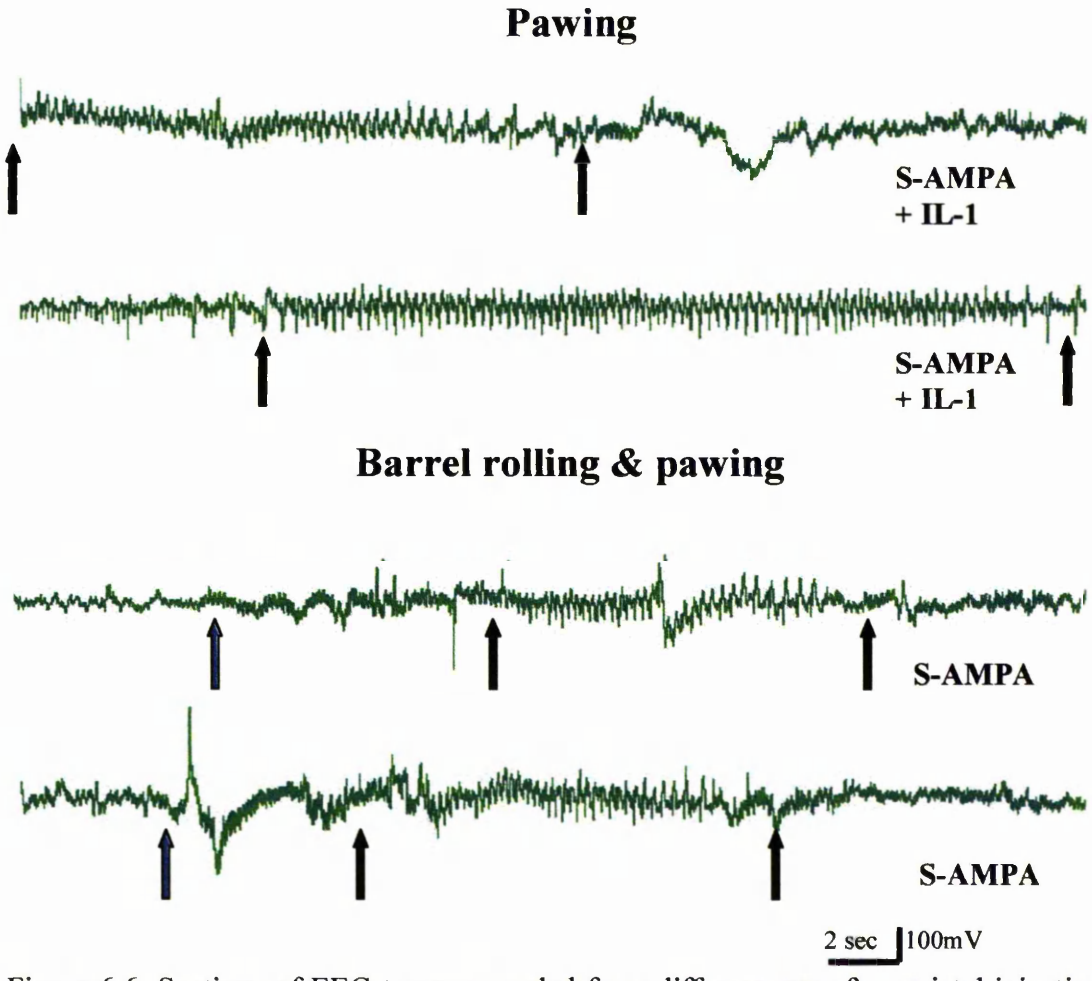

Figure 6.6: Sections of EEG traces recorded from different rats after striatal injections demonstrating EEG changes accompanying pawing or barrel rolling and pawing behaviour. Black arrows denote start and finish of pawing events, whilst blue arrows denote start of barrel rolling episode.

Rearing, and rearing and falling behaviours in response to S-AMPA with IL-1 or S-AMPA were also associated with high frequency high amplitude changes on the EEG compared to control animals. Changes in EEG frequency and amplitude seen with rearing or rearing and falling episodes were greater than those seen with pawing (Figure 6.7).

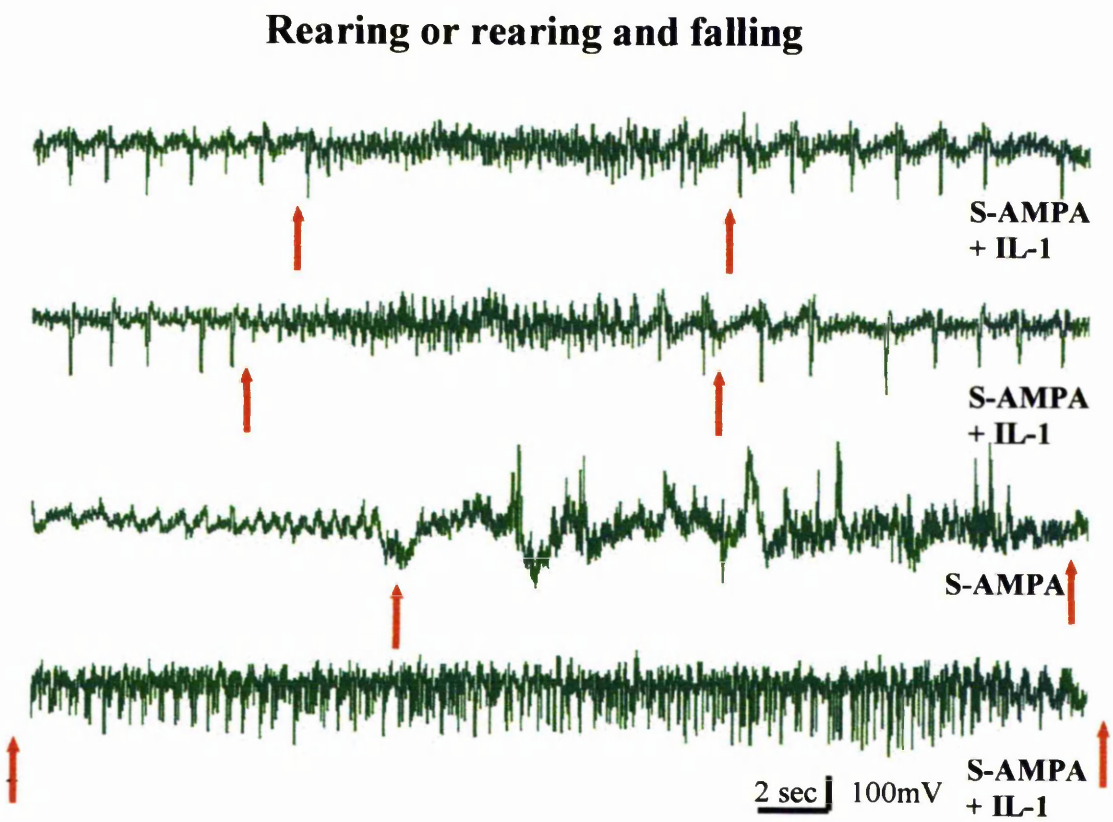

Figure 6.7. Sections of EEG traces recorded from different rats after striatal injections demonstrating EEG changes accompanying rearing and rearing and falling behaviour. Red arrows denote start and finish of rearing or rearing and falling events

6.4 Discussion

C-Fos was not observed outside the striatum consistently in response to intrastriatal injection of vehicle. Consistent with reports of icv or peripheral injection of IL-1 in rats, increased c-Fos was observed in the paraventricular nucleus of the hypothalamus (in addition to the striatum) in response to intrastriatal injection of IL-1 {Konsman, Tridon, et al. 2000; Todaka, Ishida, et al. 2000}. Overall, the regional distribution of c-Fos observed in response to S-AMPA and IL-1 or S-AMPA was similar, although, c-Fos was observed earlier in the hippocampus, and the magnitude of c-Fos induced in the neocortex (at 8 h) was greater in response to S-AMPA with IL-1 compared to S-AMPA alone after striatal injection.

C-fos is an immediate early gene that is up regulated rapidly and transiently in response to a large number of physiological and pathological stimuli including traumatic and ischaemic brain injury {Herrera & Robertson 1996; Hughes, Alexi, et al. 1999}. Increased neuronal activity induced by electrical stimulation is also a potent stimulus for c-Fos expression. Thus detection and mapping of c-Fos expression *in vivo* has been used as a method to map neuronal activity and hence metabolic activity in the brain during seizures {Herrera & Robertson 1996; Hughes, Alexi, et al. 1999}. Using c-Fos protein expression to map neuronal activity induced by seizures offers good temporal and spatial resolution although it is limited because c-Fos is only induced by neuronal activation and cells that are electrically inhibited will not be detected, and therefore, seizure pathways that involve disinhibition, may be overlooked {Dragunow & Faull 1989}. Further, whilst the temporal progression of seizures may be studied by examining c-Fos expression at different time points, detection of c-Fos protein in a single experimental subject is only a 'snap shot' view of the state of brain cellular

activity around the time of sacrifice. This is particularly important when c-Fos is used to map seizure pathways because seizures induced by various convulsants may be variable in their onset or progression {Sperk 1994}. In addition, seizures were not recorded during this experiment, and therefore variations in c-Fos expression could not be correlated to seizure activity in individual animals.

The main aims of the experiments described in this chapter were not however to map seizure activity, but to determine a) whether S-AMPA or S-AMPA with IL-1 induced neuronal activity in similar regions as those observed in response to commonly used convulsants, and b) whether increased c-Fos immunoreactivity was observed in the neocortex in response to S-AMPA with IL-1 compared to S-AMPA alone.

The time points used to study c-Fos in the present study were chosen because cell death in the neocortex in response to intrastriatal injection of S-AMPA with IL-1 was not established at 8h (chapter 4). In addition, c-Fos expression is considered to be maximal 30-60 mins after electrical stimulation {Dragunow & Robertson 1987}, and therefore c-Fos expression at 8 h after striatal injection of S-AMPA with IL-1 or S-AMPA alone was considered most important, as this was the period during which greatest differences in seizures were observed between the two groups. C-Fos expression was not observed in the neocortex at 90 minutes of striatal injections of S-AMPA or S-AMPA with IL-1, and so, 4 h was chosen as an intermediary time point (Kirk unpublished).

It is accepted widely that activation of the limbic system is a common feature in seizure models. Consistent with this, convulsive seizures induced by kainic acid, electrical stimulation, pentylentetrazole, pilocarpine, and kindling all elicit c-Fos expression in limbic brain regions especially the hippocampus and amygdala {Dragunow &

Robertson 1987; Popovici, Represa, et al. 1990; Barone, Morelli, et al. 1993; Herrera & Robertson 1996}.

Limited c-Fos was seen in the hippocampus or amygdala in response to S-AMPA 4 h after injection in this present study (Table 6.1). Equally, consistent c-Fos expression in these regions was also not observed in response to S-AMPA with IL-1 at this time point. In contrast, c-Fos was observed consistently in various allocortical and neocortical regions in response to both striatal treatments at 4 h. Activation of the hippocampal dentate gyrus is one of the earliest features of seizures induced by kainic acid (seen within 90 mins of drug administration) or kindling (within 30 mins) in the rat {Dragunow & Robertson 1987; Popovici, Represa, et al. 1990}. Seizures induced by pentylentetrazole also induce rapid up regulation of c-Fos expression in the dentate gyrus of the hippocampus {Herrera & Robertson 1996}. However, seizures induced by kainic acid or pentylentetrazole are of rapid onset, and are established within 120 minutes of injection {Morgan, Cohen, et al. 1987; Sperk 1994}. In addition, c-Fos immunohistochemistry in these studies was performed in rodents that were unanaesthetised at the time of administration of convulsant. Seizures in response to S-AMPA or S-AMPA with IL-1 began later (from 1-2 h after striatal injection, see chapter 5) than those reported in response to kainic acid or pentylentetrazole, and rodents were anaesthetised at the time of delivery of excitotoxin into the striatum in this set of experiments {Morgan, Cohen, et al. 1987; Popovici, Represa, et al. 1990}. Seizures induced by S-AMPA peaked at 4 h post injection, whilst seizures induced by S-AMPA with IL-1 peaked again 7- 8 h after striatal injections. However, hippocampal dentate gyrus and amygdala activation was observed 8 h after striatal injections in both S-AMPA and S-AMPA with IL-1 injected animals, which suggests that intrastriatal

injection of S-AMPA or S-AMPA with IL-1 recruits similar pathways associated with seizures.

Whilst c-Fos-like immunoreactivity in response to kainic acid has been reported in the dentate gyrus of the hippocampus at the time of occurrence of the first limbic motor seizure (90 min after kainic acid administration), and c-Fos-like labelling progressively involves different structures of the limbic system, limited cortical expression was observed even when the rats manifested a permanent epileptic state (3-6 h) {Popovici, Represa, et al. 1990}. This time-course was similar to that produced by kainic acid on 2-deoxyglucose consumption and correlates with the electrographic changes previously described {Ben Ari 1985}. Willoughby et al (1997) however reported widespread and early (within 1 h) c-Fos expression in the neocortex corresponding the first kainic acid induced convulsive event in the rat {Willoughby, Mackenzie, et al. 1997}. This discrepancy in results has been related to anaesthesia, the site of injection of convulsant, and differences in the strain of rat used {Willoughby, Mackenzie, et al. 1997}. Similar factors may also explain why early cortical activity was observed in response to striatal injections in this present study. Striatal injection requires that the injection needle traverse parts of the cortex during this process. Damage from passage of this needle (cortical stab injury) also induces c-Fos in the neocortex, and therefore this may also contribute to the cortical c-Fos expression observed {Dragunow & Faull 1989}. However, persistent c-Fos expression in the neocortex resulting from needle damage in the present study is unlikely as cortical c-Fos expression was not observed 4 h after striatal injection of vehicle or IL-1.

Barrel rolling behaviour induced by striatal injection of endothelin-1 in the rat also induces cortical c-Fos and so barrel rolling may also contribute to c-Fos expression observed in the cortex {Sullivan, Reynolds, et al. 1996}.

Correlation of c-Fos to individual seizure behaviours has been difficult, particularly as the onset of seizures is unpredictable, and that seizures rarely occur in isolation. Correlation between individual seizure behaviours and c-Fos expression has however been attempted at various stages of kindling {Herrera & Robertson 1996}. These published studies show that animals at stage 1 and 2 of the kindling process show either a pattern of c-Fos expression in a unilateral cortical distribution affecting the temporal lobes and parietal cortex with no changes in the hippocampus or amygdala, or a pattern of c-Fos distribution with increased expression in the hippocampus and amygdala without cortical c-Fos expression. C-Fos expression at later stages of kindling (stage 4/5) is observed in bilateral hippocampi and amygdaloid nuclei as well in bilateral neocortical, piriform and entorhinal cortices {Herrera & Robertson 1996}.

Bilateral cortical c-Fos expression at 8 h after striatal injection was also observed in response to S-AMPA with IL-1 in a greater number of animals compared to S-AMPA (66% vs 25%) alone. Bilateral c-Fos expression when observed in the neocortex, was always accompanied by bilateral c-Fos expression in the hippocampus, amygdala, piriform cortex, and entorhinal cortex. Observation of bilateral c-Fos immunoreactivity coincided with the time at which increased stage 4/5 seizures (see chapter 5) were observed in response to S-AMPA with IL-1, which is consistent with data from kindling studies presented above. However, seizures were not quantified in the present experiment, and therefore motor expression of seizures cannot be correlated directly to c-Fos expression here. Equally, whether those rodents that had no evidence of bilateral cortical c-Fos expression were those that did not develop grade 4/5 seizures also cannot be ascertained.

Despite the temporal variations in c-Fos expression pattern compared to kainic acid or pilocarpine induced seizures, the data presented in this chapter have demonstrated that intrastriatal injection of S-AMPA with IL-1 or S-AMPA alone activated similar pathways that are activated in response to a wide range of convulsants. This is in keeping with the postulate that intrastriatal injection of S-AMPA may induce seizures.

In addition to demonstrating that seizure pathways are activated by intrastriatal injection of S-AMPA or S-AMPA with IL-1, these data also suggest that the magnitude of neuronal activity (and hence metabolic activity) in the neocortex is significantly increased in response to intrastriatal injection of S-AMPA with IL-1 compared to S-AMPA alone in the rat. Increased and sustained increases in seizure activity have been correlated with neuronal damage in various experimental models of seizures in the rat {Ingvar 1986; Handforth & Ackermann 1995}. Therefore these data support the proposal that neocortical cell death induced by S-AMPA with IL-1 is related to increased seizure activity. The reason for cell death consequent to increased metabolic activity is unclear, as cerebral blood flow and metabolic rate are normally tightly coupled {Kuschinsky, Suda, et al. 1981; Sokoloff 1981}. Cerebral blood flow and metabolism studies have demonstrated that the tight coupling observed during the initial stages of seizure activity is not seen at later time points when relative hypoperfusion is observed in regions that are destined to die {Pereira, Ferrandon, et al. 2002}. Cerebral blood flow and glucose uptake studies need to be performed to investigate whether there is a perfusion/metabolic rate mismatch in this setting.

Seizures are the result of abnormal electrical discharges in the brain {Shin & McNamara 1994}. These abnormal electrical discharges may be recorded and visualised using electroencephalography (EEG). Electrical signals are recorded conventionally at

the surface of the brain, although many investigators have recorded EEG waves from various sites considered important in the seizure pathway {Ben Ari, Tremblay, et al. 1981; Vezzani, Conti, et al. 1999}. The EEG waveform recorded depends on the distance of electrical recording, duration of post-synaptic potential, number of synchronously activated post-synaptic potentials and the anatomical orientations of the current generated {Schaul 1998}.

Most of the studies using EEG to measure seizure activity employ a 'tethered system' model whereby the experimental animals are connected directly via a lead to the recording system. A telemetry-based system was used to measure EEG in the present study. It has been used previously to measure sleep EEG in rats, and seizure related EEG in guinea pigs to good effect {Mumford & Wetherell 2001; Vogel, Sanchez, et al. 2002}. Radio telemetry based systems offer the advantage of monitoring singly housed conscious freely moving animals. In addition, experimental animals can be monitored continuously over long periods of time. This feature was particularly useful as seizures occurred late in the paradigm used here. However, one disadvantage of this technique is that animals required two surgical procedures, one for implantation of EEG probe, and a second for injection of treatments into the striatum. Implantation of a striatal canula is possible and would alleviate need for a second anaesthetic and surgical procedure. However, it has been reported that implantation of a canula or electrodes interferes with latency to onset of seizures and this would have be taken into consideration {Willoughby, Mackenzie, et al. 1997}. Further, changing Home Office approval on the injection of convulsants in unanaesthetised animals would have subsequently delayed the experiments.

No single definition of seizure on the basis of the EEG exists because epilepsy is a complex and heterogeneous disorder. However, epileptiform activity may be identified on the EEG criteria on the basis that most are: asymmetric, usually followed by an after wave of slower frequency, generally multiphasic, and are distinctly different in duration form background activity {Schaul 1998}.

Multiphasic high frequency bursts were observed during control recordings (pre-injection) recordings (Figure 6.5). Rodents were not videoed during these periods, and therefore behaviour responsible for these bursts could not be analysed. Spontaneous seizures have been reported to occur in Sprague-Dawley rats, and studies will need to be performed to determine this {Willoughby & Mackenzie 1992}.

EEG recordings were performed in this present study to determine whether convulsive behaviours quantified and labelled as seizure activity correlated with EEG evidence of epileptiform activity. Each convulsive behaviour observed on video analysis was associated with a high frequency, high amplitude polyspiking wave form on the corresponding EEG recording. Further, each EEG record associated with individual convulsive bursts was comparable to EEG recordings reported elsewhere. The frequency and duration of these bursts were not quantified.

Barrel rolling behaviours were associated with a higher frequency waveform than the control EEG (during quiescence after treatment or pre-injection). In addition, EEG corresponding to barrel rolling was distinct from the EEG pattern observed with the temporally associated pawing episodes. No similar high frequency EEG recordings were observed in previous studies that have recorded and reported on EEG changes associated with barrel rolling episodes {Burke & Fahn 1983}. Whilst the reason for this

discrepancy is unclear, the EEG recordings performed in this study did allow pawing episodes to be separated from barrel rolling episodes.

The data presented in this chapter demonstrate that intrastriatal injection S-AMPA activated similar brain regions as observed with a number of convulsants, suggesting that intrastriatal injection of S-AMPA may induces seizures. It was also demonstrated that convulsive behaviours (pawing, or rearing, or rearing and falling) were associated with EEG changes consistent with seizures, although barrel rolling which was also quantified as part of seizure activity was not associated with similar changes on the EEG as pawing or rearing or rearing and falling and therefore did not represent convulsive behaviour as previously reported. However, barrel rolling was not observed at times when the greatest difference in seizures induced by striatal injections of S-AMPA compared to S-AMPA with IL-1 occurred.

Increased neuronal activity in the neocortex was observed in response to S-AMPA with IL-1 compared to S-AMPA alone, consistent with increased cortical seizure activity. These data further support the hypothesis that IL-1 increases neocortical cell death by increasing seizure duration in this paradigm of brain injury.

Chapter 7: Final discussion

7.1 Aims

Striatal injection of S-AMPA with IL-1 in the rat results in ipsilateral 'distant' neocortical cell death as well as the 'local' striatal injury seen in response to S-AMPA alone. This neocortical cell death reportedly occurs only in response to intrastriatal injection of S-AMPA with IL-1 {Lawrence, Allan, et al. 1998; Grundy 2000}. It has not been reported after intrastriatal injection of S-AMPA alone, and neither has it been observed in response to intrastriatal injection of S-AMPA with other pro-inflammatory cytokines. Therefore, neocortical cell death in this paradigm was considered to be an IL-1 specific phenomenon. Using this experimental paradigm, and by studying neocortical cell death, the overall aim of this thesis was to investigate the mechanism by which IL-1 exacerbates experimental brain injury. After validating the above-described paradigm of brain injury, the initial aim was to investigate the 'site specific site of action of IL-1' hypothesis (**section 1.10.1**).

7.2 Summary of results

7.2.1 Validation of cell death

Neocortical cell death was observed in 63-71% of rats that received intrastriatal injections of S-AMPA with IL-1, but no neocortical cell death was observed in response to S-AMPA alone. Striatal injection of S-AMPA with IL-1 also resulted in a three-fold increase in lesion volume compared to S-AMPA alone in the rat. These data were consistent with those previously reported {Lawrence, Allan, et al. 1998; Grundy 2000}.

Using fluoro-jade staining, it was also observed that 'distant' subcortical and allocortical neuronal damage occurred in response to intrastriatal injection of S-AMPA

or S-AMPA with IL-1. The total number of regions in which neuronal damage was observed was greater (1.5-fold) in S-AMPA with IL-1 *vs* S-AMPA treated animals. Cell death in the neocortex in response to S-AMPA with IL-1 has been termed 'distant' cell death. Observations of 'distant' cell death (albeit in subcortical and allocortical regions) in response to S-AMPA alone suggest that 'distant' cell death was an S-AMPA dependent process rather than an IL-1 specific process.

7.2.2 Immunoreactive IL-1β expression

Using immunohistochemistry to identify the temporal and spatial distribution of IL-1β in response to intrastriatal S-AMPA *vs* S-AMPA with IL-1, the aim of the study was to identify a 'putative pathway' for IL-1 action in acute neurodegeneration. The results from this series of experiments demonstrated that:

- the temporo-spatial progression of irIL-1β in response to intrastriatal injection of S-AMPA or S-AMPA with IL-1 was variable.
- irIL-1β was observed in more brain regions in response to S-AMPA with IL-1 compared to S-AMPA, although the spatial distribution of irIL-β was similar in response to both treatments.
- irIL-1β was observed in the neocortex in response to both S-AMPA alone, and S-AMPA with IL-1, and was associated with neocortical neuronal degeneration.
- irIL-1β in the neocortex was up-regulated earlier and more frequently in response to S-AMPA with IL-1 compared to S-AMPA. In addition, irIL-1β appeared to precede neuronal damage in the neocortex in response to S-AMPA with IL-1.
- Little hypothalamic irIL-1β was observed in response to either treatment.

These results did not allow delineation of a 'putative pathway' for IL-1 action since, irIL-1β was observed in similar sites in response to S-AMPA or S-AMPA with IL-1,

neocortical cell death cell death was observed in response to S-AMPA alone, and hypothalamic (a site through which IL-1 is thought to act to exacerbate brain injury {Allan, Parker, et al. 2000}) irIL-1β was rarely observed. These data therefore, argue against the postulate that IL-1 acts through specific brain regions to exacerbate acute neurodegeneration.

Instead, the data suggest that irIL-1β and neuronal cell death occurred as a result of an S-AMPA dependent process. That S-AMPA with IL-1 resulted in an increased frequency of neocortical cell death, suggested that IL-1 lead to cell death by increasing the S-AMPA dependent process that causes 'distant' cell death.

7.2.3 IL-1, seizures and cell death

'Distant' cell death is observed in response to intrahippocampal injection of S-AMPA or kainic acid in the rat {Lees & Leong 2001}, and has been related to seizure activity {Ben Ari, Tremblay, et al. 1980}. IL-1 increases seizure activity {Vezzani, Conti, et al. 1999}, and therefore it was hypothesised that IL-1 could cause neocortical cell death in this paradigm by increasing seizures.

Co-infusion of S-AMPA with IL-1 significantly increased seizure duration, frequency, and cortical cell death compared to S-AMPA alone. This increased seizure duration occurred 7-8 h after treatments, which is prior to development of cell death, and resulted mainly from an increase in 'severe' stage 4 or stage 5 seizures. The anticonvulsant diazepam reduced the IL-1 induced cell death and prevented the late increase in seizure duration induced by striatal injection of S-AMPA with IL-1β. In addition, significant correlation was observed between seizure duration and lesion volume. These data

suggests that IL-1 exacerbates S-AMPA induced cell death by increasing the duration and intensity of seizures.

7.2.4 Neuronal activity and EEG correlates of behaviour induced by intrastriatal injections of S-AMPA ± IL-1

It has been suggested that behaviours described in chapter 5 may not related to seizures, as the striatum is not a recognised site at which seizures may be elicited {Goddard, McIntyre, et al. 1969}. Using c-fos immunohistochemistry as a marker of neuronal activation, it was demonstrated that intrastriatal injection of S-AMPA or S-AMPA with IL-1 induced irc-fos in similar brain regions to those in which c-fos is up regulated in response to seizures {Herrera & Robertson 1996}. In addition stage 3 (pawing), stage 4 or 5 (rearing, or rearing and falling) behaviours were all associated with EEG evidence of seizure activity. Finally, significantly increased neuronal activity (number of irc-fos cells) was observed in the neocortex in response to S-AMPA with IL-1 compared to S-AMPA alone.

These data suggest that intrastriatal injection of S-AMPA activated neurones along well-characterised seizure pathways. In addition, co-infusion of S-AMPA with IL-1 significantly increased neuronal activity (consistent with increased seizure activity) in the neocortex, compared to S-AMPA alone.

The data reported in this thesis therefore supports the hypothesis that IL-1 exacerbates neocortical cell death induced by intrastriatal injection of S-AMPA in the rat by exacerbating seizures. Detailed discussion of the findings has been presented in the relevant chapters. The discussion here will focus on a) the validity of the model used, and b) addressing the role of seizures in cerebral ischaemia and trauma.

7.3 Relevance of experimental paradigm used

Neocortical cell death induced by striatal injection of S-AMPA with IL-1 does not share the vascular, meningeal, or contusional disruption of the brain seen in response to traumatic brain injury {Leker & Shohami 2002}. Neither does it have the primary vascular occlusion that leads to cerebral infarction at its core as seen in response to MCAO {Leker & Shohami 2002}. However, the central process that leads to progression of neuronal cell death after the primary insult (vascular occlusion, trauma) is excitotoxicity, and on this basis, intracerebral injection of NMDA agonists have been used widely to mimic acute brain injury {Lawrence, Allan, et al. 1998; Doble A 1999; Pearson, Rothwell, et al. 1999}. Cell death in the neocortex in response to intrastriatal injection of S-AMPA with IL-1 is inhibited by NMDA antagonists {Allan & Rothwell 2000} indicating that the mechanism by which cell death occurs in the neocortex in the paradigm used here is similar to seen in experimental stroke or head injury.

The progression of injury induced by intrastriatal injection of S-AMPA is also similar to that seen in response to MCAO as it occurs rapidly (neocortical cell death is complete by 24 h), and has features of primary (intrastriatal) and secondary (neocortical) injury {Davies, Loddick, et al. 1999}.

7.4 Seizures in stroke and head injury.

Data with regard to seizures in experimental stroke are uncommon. However, focal seizure activity on EEG recordings has been observed in the cortex in rats within one hour of MCAO {Hartings, Williams, et al. 2003; Williams & Tortella 2002}. Whilst no direct relationship between seizures and neurological outcome has been demonstrated, reduction of seizure activity by anticonvulsants has been associated with a decrease in infarct volume in rats {Williams & Tortella 2002}.

Stroke is the most common cause of seizures in the elderly, and seizures are the most common neurological sequelae of stroke {Silverman, Restrepo, et al. 2002}. Early seizures (those that occur within two weeks of stroke) occur most commonly within 24 h of stroke onset, and have been reported to occur in 43-90% of patients after a stroke {Silverman, Restrepo, et al. 2002}.

The impact of seizures on outcome after a stroke is not clear. Several studies have reported that the outcome in those patients that have seizures after a stroke is no different compared to outcome in patients that have no seizures {Reith, Jorgensen, et al. 1997}. Equally, it has been reported that those patients that have seizures within 48 h of a stroke are at significantly greater risk of death than those patients that do not have seizures {Arboix, Garcia-Eroles, et al. 1997}.

Seizures are also seen in response to experimental head injury and generalised seizure activity is evident from within two min of injury in the rat {Nilsson, Ronne-Engstrom, et al. 1994}. Seizures are also a common feature of severe head injury (SHI) in patients, and are seen in up to 22% of SHI patients {Vespa, Nuwer, et al. 1999}. The impact of early seizures on outcome is also unclear as patient numbers in studies on seizures and head injury have been small. However in one study, all patients that developed persistent seizures died {Vespa, Nuwer, et al. 1999}.

IL-1 exacerbates experimental, ischaemic, and traumatic brain injury, and data from this thesis suggest that IL-1 increased excitotoxin induced cell death by increasing seizure activity. Data presented above suggest that seizures are a common accompanying feature of experimental and clinical acute neurodegenerative conditions.

Therefore, IL-1 may also exacerbate cell death in these conditions through its effects on seizure activity and some of the findings in this thesis may be extended to more clinically relevant experimental models.

7.5 Future work

Whilst this study has suggested that IL-1 increases excitotoxin induced cell death by increasing seizure activity, it also raises a number of questions.

7.5.1 IL-1, cerebral ischaemia and seizures

As discussed above, seizures are observed in the cortex of rats early after middle cerebral artery occlusion; so, IL-1 may also exacerbate ischaemic brain injury by increasing seizures. The effect of IL-1 on seizures induced by middle cerebral artery occlusion has not been investigated previously.

Seizures are characterised by increased neuronal activity, and as discussed above, seizures are observed in the cortex of rats early after middle cerebral artery occlusion {Hartings, Williams, et al. 2003; Williams & Tortella 2002}. Increased seizure activity in the region of the penumbra may exacerbate cell death through a further depletion of limited energy supplies, and hence lead to increased cell death {Katsura, Folbergrova, et al. 1994}.

7.5.2 Mechanism of cell death in the neocortex induced by S-AMPA with IL-1

Whilst we have demonstrated that IL-1 induced cell death in the neocortex is due to increased seizure activity, the mechanism(s) by which cell death occurs is unclear. As proposed above, seizure related cell death in stroke may occur as a result of increased

neuronal activity outstripping a limited energy supply in the region of the penumbra leading to death as a result of a mismatch between blood flow and metabolism {Katsura, Folbergrova, et al. 1994}.

A mismatch in blood flow and metabolism has been observed in regions that subsequently die in response to persistent seizure activity {Pereira, Ferrandon, et al. 2002}. However no studies have investigated whether this is applicable in the experimental paradigm used in this thesis.

IL-1 is an important mediator of neutrophil accumulation and entry at the site of injury or inflammation. Intraparenchymal injection of IL-1 into the CNS results in an intense myelomonocytic recruitment in the meninges surrounding the brain {Andersson, Perry, et al. 1992}. Neutrophil accumulation has been shown to obstruct the cerebral microvasculature and has been proposed to reduce cerebral blood flow and hence lead to an increase in cerebral infarct volume in stroke {del Zoppo, Schmid-Schonbein, et al. 1991}. Consistent with this, neutrophil depletion in mice results in an increase in cerebral blood flow which is accompanied with a reduced infarct volume as compared to control mice in which neutrophils were not depleted {Connolly, Winfree, et al. 1996}.

Based on these data, it is hypothesised that a relative reduction in blood flow resulting from IL-1 dependent neutrophil accumulation in the meninges leads to a perfusion/ metabolism mismatch and hence contributes to cell death in the neocortex.

7.5.3 IL-1 and seizures

The mechanism by which IL-1 causes seizures is also unknown, and some potential mechanisms have been discussed in chapter 5. Exogenous IL-1 does not alter latency to onset of kainic acid seizures {Vezzani, Conti, et al. 1999}, and IL-1ra does not modify bicuculline-induced interictal spiking in the mouse. These data suggest that IL-1 does not influence focal neuronal excitability or influence the mechanisms of seizure generation. However, the report that the bicuculline-induced bilateral, neocortical c-fos expression is reduced or absent in mice over expressing IL-1ra (*vs* wild-type mice), suggests that IL-1 influences seizure generalisation {Vezzani, Moneta, et al. 2000}. Racine stage 4 and 5 seizures may represent 'generalised' seizures {de Simoni, Perego, et al. 2000}, and therefore data presented here would also support the proposal that IL-1 is involved in the generalisation of seizures. In addition, bilateral cortical c-fos expression (8 h, chapter 6) was observed in more rats in response intrastriatal injection of S-AMPA with IL-1 compared to S-AMPA alone. These data support the hypothesis that IL-1 lowers the threshold for generalisation of seizures.

The findings of this thesis suggest that IL-1 exacerbates excitotoxin induced brain injury by increasing seizure activity. However, IL-1 is a plieotropic cytokine, and so this may represent only one mechanism by which IL-1 exacerbates acute brain injury. Thus, each of the possible detrimental effects of IL-1 (increasing temperature, BBB breakdown, neutrophil recruitment etc) need to be addressed in order to understand fully the impact of this cytokine on acute brain injury. Hopefully, along the way, this will lead a better understanding of acute brain injury and ultimately to development of a successful treatment.

References

1. Allan SM, Parker LC, Collins B, Davies, R, Luheshi GN et al. Cortical cell death induced by IL-1 is mediated via actions in the hypothalamus of the rat. *Proc Natl Acad Sci USA* 2000; 97(10):5580-5585.

2. Allan SM, Harrison DC, Read S, Collins B, Parsons AA, Philpott K et al. Selective increases in cytokine expression in the rat brain in response to striatal injection of alpha-amino-3-hydroxy-5-methyl-4-isoxazolepropionate and interleukin-1. *Brain Res Mol Brain Res* 2001; 93(2):180-189.

3. Allan SM. Varied actions of proinflammatory cytokines on excitotoxic cell death in the rat central nervous system. *J Neurosci Res* 2002; 67(4):428-434.

4. Alnemri ES, Fernandes-Alnemri T, Litwack G. Cloning and expression of four novel isoforms of human interleukin-1 beta converting enzyme with different apoptotic activities. *J Biol Chem* 1995; 270(9):4312-4317.

5. Alsbo CW, Wrang ML, Johansen FF, Diemer NH. Quantitative PCR analysis of AMPA receptor composition in two paradigms of global ischemia. *Neuroreport* 2000; 11(2):311-315.

6. Andersson PB, Perry VH, Gordon S. Intracerebral injection of proinflammatory cytokines or leukocyte chemotaxins induces minimal myelomonocytic cell recruitment to the parenchyma of the central nervous system. *J Exp Med* 1992; 176(1):255-259.

7. Anforth HR, Bluthe RM, Bristow A, Hopkins S, Lenczowski MJ, Luheshi G et al. Biological activity and brain actions of recombinant rat interleukin-1alpha and interleukin-1beta. *Eur Cytokine Netw* 1998; 9(3):279-288.

8. Anthony D, Dempster R, Fearn S, Clements J, Wells G, Perry VH et al. CXC chemokines generate age-related increases in neutrophil-mediated brain inflammation and blood-brain barrier breakdown. *Curr Biol* 1998; 8:923-926.

9. Anthony DC, Bolton SJ, Fearn S, Perry VH. Age-related effects of interleukin-1 beta on polymorphonuclear neutrophil-dependent increases in blood-brain barrier permeability in rats. *Brain* 1997; 120(Pt 3):435-444.

10. Arboix A, Garcia-Eroles L, Massons JB, Oliveres M, Comes E. Predictive factors of early seizures after acute cerebrovascular disease. *Stroke* 1997; 28(8):1590-1594.

11. Asensio VC, Campbell IL. Chemokines in the CNS: plurifunctional mediators in diverse states. *Trends Neurosci* 1999; 22(11):504-512.

12. Badovinac V, Mostarica-Stojkovic M, Dinarello CA, Stosic-Grujicic S. Interleukin-1 receptor antagonist suppresses experimental autoimmune encephalomyelitis (EAE) in rats by influencing the activation and proliferation of encephalitogenic cells. *J Neuroimmunol* 1998; 85(1):87-95.

13. Ban EM. Interleukin-1 receptors in the brain: characterization by quantitative in situ autoradiography. *Immunomethods* 1994; 5(1):31-40.

14. Barone FC, Feuerstein GZ. Inflammatory mediators and stroke: new opportunities for novel therapeutics. *J Cereb Blood Flow Metab* 1999; 19(8):819-834.

15. Barone P, Morelli M, Cicarelli G, Cozzolino A, DeJoanna G, Campanella G et al. Expression of c-fos protein in the experimental epilepsy induced by pilocarpine. *Synapse* 1993; 14(1):1-9.

16. Bath PM, Lees KR. ABC of arterial and venous disease. Acute stroke. *BMJ* 2000; 320(7239):920-923.

17. Ben-Ari Y, Tremblay E, Ottersen OP, Meldrum BS. The role of epileptic activity in hippocampal and "remote" cerebral lesions induced by kainic acid. *Brain Res* 1980; 191(1):79-97.

18. Ben Ari Y, Lagowska Y, Le Gal LS, Tremblay E, Ottersen OP, Naquet R. Diazepam pretreatment reduces distant hippocampal damage induced by intra-amygdaloid injections of kainic acid. *Eur J Pharmacol* 1978; 52(3-4):419-420.

19. Ben Ari Y, Tremblay E, Ottersen OP, Naquet R. Evidence suggesting secondary epileptogenic lesion after kainic acid: pre treatment with diazepam reduces distant but not local brain damage. *Brain Res* 1979; 165(2):362-365.

20. Ben Ari Y, Tremblay E, Riche D, Ghilini, G, Naquet R. Electrographic, clinical and pathological alterations following systemic administration of kainic acid, bicuculline or pentetrazole: metabolic mapping using the deoxyglucose method with special reference to the pathology of epilepsy. *Neuroscience* 1981; 6(7):1361-1391.

21. Ben Ari Y. Limbic seizure and brain damage produced by kainic acid: mechanisms and relevance to human temporal lobe epilepsy. *Neuroscience* 1985; 14(2):375-403.

22. Benveniste EN. Cytokine actions in the central nervous system. *Cytokine Growth Factor Rev* 1998; 9(3-4):259-275.

23. Berman FW, Murray TF. Domoic acid neurotoxicity in cultured cerebellar granule neurons is mediated predominantly by NMDA receptors that are activated as a consequence of excitatory amino acid release. *J Neurochem* 1997; 69(2):693-703.

24. Bethea JR, Chung IY, Sparacio SM, Gillespie GY, Benveniste EN. Interleukin-1 beta induction of tumor necrosis factor-alpha gene expression in human astroglioma cells. *J Neuroimmunol* 1992; 36(2-3):179-191.

25. Betz AL, Schielke GP, Yang G-Y. Interleukin-1 in cerebral ischemia. Keio Journal of Medicine 45(3), 230-238. 1996.

26. Blamire AM, Anthony DC, Rajagopalan B, Sibson NR, Perry VH, Styles P. Interleukin-1beta -induced changes in blood-brain barrier permeability, apparent diffusion coefficient, and cerebral blood volume in the rat brain: a magnetic resonance study. *J Neurosci* 2000; 20(21):8153-8159.

27. Blasi F, Riccio M, Brogi A, Strazza M, Taddei ML, Romagnoli S et al. Constitutive expression of interleukin-1beta (IL-1beta) in rat oligodendrocytes. *Biol Chem* 1999; 380(2):259-264.

28. Bleakman D, Lodge D. Neuropharmacology of AMPA and kainate receptors. *Neuropharmacology* 1998; 37(10-11):1187-1204.

29. Boakes RJ, Ednie JM, Edwardson JA, Keith AB, Sahal A, Wright C. Abnormal behavioural changes associated with vasopressin induced barrel rotations. *Brain Res* 1985; 326:250-256.

30. Boutin H, LeFeuvre RA, Horai R, Asano M, Iwakura Y, Rothwell NJ. Role of IL-1alpha and IL-1beta in ischemic brain damage. *J Neurosci* 2001; 21(15):5528-5534.

31. Bradford HF. Glutamate, GABA and epilepsy. *Prog Neurobiol* 1995; 47(6):477-511.

32. Brorson JR, Manzolillo PA, Gibbons SJ, Miller RJ. AMPA receptor desensitization predicts the selective vulnerability of cerebellar Purkinje cells to excitotoxicity. *J Neurosci* 1995; 15(6):4515-4524.

33. Bruce AJ, Boling W, Kindy MS, Peschon J, Kraemer PJ, Carpenter MK et al. Altered neuronal and microglial responses to excitotoxic and ischemic brain injury in mice lacking TNF receptors. *Nat Med* 1996; 2(7):788-794.

34. Burke RE, Fahn S. Electroencephalographic studies of chlorpromazine methiodide and somatostatin-induced barrel rotation in rats. *Exp Neurol* 1983; 79(3):704-713.

35. Busto R, Dietrich WD, Globus MYT, Valdés I, Scheinberg P, Ginsberg MD. Small differences in intraischemic brain temperature critically determine the extent of ischemic neuronal injury. *J Cerebr Blood Flow Metab* 1987; 7(6):729-738.

36. Busto R, Globus MYT, Dietrich WD, Martinez E, Valdés I, Ginsberg MD. Effect of mild hypothermia on ischemia-induced release of neurotransmitters and free fatty acids in rat brain. *Stroke* 1989; 20(7):904-910.

37. Buttini M, Sauter A, Boddeke HW. Induction of interleukin-1 beta mRNA after focal cerebral ischaemia in the rat. *Brain Res Mol Brain Res* 1994; 23(1-2):126-134.

38. Cammermeyer J. The impportance of avoiding 'dark' neurones in experimental neuropathology. *Acta Neuropathol* 1961; 1:245-270.

39. Carriedo SG, Sensi SL, Yin HZ, Weiss JH. AMPA exposures induce mitochondrial Ca(2+) overload and ROS generation in spinal motor neurons in vitro. *J Neurosci* 2000; 20(1):240-250.

40. Cartmell T, Luheshi GN, Rothwell NJ. Brain sites of action of endogenous interleukin-1 in the febrile response to localized inflammation in the rat. *J Physiol* 1999; 518 (Pt 2):585-594.

41. Cartmell T, Luheshi GN, Hopkins SJ, Rothwell NJ, Poole S. Role of endogenous interleukin-1 receptor antagonist in regulating fever induced by localised inflammation in the rat. *J Physiol* 2001; 531(Pt 1):171-180.

42. Cheng B, Christakos S, Mattson MP. Tumor necrosis factors protect neurons against metabolic-excitotoxic insults and promote maintenance of calcium homeostasis. *Neuron* 1994; 12(1):139-153.

43. Choi DW. Glutamate neurotoxicity in cortical cell culture is calcium dependent. *Neurosci Lett* 1985; 58(3):293-297.

44. Choi DW. Glutamate neurotoxicity and diseases of the nervous system. *Neuron* 1988; 1(8):623-634.

45. Choi DW. Glutamate receptors and the induction of excitotoxic neuronal death. *Prog Brain Res* 1994; 100:47-51.

46. Chung IY, Benveniste EN. Tumor necrosis factor-alpha production by astrocytes. Induction by lipopolysaccharide, IFN-gamma, and IL-1 beta. *J Immunol* 1990; 144(8):2999-3007.

47. Clark WM, Rinker LG, Lessov NS, Hazel K, Hill JK, Stenzel-Poore M et al. Lack of interleukin-6 expression is not protective against focal central nervous system ischemia. *Stroke* 2000; 31(7):1715-1720.

48. Clifton GL, Jiang JY, Lyeth BG, Jenkins LW, Hamm RJ, Hayes RL. Marked protection by moderate hypothermia after experimental traumatic brain injury. *J Cereb Blood Flow Metab* 1991; 11(1):114-121.

49. Collingridge GL, Singer W. Excitatory amino acid receptors and synaptic plasticity. *Trends Pharmacol Sci* 1990; 11(7):290-296.

50. Connolly ES, Jr., Winfree CJ, Springer TA, Naka Y, Liao H, Yan SD et al. Cerebral protection in homozygous null ICAM-1 mice after middle cerebral artery occlusion. Role of neutrophil adhesion in the pathogenesis of stroke. *J Clin Invest* 1996; 97(1):209-216.

51. Davies CA, Loddick SA, Toulmond S, Stroemer RP, Hunt J, Rothwell NJ. The progression and topographic distribution of interleukin-1beta expression after permanent middle cerebral artery occlusion in the rat *J Cereb Blood Flow Metab* 1999; 19(1):87-98.

52. de Simoni MG, Perego C, Ravizza T, Moneta D, Conti M, Marchesi F et al. Inflammatory cytokines and related genes are induced in the rat hippocampus by limbic status epilepticus. *Eur J Neurosci* 2000; 12(7):2623-2633.

53. de Vries HE, Blom-Roosemalen MC, van Oosten M, de Boer AG, van Berkel TJ, Breimer DD et al. The influence of cytokines on the integrity of the blood-brain barrier in vitro. *J Neuroimmunol* 1996; 64(1):37-43.

54. del Zoppo GJ, Schmid-Schonbein GW, Mori E, Copeland BR, Chang CM. Polymorphonuclear leukocytes occlude capillaries following middle cerebral artery occlusion and reperfusion in baboons. *Stroke* 1991; 22(10):1276-1283.

55. Diamant NH, de Weid D. Simultaneous occurrence of barrel rotation and hypothermia in rats following central injection of AVP. *Ann N Y Acad Sci* 1993; 689:582-588.

56. Dinarello CA. The interleukin-1 family: 10 years of discovery. *FASEB Journal* 1994; 8:1314-1325.

57. Dinarello CA. The role of the interleukin-1-receptor antagonist in blocking inflammation mediated by interleukin-1. *N Engl J Med* 2000; 343(10):732-734.

58. Doble A. The role of Excitotoxicity in Neurodegenerative Disease:Implications for therapy. *Pharmacol Ther* 1999; 81(3):163-221.

59. Dragunow M, Robertson HA. Kindling stimulation induces c-fos protein(s) in granule cells of the rat dentate gyrus. *Nature* 1987; 329(6138):441-442.

60. Dragunow M, Faull R. The use of c-fos as a metabolic marker in neuronal pathway tracing. *J Neurosci Methods* 1989; 29(3):261-265.

61. Enari M, Hug H, Nagata S. Involvement of an ICE-like protease in Fas-mediated apoptosis. *Nature* 1995; 375(6526):78-81.

62. Ericsson A, Liu C, Hart RP, Sawchenko PE. Type 1 interleukin-1 receptor in the rat brain: distribution, regulation, and relationship to sites of IL-1-induced cellular activation. *J Comp Neurol* 1995; 361:681-698.

63. Eriksson C, Winblad B, Schultzberg M. Kainic acid induced expression of interleukin-1 receptor antagonist mRNA in the rat brain. *Brain Res Mol Brain Res* 1998; 58(1-2):195-208.

64. Eriksson C, Van Dam AM, Lucassen PJ, Bol JG, Winblad B, Schultzberg M. Immunohistochemical localization of interleukin-1beta, interleukin-1 receptor antagonist and interleukin-1beta converting enzyme/caspase-1 in the rat brain after peripheral administration of kainic acid. *Neuroscience* 1999; 93(3):915-930.

65. Fabian RH, Perez-Polo JR, Kent TA. Electrochemical monitoring of superoxide anion production and cerebral blood flow: effect of interleukin-1 beta pretreatment in a model of focal ischemia and reperfusion. *J Neurosci Res* 2000; 60(6):795-803.

66. Faraci FM, Breese KR. Dilatation of cerebral arterioles in response to N-methyl-D-aspartate: role of CGRP and acetylcholine. *Brain Res* 1994; 640(1-2):93-97.

67. Farrar WL, Kilian PC, Ruff MR, Hill JM, Pert CB. Visualization and characterization of interleukin 1 receptors in brain. *J Immunol* 1987; 139(2):459-463.

68. Foutz AS, Champagnat J, Denavit-Saubie M. Respiratory effects of the N-methyl-D-aspartate (NMDA) antagonist, MK-801, in intact and vagotomized chronic cats. *Eur J Pharmacol* 1988; 154(2):179-184.

69. Freeman BD, Buchman TG. Interleukin-1 receptor antagonist as therapy for inflammatory disorders. *Expert Opin Biol Ther* 2001; 1(2):301-308.

70. French RA, VanHoy RW, Chizzonite R, Zachary JF, Dantzer R, Parnet P et al. Expression and localization of p80 and p68 interleukin-1 receptor proteins in the brain of adult mice. *J Neuroimmunol* 1999; 93(1-2):194-202.

71. Garabedian BV, Lemaigre-Dubreuil Y, Mariani J. Central origin of IL-1beta produced during peripheral inflammation: role of meninges. *Brain Res Mol Brain Res* 2000; 75(2):259-263.

72. Garcia JH, Kamijioyo Y. Cerebral infarction:evolution of histopathological changes after occlusion of a middle cerebral artery in primates. *J Neuropathol Exp Neurol* 1974; 33:409-421.

73. Garthwaite G, Hajos F, Garthwaite J. Ionic requirements for neurotoxic effects of excitatory amino acid analogues in rat cerebellar slices. *Neuroscience* 1986; 18(2):437-447.

74. Garthwaite G, Garthwaite J. AMPA Neurotoxicity in Rat Cerebellar and Hippocampal Slices: Histological Evidence for Three Mechanisms. *Eur J Neurosci* 1991; 3(8):715-728.

75. Gary DS, Bruce-Keller AJ, Kindy MS, Mattson MP. Ischemic and excitotoxic brain injury is enhanced in mice lacking the p55 tumor necrosis factor receptor. *J Cereb Blood Flow Metab* 1998; 18(12):1283-1287.

76. Gayle D, Ilyin SE, Romanovitch AE, Peloso E, Satinoff E, Plata-Salaman CR. Basal and IL-1beta-stimulated cytokine and neuropeptide mRNA expression in brain regions of young and old Long-Evans rats. *Brain Res Mol Brain Res* 1999; 70(1):92-100.

77. Ginsberg MD. Temperature influence on ischaemic brain injury. In: Hsu CY, editor. *Ischaemic stroke: from basic mechamnisms to new drug development.* Basel: Krager, 1998:65-88.

78. Giulian D, Vaca K, Corpuz M. Brain glia release factors with opposing actions upon neuronal survival. *J Neurosci* 1993; 13(1):29-37.

79. Goddard GV, McIntyre DC, Leech CK. A permanent change in brain function resulting from daily electrical stimulation. *Exp Neurol* 1969; 25(3):295-330.

80. Greenfeder SA, Nunes P, Kwee L, Labow M, Chizzonite RA, Ju G. Molecular cloning and characterization of a second subunit of the interleukin 1 receptor complex. *J Biol Chem* 1995; 270:13757-13765.

81. Grundy RI, Rothwell NJ, Allan SM. Dissociation between the effects of interleukin-1 on excitotoxic brain damage and body temperature in the rat. *Brain Res* 1999; 830(1):32-37.

82. Grundy RI. The role of IL-1 in AMPA mediated excitotoxic cell death. 2000. Unversity of Manchester.

83. Grundy RI, Rothwell NJ, Allan SM. Site-specific actions of interleukin-1 on excitotoxic cell death in the rat striatum. *Brain Res* 2002; 926(1-2):142-148.

84. Hallegua DS, Weisman MH. Potential therapeutic uses of interleukin 1 receptor antagonists in human diseases. *Ann Rheum Dis* 2002; 61(11):960-967.

85. Handforth A, Ackermann RF. Mapping of limbic seizure progressions utilizing the electrogenic status epilepticus model and the 14C-2-deoxyglucose method. *Brain Res Brain Res Rev* 1995; 20(1):1-23.

86. Hartings JA, Williams AJ, Tortella FC. Occurrence of nonconvulsive seizures, periodic epileptiform discharges, and intermittent rhythmic delta activity in rat focal ischemia. *Exp Neurol* 2003; 179(2):139-149.

87. Herrera DG, Robertson HA. Activation of c-fos in the brain. *Prog Neurobiol* 1996; 50(2-3):83-107.

88. Holmin S, Mathiesen T. Intracerebral administration of interleukin-1beta and induction of inflammation, apoptosis, and vasogenic edema. *J Neurosurg* 2000; 92(1):108-120.

89. Hoozemans JJ, Veerhuis R, Janssen I, Rozemuller AJ, Eikelenboom P. Interleukin-1beta induced cyclooxygenase 2 expression and prostaglandin E2 secretion by human neuroblastoma cells: implications for Alzheimer's disease. *Exp Gerontol* 2001; 36(3):559-570.

90. Hopkins SJ, Rothwell NJ. Cytokines and the nervous system I : Expression and recognition. *Trends Neurosci* 1995; 18(2):83-88.

91. Hosoi T, Okuma Y, Nomura Y. Leptin induces IL-1 receptor antagonist expression in the brain. *Biochem Biophys Res Commun* 2002; 294(2):215-219.

92. Hughes PE, Alexi T, Walton M, Williams CE, Dragunow M, Clark RG et al. Activity and injury-dependent expression of inducible transcription factors, growth factors and apoptosis-related genes within the central nervous system. *Prog Neurobiol* 1999; 57(4):421-450.

93. Ianotti F, Kida S, Weller R, Buhagiar G, Hillhouse EW. Interleukin-1β in focal cerebral ischaemia in rats. *JENPO* 1993; 137:115.

94. Ingvar M. Cerebral blood flow and metabolic rate during seizures. Relationship to epileptic brain damage. *Ann N Y Acad Sci* 1986; 462:194-206.

95. Issekutz TB. In vivo blood monocyte migration to acute inflammatory reactions, IL-1 alpha, TNF-alpha, IFN-gamma, and C5a utilizes LFA-1, Mac-1, and VLA-4. The relative importance of each integrin. *J Immunol* 1995; 154(12):6533-6540.

96. Jankowsky JL, Patterson PH. The role of cytokines and growth factors in seizures and their sequelae. *Prog Neurobiol* 2001; 63(2):125-149.

97. Kaplanski G, Farnarier C, Kaplanski S, Porat R, Shapiro L, Bongrand P et al. Interleukin-1 induces interleukin-8 secretion from endothelial cells by a juxtacrine mechanism. *Blood* 1994; 84(12):4242-4248.

98. Karibe H, Chen J, Zarow GJ, Graham SH, Weinstein PR. Delayed induction of mild hypothermia to reduce infarct volume after temporary middle cerebral artery occlusion in rats. *J Neurosurg* 1994; 80(1):112-119.

99. Kassel N, Sasaki T, Colohan A. Cerebral vasospasm following aneurysmal subarachnoid haemorrhage. *Stroke* 1985; 16:562-572.

100. Katabami T, Shimizu M, Okano K, Yano Y, Nemoto K, Ogura et al. Intracellular signal transduction for interleukin-1 beta-induced endothelin production in human umbilical vein endothelial cells. *Biochemical & Biophysical Research Communications* 1992; 188(2):565-570.

101. Kato H, Walz W. The initiation of the microglial response. *Brain Pathol* 2000; 10(1):137-143.

102. Katsura K, Folbergrova J, Gido G, Siesjo BK. Functional, metabolic, and circulatory changes associated with seizure activity in the postischemic brain. *J Neurochem* 1994; 62(4):1511-1515.

103. Keinanen K, Wisden W, Sommer B, Werner P, Herb A, Verdoorn TA et al. A family of AMPA-selective glutamate receptors. *Science* 1990; 249(4968):556-560.

104. Keyser J, Sulter G, Luiten P. Clinical trials with neuroprotective drugs in acute ischaemic stroke: are we doing the right thing? *Trends Neurosci* 2000; 22(12):535-540.

105. Kluger MJ, Kozak W, Leon LR, Soszynski D, Conn CA. Cytokines and fever. *Neuroimmunomodulation* 1995; 2(4):216-223.

106. Konsman JP, Tridon V, Dantzer R. Diffusion and action of intracerebroventricularly injected interleukin-1 in the CNS. *Neuroscience* 2000; 101(4):957-967.

107. Kreutzberg GW. Microglia: a sensor for pathological events in the CNS. *Trends Neurosci* 1996; 19(8):312-318.

108. Kuschinsky W, Suda S, Sokoloff L. Local cerebral glucose utilization and blood flow during metabolic acidosis. *Am J Physiol* 1981; 241(5):H772-H777.

109. Lawrence CB, Allan SM, Rothwell NJ. Interleukin-1beta and the interleukin-1 receptor antagonist act in the striatum to modify excitotoxic brain damage in the rat. *Eur J Neurosci* 1998; 10(3):1188-1195.

110. Lees GJ, Leong W. The non-NMDA glutamate antagonist NBQX blocks the local hippocampal toxicity of kainic acid, but not the diffuse extrahippocampal damage. *Neurosci Lett* 1992; 143(1-2):39-42.

111. Lees GJ, Leong W. NBQX prevents contralateral but not ipsilateral seizure-induced cytotoxicity of kainate but not AMPA-reversal at high doses of NBQX. *Neuroreport* 1994; 5(16):2153-2156.

112. Lees GJ, Leong W. In vivo, the direct and seizure-induced neuronal cytotoxicity of kainate and AMPA is modified by the non-competitive antagonist, GYKI 52466. *Brain Res* 2001; 890(1):66-77.

113. Leker.R, Shohami E. Cerbral ischaemia and trauma- different etiologies yet similar mechanisms:neuroprotective opportunities. *Brain Res Rev* 2002; 39:55-73.

114. Liu T, McDonnell PC, Young PR, White RF, Siren AL, Hallenbeck JM et al. Interleukin-1 beta mRNA expression in ischemic rat cortex. *Stroke* 1993; 24(11):1746-1750.

115. Loddick SA, Rothwell NJ. Neuroprotective effects of human recombinant interleukin-1 receptor antagonist in focal cerebral ischaemia in the rat. *J Cereb Blood Flow Metab* 1996a; 16(5):932-940.

116. Loddick SA, MacKenzie A, Rothwell NJ. An ICE inhibitor, z-VAD-DCB attenuates ischaemic brain damage in the rat. *Neuroreport* 1996b; 7(9):1465-1468.

117. Loddick SA, Turnbull AV, Rothwell NJ. Cerebral interleukin-6 is neuroprotective during permanent focal cerebral ischemia in the rat. *J Cereb Blood Flow Metab* 1998a; 18(2):176-179.

118. Loddick SA, Liu C, Takao T, Hashimoto K, De Souza EB. Interleukin-1 receptors: cloning studies and role in central nervous system disorders. *Brain Res - Brain Res Reviews* 1998b; 26(2-3):306-319.

119. Loscher W. Pharmacology of glutamate receptor antagonists in the kindling model of epilepsy. *Prog Neurobiol* 1998; 54(6):721-741.

120. Lu YM, Yin HZ, Chiang J, Weiss JH. Ca(2+)-permeable AMPA/kainate and NMDA channels: high rate of Ca2+ influx underlies potent induction of injury. *J Neurosci* 1996; 16(17):5457-5465.

121. Marcus BC, Wyble CW, Hynes KL, Gewertz BL. Cytokine-induced increases in endothelial permeability occur after adhesion molecule expression. *Surgery* 1996; 120(2):411-416.

122. Marshall L, Gautille T, Klauber T, et al. The outcome after closed head injury. *J Neurosurg* 1991; 75(Suppl):S28-S36.

123. Martin D, Chinookoswong N, Miller G. The interleukin-1 receptor antagonist (rhIL-1ra) protects against cerebral infarction in a rat model of hypoxia-ischemia. *Exp Neurol* 1994; 130(2):362-367.

124. Martin D, Near SL. Protective effect of interleukin-1 receptor antagonist (IL-1ra) on experimental allergic encephalomyelitis in rats. *J Neuroimmunol* 1995; 61(1):241-245.

125. Mathiesen T, Edner G, Ulfarsson E, Andersson B. Cerebrospinal fluid interleukin-1 receptor antagonist and tumor necrosis factor- α following subarachnoid hemorrhage. *J Neurosurg* 87 (2), 215-220. 1997.

126. Mayne M, Ni W, Yan HJ, Xue M, Johnston JB, Del Bigio MR et al. Antisense oligodeoxynucleotide inhibition of tumor necrosis factor-alpha expression is neuroprotective after intracerebral hemorrhage. *Stroke* 2001; 32(1):240-248.

127. Mazzari S, Aldinio C, Beccaro M, Toffano G, Schwarcz R. Intracerebral quinolinic acid injection in the rat:effects on dopaminergic neurones. *Brain Res* 1986; 380:309-316.

128. McClain CJ, Cohen D, Ott L, Dinarello CA, Young B. Ventricular fluid interleukin-1 activity in patients with head injury. *J Lab Clin Med* 1987; 110:48-54.

129. McDonald JW, Johnston MV. Physiological and pathophysiological roles of excitatory amino acids during central nervous system development. *Brain Res - Brain Res Reviews*1990; 15(1):41-70.

130. Meldrum B. Excitatory amino acids and anoxic/ischaemic brain damage. *Trends Neurosci* 1985; 8(2):47-48.

131. Meldrum B, Garthwaite J. Excitatory amino acid neurotoxicity and neurodegenerative diseases. *Trends Pharmacol Sci* 1990; 11(11):379-87.

132. Miller LG, Galpern WR, Dunlap K, Dinarello CA, Turner TJ. Interleukin-1 augments gamma-aminobutyric acidA receptor function in brain. *Molecular Pharmacology* 1991; 39(2):105-108.

133. Minami M, Kuraishi Y, Yabuuchi K, Yamazaki A, Satoh M. Induction of interleukin-1β mRNA in rat brain after transient forebrain ischemia. *J Neurochem* 1992; 58(1):390-392.

134. Monyer H, Seeburg PH, Wisden W. Glutamate-operated channels: developmentally early and mature forms arise by alternative splicing. *Neuron* 1991; 6(5):799-810.

135. Morgan JI, Cohen DR, Hempstead JL, Curran T. Mapping patterns of c-fos expression in the central nervous system after seizure. *Science* 1987; 237(4811):192-197.

136. Morikawa E, Ginsberg MD, Dietrich WD, Duncan RC, Kraydieh S, Globus MY et al. The significance of brain temperature in focal cerebral ischemia: histopathological consequences of middle cerebral artery occlusion in the rat. *J Cereb Blood Flow Metab* 1992; 12(3):380-389.

137. Mumford H, Wetherell JR. A simple method for measuring EEG in freely moving guinea pigs. *J Neurosci Methods* 2001; 107(1-2):125-130.

138. Munoz-Fernandez MA, Fresno M. The role of tumour necrosis factor, interleukin 6, interferon-gamma and inducible nitric oxide synthase in the development and pathology of the nervous system. *Prog Neurobiol* 1998; 56(3):307-340.

139. Murray CA, McGahon B, McBennett S, Lynch MA. Interleukin-1 beta inhibits glutamate release in hippocampus of young, but not aged, rats. *Neurobiol Aging* 1997; 18(3):343-348.

140. Nawashiro H, Martin D, Hallenbeck JM. Neuroprotective effects of TNF binding protein in focal cerebral ischemia. *Brain Res* 1997; 778(2):265-271.

141. Nicholls D, Attwell D. The release and uptake of excitatory amino acids. *Trends Pharmacol Sci* 1990; 11(11):462-468.

142. Nilsson P, Ronne-Engstrom E, Flink R, Ungerstedt U, Carlson H, Hillered L. Epileptic seizure activity in the acute phase following cortical impact trauma in rat. *Brain Res* 1994; 637(1-2):227-232.

143. Olsen RW, Szamraj O, Houser CR. [3H]AMPA binding to glutamate receptor subpopulations in rat brain. *Brain Res* 1987; 402(2):243-254.

144. Ozawa S, Kamiya H, Tsuzuki K. Glutamate receptors in the mammalian central nervous system. *Prog Neurobiol* 1998; 54(5):581-618.

145. Parnet P, Kelley KW, Bluthe RM, Dantzer R. Expression and regulation of interleukin-1 receptors in the brain. Role in cytokines-induced sickness behavior. *J Neuroimmunol* 2002; 125(1-2):5-14.

146. Paxinos G, Watson C. *The rat brain in stereotaxic coordinates*, Second Edition ed. London: Academic Press, 1986.

147. Pearson VL, Rothwell NJ, Toulmond S. Excitotoxic brain damage in the rat induces interleukin-1beta protein in microglia and astrocytes: correlation with the progression of cell death. *Glia* 1999; 25(4):311-323.

148. Penkowa M, Moos T, Carrasco J, Hadberg H, Molinero A, Bluethmann H et al. Strongly compromised inflammatory response to brain injury in interleukin-6-deficient mice. *Glia* 1999; 25(4):343-357.

149. Pereira d, V, Ferrandon A, Nehlig A. Local cerebral blood flow during lithium-pilocarpine seizures in the developing and adult rat: role of coupling between blood flow and metabolism in the genesis of neuronal damage. *J Cereb Blood Flow Metab* 2002; 22(2):196-205.

150. Perry VH, Bell MD, Brown HC, Matyszak MK. Inflammation in the nervous system. *Curr Opin Neurobiol* 1995; 5(5):636-641.

151. Petralia RS, Wenthold RJ. Light and electron immunocytochemical localization of AMPA-selective glutamate receptors in the rat brain. *J Comp Neurol* 1992; 318(3):329-354.

152. Pinteaux E, Parker LC, Rothwell NJ, Luheshi GN. Expression of interleukin-1 receptors and their role in interleukin-1 actions in murine microglial cells. *J Neurochem* 2002; 83(4):754-763.

153. Plata-Salaman CR, Ffrench-Mullen JM. Interleukin-1 beta depresses calcium currents in CA1 hippocampal neurons at pathophysiological concentrations. *Brain Res Bull* 1992; 29(2):221-223.

154. Popovici T, Represa A, Crepel V, Barbin G, Beaudoin M, Ben Ari Y. Effects of kainic acid-induced seizures and ischemia on c-fos-like proteins in rat brain. *Brain Res* 1990; 536(1-2):183-194.

155. Prehn JH, Backhauss C, Krieglstein J. Transforming growth factor-beta 1 prevents glutamate neurotoxicity in rat neocortical cultures and protects mouse neocortex from ischemic injury in vivo. *J Cereb Blood Flow Metab* 1993; 13(3):521-525.

156. Proescholdt MG, Chakravarty S, Foster JA, Foti SB, Briley EM, Herkenham M. Intracerebroventricular but not intravenous interleukin-1beta induces widespread vascular-mediated leukocyte infiltration and immune signal mRNA expression followed by brain-wide glial activation. *Neuroscience* 2002; 112(3):731-749.

157. Racine RJ. Modification of seizure activity by electrical stimulation. II. Motor seizure. *Electroencephalogr Clin Neurophysiol* 1972; 32(3):281-294.

158. Reimann-Philipp U, Ovase R, Weigel PH, Grammas P. Mechanisms of cell death in primary cortical neurons and PC12 cells. *J Neurosci Res* 2001; 64(6):654-660.

159. Reith J, Jorgensen H, Pedersen P, et al. Body temperature in acute stroke:relation to stroke severity infarct size mortality and outcome. *Lancet* 1996; 327:422-425.

160. Reith J, Jorgensen HS, Nakayama H, Raaschou HO, Olsen TS. Seizures in acute stroke: predictors and prognostic significance. The Copenhagen Stroke Study. *Stroke* 1997; 28(8):1585-1589.

161. Relton JK, Rothwell NJ. Interleukin-1 receptor antagonist inhibits ischaemic and excitotoxic neuronal damage in the rat. *Brain Res Bull* 1992; 29(2):243-246.

162. Rogers HW, Tripp CS, Schreiber RD, Unanue ER. Endogenous IL-1 is required for neutrophil recruitment and macrophage activation during murine listeriosis. *J Immunol* 1994; 153(5):2093-2101.

163. Rosa ML, Jefferys JG, Sanders MW, Pearson RC. Expression of mRNAs encoding flip isoforms of GluR1 and GluR2 glutamate receptors is increased in rat hippocampus in epilepsy induced by tetanus toxin. *Epilepsy Res* 1999; 36(2-3):243-251.

164. Rothwell N, Allan S, Toulmond S. The role of interleukin 1 in acute neurodegeneration and stroke: pathophysiological and therapeutic implications. *J Clin Invest* 1997; 100(11):2648-2652.

165. Rothwell NJ, Hopkins SJ. Cytokines and the nervous system II: Actions and mechanisms of action. *Trends Neurosci* 1995; 18(3):130-136.

166. Rothwell NJ. Annual review prize lecture cytokines - killers in the brain?. *Journal of Physiology* 1999; 514(Pt 1):3-17.

167. Rothwell NJ, Luheshi G. Interleukin-1 in the brain: biology, pathology and therapeutic targets. *Trends Neurosci* 2000; 23(12):618-625.

168. Ruocco A, Nicole O, Docagne F, Ali C, Chazalviel L, Komesli S et al. A transforming growth factor-beta antagonist unmasks the neuroprotective role of this endogenous cytokine in excitotoxic and ischemic brain injury. *J Cereb Blood Flow Metab* 1999; 19(12):1345-1353.

169. Sanderson KL, Raghupathi R, Saatman KE, Martin D, Miller G, McIntosh TK. Interleukin-1 receptor antagonist attenuates regional neuronal cell death and cognitive dysfunction after experimental brain injury. *J Cereb Blood Flow Metab* 1999; 19(10):1118-1125.

170. Scharfman HE, Schwartzkroin PA. Protection of dentate hilar cells from prolonged stimulation by intracellular calcium chelation. *Science* 1989; 246(4927):257-260.

171. Schaul N. The fundamental neural mechanisms of electroencephalography. *Electroencephalogr Clin Neurophysiol* 1998; 106(2):101-107.

172. Schmued LC, Albertson C, Slikker W, Jr. Fluoro-Jade: a novel fluorochrome for the sensitive and reliable histochemical localization of neuronal degeneration. *Brain Res* 1997; 751(1):37-46.

173. Seifert G, Schroder W, Hinterkeuser S, Schumacher T, Schramm J, Steinhauser C. Changes in flip/flop splicing of astroglial AMPA receptors in human temporal lobe epilepsy. *Epilepsia* 2002; 43 Suppl 5:162-167.

174. Sensi SL, Yin HZ, Weiss JH. AMPA/kainate receptor-triggered Zn2+ entry into cortical neurons induces mitochondrial Zn2+ uptake and persistent mitochondrial dysfunction. *Eur J Neurosci* 2000; 12(10):3813-3818.

175. Sheng JG, Boop FA, Mrak RE, Griffin WS. Increased neuronal beta-amyloid precursor protein expression in human temporal lobe epilepsy: association with interleukin-1 alpha immunoreactivity. *J Neurochem* 1994; 63(5):1872-1879.

176. Shibata M, Parfenova H, Zuckerman SL, Seyer JM, Krueger JM, Leffler CW. Interleukin-1β peptides induce cerebral pial arteriolar dilation in anaesthetized newborn pigs. *Am J Physiol* 1996; 270(5 Pt 2):R1044-R1050.

177. Shin C, McNamara JO. Mechanism of epilepsy. *Annu Rev Med* 1994; 45:379-389.

178. Siesjo BK. Pathophysiology and treatment of focal cerebral ischemia. Part II: Mechanisms of damage and treatment. *J Neurosurg* 1992a; 77(3):337-354.

179. Siesjo BK. Pathophysiology and treatment of focal cerebral ischemia. Part II: Mechanisms of damage and treatment. *J Neurosurg* 1992b; 77(3):337-354.

180. Siesjo BK. Basic mechanisms of traumatic brain damage. *Ann Emerg Med* 1993; 22(6):959-969.

181. Silverman IE, Restrepo L, Mathews GC. Poststroke seizures. *Arch Neurol* 2002; 59(2):195-201.

182. Sokoloff L. Relationships among local functional activity, energy metabolism, and blood flow in the central nervous system. *Fed Proc* 1981; 40(8):2311-2316.

183. Sommer B, Keinanen K, Verdoorn TA, Wisden W, Burnashev N, Herb A et al. Flip and flop: a cell-specific functional switch in glutamate-operated channels of the CNS. *Science* 1990; 249(4976):1580-1585.

184. Sperk G. Kainic acid seizures in the rat. *Prog Neurobiol* 1994; 42:1-32.

185. Stanimirovic D, Satoh K. Inflammatory mediators of cerebral endothelium: a role in ischemic brain inflammation. *Brain Pathol* 2000; 10(1):113-126.

186. Sternberg EM. Neural-immune interactions in health and disease. *J Clin Invest* 1997; 100(11):2641-2647.

187. Stochetti N, Rossi S, Buzzi F. Intracranial pressure monitoring in head injury; management and results. *Intensive Care Medicine* 1999; 25:371-376.

188. Stoll G, Jander S, Schroeter M. Inflammation and glial responses in ischemic brain lesions. *Prog Neurobiol* 1998; 56(2):149-171.

189. Stoll G, Jander S. The role of microglia and macrophages in the pathophysiology of the CNS. *Prog Neurobiol* 1999; 58(3):233-247.

190. Strijbos PJLM, Rothwell NJ. Interleukin-1β attenutates excitatory amino acid-induced neurodegeneration in vitro: involvement of nerve growth factor. *J Neurosci* 1995; 15(5):3468-3474.

191. Stroemer RP, Rothwell NJ. Cortical protection by localized striatal injection of IL-1ra following cerebral ischemia in the rat. *J Cereb Blood Flow Metab* 1997; 17(6):597-604.

192. Stroemer RP, Rothwell NJ. Exacerbation of ischemic brain damage by localized striatal injection of interleukin-1beta in the rat. *J Cereb Blood Flow Metab* 1998; 18(8):833-839.

193. Sullivan AM, Reynolds DS, Thomas KL, Morton AJ. Cortical induction of c-fos by intrastriatal endothelin-1 is mediated via NMDA receptors. *Neuroreport* 1996; 8(1):211-216.

194. Sutcliffe IT, Smith HA, Stanimirovic D, Hutchison JS. Effects of moderate hypothermia on IL-1 beta-induced leukocyte rolling and adhesion in pial microcirculation of mice and on proinflammatory gene expression in human cerebral endothelial cells. *J Cereb Blood Flow Metab* 2001; 21(11):1310-1319.

195. Tanaka H, Grooms SY, Bennett MV, Zukin RS. The AMPAR subunit GluR2: still front and center-stage. *Brain Res* 2000; 886(1-2):190-207.

196. Terao A, Matsumura H, Saito M. Interleukin-1 induces slow-wave sleep at the prostaglandin D2-sensitive sleep-promoting zone in the rat brain. *J Neurosci* 1998; 18(16):6599-6607.

197. Todaka K, Ishida Y, Ishizuka Y, Hashiguchi H, Mitsuyama Y, Kannan H et al. Fos expression in neurons immunoreactive for neuronal nitric oxide synthase in the rat paraventricular nucleus after intraperitoneal injection of interleukin-1 beta. *Neurosci Res* 2000; 38(3):321-324.

198. Toulmond S, Rothwell NJ. Time-course of IL-1 receptor antagonist (IL-1ra) expression after brain trauma in the rat. *Soc Neurosci Abstr* 1995; 21:200.2.

199. Touzani O, Boutin H, Chuquet J, Rothwell N. Potential mechanisms of interleukin-1 involvement in cerebral ischaemia. *J Neuroimmunol* 1999; 100(1-2):203-215.

200. Turski WA, Cavalheiro EA, Calderazzo-Filho LS, Kleinrok Z, Czuczwar SJ, Turski L. Injections of picrotoxin and bicuculline into the amygdaloid complex of the rat: an electroencephalographic, behavioural and morphological analysis. *Neuroscience* 1985; 14(1):37-53.

201. Vandenberghe W, Robberecht W, Brorson JR. AMPA receptor calcium permeability, GluR2 expression, and selective motoneuron vulnerability. *J Neurosci* 2000; 20(1):123-132.

202. Vespa PM, Nuwer MR, Nenov V, Ronne-Engstrom E, Hovda DA, Bergsneider M et al. Increased incidence and impact of nonconvulsive and convulsive seizures after traumatic brain injury as detected by continuous electroencephalographic monitoring. *J Neurosurg* 1999; 91(5):750-760.

203. Vezzani A, Conti M, De Luigi A, Ravizza T, Moneta D, Marchesi F et al. Interleukin-1beta immunoreactivity and microglia are enhanced in the rat hippocampus by focal kainate application: functional evidence for enhancement of electrographic seizures. *J Neurosci* 1999; 19(12):5054-5065.

204. Vezzani A, Moneta D, Conti M, Richichi C, Ravizza T, De Luigi A et al. Powerful anticonvulsant action of IL-1 receptor antagonist on intracerebral injection and astrocytic overexpression in mice. *Proc Natl Acad Sci U S A* 2000; 97(21):11534-11539.

205. Vitkovic L, Bockaert J, Jacque C. "Inflammatory" cytokines: neuromodulators in normal brain? *J Neurochem* 2000; 74(2):457-471.

206. Vogel V, Sanchez C, Jennum P. EEG measurements by means of radiotelemetry after intracerebroventricular (ICV) cannulation in rodents. *J Neurosci Methods* 2002; 118(1):89-96.

207. Watkins JC, Evans RH. Excitatory amino acid transmitters. *Annu Rev Pharmacol Toxicol* 1981; 21:165-204.

208. Weiss JH, Sensi SL. Ca2+-Zn2+ permeable AMPA or kainate receptors: possible key factors in selective neurodegeneration. *Trends Neurosci* 2000; 23(8):365-371.

209. Williams AJ, Tortella FC. Neuroprotective effects of the sodium channel blocker RS100642 and attenuation of ischemia-induced brain seizures in the rat. *Brain Res* 2002; 932(1-2):45-55.

210. Willoughby JO, Mackenzie L. Nonconvulsive electrocorticographic paroxysms (absence epilepsy) in rat strains. *Lab Anim Sci* 1992; 42(6):551-554.

211. Willoughby JO, Mackenzie L, Medvedev A, Hiscock JJ. Fos induction following systemic kainic acid: early expression in hippocampus and later widespread expression correlated with seizure. *Neuroscience* 1997; 77(2):379-392.

212. Xue D, Huang ZG, Barnes K, Lesiuk HJ, Smith KE, Buchan AM. Delayed treatment with AMPA, but not NMDA, antagonists reduces neocortical infarction. *J Cereb Blood Flow Metab* 1994; 14(2):251-261.

213. Yabuuchi K, Minami M, Katsumata S, Satoh M. In situ hybridization study of interleukin-1 beta mRNA induced by kainic acid in the rat brain. *Brain Res Mol Brain Res* 1993; 20(1-2):153-161.

214. Yamasaki Y, Matsuura N, Shozuhara H, Onodera H, Itoyama Y, Kogure K. Interleukin-1 as a pathogenetic mediator of ischemic brain damage in rats. *Stroke* 1995; 26(4):676-681.

215. Ye ZC, Sontheimer H. Cytokine modulation of glial glutamate uptake: a possible involvement of nitric oxide. *Neuroreport* 1996; 7(13):2181-2185.

216. Ying HS, Weishaupt JH, Grabb M, Canzoniero LM, Sensi SL, Sheline CT et al. Sublethal oxygen-glucose deprivation alters hippocampal neuronal AMPA receptor expression and vulnerability to kainate-induced death. *J Neurosci* 1997; 17(24):9536-9544.

217. Zaczek R, Simonton S, Coyle JT. Local and distant neuronal degeneration following intrastriatal injection of kainic acid. *J Neuropathol Exp Neurol* 1980; 39:245-264.

218. Zhang Z, Chopp M, Goussev A, Powers C. Cerebral vessels express interleukin 1beta after focal cerebral ischemia. *Brain Res* 1998; 784(1-2):210-217.

219. Zhao X, Bausano B, Pike BR, Newcomb-Fernandez JK, Wang KK, Shohami E et al. TNF-alpha stimulates caspase-3 activation and apoptotic cell death in primary septo-hippocampal cultures. *J Neurosci Res* 2001; 64(2):121-131.

220. Zhou QQ, Imbe H, Zou S, Dubner R, Ren K. Selective upregulation of the flip-flop splice variants of AMPA receptor subunits in the rat spinal cord after hindpaw inflammation. *Brain Res Mol Brain Res* 2001; 88(1-2):186-193.